



**MECHANICAL PROPERTIES OF A THERMAL TREATED COMMERCIALY PURE
GRADE 2 TITANIUM PLATE (CP TI GRADE 2)**

By

DUMO MPUMLWANA

Thesis submitted in fulfilment of the requirements for the degree

Master of Engineering: Mechanical Engineering

in the Faculty of Engineering

at the Cape Peninsula University of Technology

Supervisor: Dr V. Msomi

Bellville

October 2020

DECLARATION

I, Dumo Mpumlwana, announce that the substance of this dissertation speak to my very own independent work, and that this dissertation has not recently been submitted for scholarly assessment towards any capability. Besides, it speaks to my own assessments and not really those of the Cape Peninsula University of Technology.



Signature

October 2020

Date

ABSTRACT

The significant improvement when titanium is utilized in different designing fields is its high explicit quality and resilience against high temperatures while maintaining its quality within a wide temperature range. Titanium is produced for commercial use in two different formats; commercially pure and alloyed. Titanium additionally shows high corrosion resistance, high malleability, exhaustion quality, and high strength to mass temperature ratios in most force application media. Commercially pure titanium grade 2 (CP-Ti grade 2) has a yield strength of 540 MPa joined with great flexibility, formability, and phenomenal weldability. Grade 2 titanium has a density of 4.51 g/cm³ which is 60 % less compared to steel.

This research presents the examination of the mechanical properties of (CP-Ti) hot-rolled plates through the microstructure analysis, tensile testing, microhardness testing and scanning electron microscope (SEM) analysis. The samples were prepared through the use of a water-jet cutter to prevent an introduction of unnecessary heat to the samples. The prepared samples were then heat-treated using a standard furnace by soaking them in a furnace oven at 900°C for different soaking times. The tensile testing, microhardness testing, microstructural analysis and scanning electron microscope (SEM) were performed in all heat treated and non-treated samples, and the results were compared to the non-treated samples.

Performing a tensile test in all heat-treated and non-treated samples allowed the analysis of different mechanical properties and distinguished between elastic and plastic deformation. Performing the microstructure test in treated and untreated samples allowed the analysis of the surface coordinates of each particle of the tested samples. The hardness test of heat-treated and non-treated samples determined the appropriateness of a material for a specified application, or the particular treatment to which the material has been subjected. SEM for heat-treated and non-treated samples determined the surface fracture.

It was noticeable that the heating period had an impact on the hardness of the samples. The largest hardness was found on the 90 minutes treatment. In microstructural analyses it was noticeable that heat treatment influences the growth of grains. There was a decrease in tensile strength in all heat-treated samples compared with the non-treated samples. A ductile fracture was noticeable in all heat-treated samples.

Keywords: Cp Ti, Cp Ti grade 2, microstructure, phase transformation thermal expansion, physical properties, mechanical properties, grains, α phase, β phase, β transus, $\alpha - \beta$ alloys, water quenching, annealing.

ACKNOWLEDGEMENTS

I would hereby, like to appreciate the following individuals and organisations instrumental in the completion of my research project:

- Firstly, to God Almighty be the glory and honour for the strength and wisdom throughout my research;
- Thank you to my supervisor, Dr V. Msomi for the supervision, motivations, support and, much needed advice;
- I thank Walter Sisulu University (WSU) my employer for allowing me some allocated time during working hours to spend on my research and travelling to Cape Town when needed to;
- Many thanks to my sponsor MerSeta for funding all of my research.
- Thank you to Dr. A.K. Masha, and Dr. C.J.S. Fourie for their support and motivations;
- My gratitude toward Dr. C.J.S. Fourie for proof reading and language editing of the document;
- I thank the CPUT mechanical Engineering laboratory technician staff Mr. Moni and Mr Matthew for their assistance and help during my research practical at the laboratory, I sincerely appreciate their assistance;
- I thank Ms Shahheda for her support during my research practical at the meturlugy laboratory.
- My work colleagues in particular Mr. M. Mbola, Mr. M. Tyokolo and Mr. S. Mawisa for their assistance, motivations and support;
- My loving wife for all her support and prayers during the research project. I couldn't have done it without her;

TABLE OF CONTENTS

TITLE PAGE.....	i
DECLARATION.....	i
ABSTRACT.....	ii
ACKNOWLEDGEMENTS.....	iii
TABLE OF CONTENTS.....	iv
LIST OF FIGURES.....	v
LIST OF TABLES.....	vi
GLOSSARY.....	viii
Acronyms/Abbreviations.....	viii
GLOSSARY OF TERMS.....	x
Nomenclature.....	xii
CHAPTER 1: INTRODUCTION.....	1
1.1 OVERVIEW OF TITANIUM.....	1
1.2 PROBLEM STATEMENT.....	2
1.3 BACKGROUND.....	2
1.3.1 Commercially Pure Titanium and Physical Metallurgy.....	4
1.3.2 α/β Titanium.....	5
1.3.3 Crystal Construction of Titanium (Ti).....	6
1.3.4 Effects of Alloying Elements of Titanium (Ti).....	6
1.3.5 Titanium Alloys Classification.....	7
1.3.6 β -stabilizers.....	8
1.3.7 α –Stabilizers.....	9
1.3.8 Impartial fundamentals of Ti.....	10
1.3.9 Microstructure of CP Ti grade 2.....	10
1.4 OBJECTIVES.....	11
1.5 THESIS OVERVIEW.....	11
CHAPTER 2: LITERATURE REVIEW.....	12
2.1 Heat treatment on tensile properties.....	12
2.2 Heat treatment on microstructure.....	16
2.3 Heat treatment on micro hardness.....	20
2.4 Heat treatment on Scanning Electron Microscope (SEM).....	24
2.5 Chapter Summary.....	26
CHAPTER 3: EXPERIMENTAL SETUP AND PERFORMANCE.....	27
3.1 LIST OF EQUIPMENT USED DURING HEAT-TREATMENT.....	27
3.2 EQUIPMENT DISCRPTION.....	27
3.2.1 Vulcan Furnace Oven.....	27
3.2.2 Thermometer.....	28
3.2.3 Stop watch.....	28
3.2.4 Performance of Heat Treatment.....	29
3.3 EQUIPMENT USED FOR THE ANALYSIS OF THE RESULTS.....	31
3.4 EQUIPMENT DISCRPTION.....	31
3.4.1 Motic AE2000MET inverted microscope.....	31
3.4.2 Instron tensile testing machine.....	31
3.4.3 MIRA Scanning Electron Microscope.....	32
3.4.4 Micro hardness Tester machine.....	32
3.5 PERFORMANCE OF ANALYSIS.....	32
3.5.1 Microstructure.....	32
3.5.1.1 Hot Mounting.....	33
3.5.1.2 Polishing.....	33
3.5.1.3 Etching.....	34
3.5.1.4 Microscope Analysis.....	34
3.5.2 Tensile.....	35
3.5.3 Scanning Electron Microscope (SEM).....	36
3.5.4 Micro Hardness.....	37

CHAPTER 4: RESULTS AND DISCUSSIONS	40
4.1 TENSILE.....	40
4.1.1 Parent vs 30 minutes-soaked results	40
4.1.2 Parent vs 60 minutes heat treatment results	42
4.1.3 Parent vs 90 minutes-soaked results	44
4.2 Summary of Tensile Behaviour	46
4.3 Scanning Electron Microscope (SEM).....	46
4.4 Microstructure grain sizes investigation and Structure Analysis	48
4.5 Micro hardness	51
4.5.1 Parent.....	51
4.5.2 30 Minutes Heat Treatment.....	52
4.5.3 60 Minutes Heat Treatment.....	53
4.5.4 90 Minutes heat treatment	54
CHAPTER 5: CONCLUSION AND RECOMMENDATION	56
5.1. Conclusion.....	56
5.2 Recommendations for future work	57
REFERENCES	58

LIST OF FIGURES

Figure 1.1 A tensile strength vs. temperature for various materials.....	3
Figure 1.2 Component cell of alpha (α) and beta (β) phases of Ti.....	6
Figure 1.3 “Precise strength vs use temperature (K).....	7
Figure 1.4 3-D phase diagram to classifying Titanium (Ti) alloys	8
Figure 1.5 Displays diverse kinds of stages illustrations of Titanium	9
Figure 1.6 As received microstructure of commercially pure titanium grade 2.....	10
Figure 3.1: Vulcan Furnace 3 – 1750 Oven	28
Figure 3.2: Thomas Traceable Kangaroo Thermometer	28
Figure 3.3: Ciccio stop watch.....	28
Figure 3.4: Heat Treatment process diagram.....	29
Figure 3.5: Treated and untreated samples	30
Figure 3.6: Hot mounted microstructure samples.....	32
Figure 3.7: Mounting machines.....	33
Figure 3.8: Polisher machine used in preparation of microscope samples	34
Figure 3.9: Motic AE2000MET inverted microscope	35
Figure 3.10: Prepared tensile sample	35
Figure 3.11: Instron Tensile Machine.....	36
Figure 3.12: Prepare SEM samples	36
Figure 3.13: Tescan Mira 3 machine.....	37
Figure 3.14: Innova Test Falcon 500 Micro Hardness Machine	38
Figure 3.15: Micro hardness test pattern followed.....	39
Figure 4.1: Parent Sample Stress-strain curve graph.....	40
Figure 4.2: 30 Minutes Heat Treatment Stress-strain curve graph	41
Figure 4.3: Fractured tensile samples, (A) Parent, (B) 30 Minutes	42
Figure 4.4: 60 minutes soaking Stress-strain curve.....	43
Figure 4.5: Fractured tensile samples, (A) Parent, (B) 60 Minutes	44
Figure 4.6: Parent compared with 90 minutes soaking Stress-strain curve	45
Figure 4.7: Fractured tensile Samples, (A) Parent, (B) 90 Minutes	46
Figure 4.8: Fracture morphology of different samples after the tensile test (A) parent, (B) 30 Min, (C) 60 Min, (D) 90 Min.....	47
Figure 4.9: Microstructure of a parent material.....	49
Figure 4.10: Microstructure of 30 minutes heat treatment sample.....	49
Figure 4.11: Microstructure of 60 minutes heat treatment sample.....	50
Figure 4.12: Microstructure of 90 minutes heat treatment sample.....	50
Figure 4.13: Hardness (HV) vs hardness points.....	52
Figure 4.14: 30 minutes heat treatment Hardness (HV) vs hardness points graph.....	53
Figure 4.15: Hardness (HV) vs hardness points.....	54
Figure 4.16: 90 Minutes Hardness (HV) vs hardness points graph	55
APPENDICES	63
Figure A1: Images around micro hardness points measured for Parent sample	63
Figure A2: Images around micro hardness points measured for 30 minutes heat treated sample.....	67
Figure A3: Images around micro hardness points measured for 60 minutes heat treated sample.....	71
Figure A4: Images around micro hardness points measured for 90 minutes heat treated sample.....	75
APPENDIX AB.....	79
Figure B1: Raw titanium(Sponge)	79

LIST OF TABLES

Table 1. 1 Maximum working temperature for several Ti alloys (The IMI designations).....	3
Table 1.2 Mechanical properties of CP Ti grade 2	4
Table 1.3 Commercial alpha and beta (α/β) alloys list.....	5
Table 3.1 Micro hardness information entered loaded on the machine	39
Table 4.1: 30 Minutes results compared with parent material results at yield point	40
Table 4.2: 60 minutes results compared with parent material at yield point.....	42
Table 4.3: 90 minutes results compared with parent material at yield point.....	44
Table 4.4: Average grain size measurement for Cp Ti grade 2 samples (μn)	48
Table 4.5: Average micro hardness results	51
Table 4.6: Micro hardness results measured at different point	51
Table 4.7: Micro hardness results for 30 minutes sample	52
Table 4.8: 60 Minutes micro hardness results.....	53
Table 4.9: 90 Minutes micro hardness results.....	54

GLOSSARY

Acronyms/Abbreviations

AC	Air Cooling
Al	Aluminium
ASTM	American Society of Testing Materials
BCC	Body centered cubic
Bi	Bismuth
C	Carbon
CAD	Computer Aided Drawings
Cl	Chlorine
CP	Commercially Pure
CPUT	Cape Peninsula University of Technology
Cp-Ti	Commercially-Pure Titanium
Cp-Ti grade 2	Commercially-Pure Grade 2 Titanium
CIP	Cold Isostatic Press
Cr	Chromium
Cu	Copper
DIC	Digital Image Correlation
EDS	Energy Dispersive Spectroscopy
EDX	Energy Dispersive X-Ray Spectroscopy
EIS	Electrochemical Impedance Spectroscopy
ELI	Extra Low Interstitial
F	Flourine
FC	Furnace Cooling
Fe	Iron
FESEM	Field Emission Scanning Electron Microscopy
FGMs	Functionally – Graded Materials
FGCs	Functionally Graded Composites
G	Gallium
Ge	Germanium
H	Hydrogen
HAZ	Heat Affected Zone
HCP	Hexagonal Close-Pack crystal structure
HV	Vickers Micro hardness
Kgf	Refers to Brinell Hardness load range
LOM	Light Optical Microscopy
MC	Composite Metal

MMC	Metal Matrix Composites
MAM	Material Accretion Manufacturing
Mo	Molybdenum
Mn	Manganese
Mo	Molybdenum
N	Nitrogen
Nb	Niobium
Na	Sodium
Nb	Niobium
NQ	Nitrogen Quenching
Ni	Nickel
O	Oxygen
OC	Oil Quenching
S	Sulfur
SEM	Scanning Electron Microscopy
Si	Silicon
Sn	Tin
SPS	Spark plasma sintering
Ta	Tantalum
TiC	Titanium carbide
Ti	Titanium
Ti-6Al-4V	Titanium-6Aluminium-4Vanadium
TNTZ	Ti-29Nb-13Ta-4.6Zr
TEMs	Transmission Electron Microscope
UTS	Ultimate tensile strength
UV	Ultraviolet
V	Vanadium
W	Tungsten
WQ	Water Quenching
Zr	Zirconium

GLOSSARY OF TERMS

Alloy – A material with metallic elements and actuality made from at least two synthetic components of which at any rate one of which is a metal.

Alloying Element – Is a component additional to a metal, and the remoulding of the metal.

Brittleness – Is the propensity of a material, to break exclusive of first undergoing significant plastic distortion.

Brittle fracture – Fast breakage from minimal or tiny plastic distortion.

Cavitation's wear testing – A procedure of wear, whereby the erosive medium or counter form is a liquid. A corrosion could be encompassed in wear phenomenon, however, harm will be bigger and achieved from chemical reactions instead of mechanical action.

Characterization – Refers to the usage of exterior methods to probe into the interior structure and belongings of a material. Characterization can take the form of real materials examination.

Columnar epithelial – Are epithelial cells whose height are at least four times their width.

Ductility – A quantity of the aptitude of a material to experience plastic distortion prior fracture which is typically articulated as percentage elongation.

% Elongation – Is the overall percent upsurge in the distance measure of a sample following a tensile examination.

Elastic deformation – Is the distortion of the material that is recovered when load is applied.

Elastic region – A material is alleged to be stressed inside the elastic area when the working stress does not exceed the elastic limit.

Elastic limit – The highest stress which a material is capable of sustaining without any lasting strain remaining upon complete release of the stress.

Elongation – The growth in gauge distance of a body exposed to a tension energy, referenced to a gauge length of a body.

Etching – Applying a surface treatment using an suitable chemical reagent to reveal the microstructure of a material.

Engineering strain – This is a dimensionless value that variate in distance per unit length of the original linear dimension.

Equixed – Are crystals that contain axes of about the similar length/ having approximately same dimensions in all directions utilised particularly of a crystal in a metal.

Grain – A single crystal in a polycrystalline material.

Grain Size – The average grain diameter determined from a random cross section.

Grain Growth – This is a phenomenon that happens once the temperature of a metal is increased; the grains grow and their size may ultimately exceed the original grain size.

Grain Boundary – An interface separating two grains, where the orientation variation is minor, the boundary is occasionally referred to as a sub-boundary structure.

Grinding – Eliminating material from the surface of the work piece by means of a grinding wheel or abrasive grinding papers.

Hardness – A term utilised for unfolding the resistance of a material to plastic distortion.

Hardness test – Measure the resistance of a material to penetration by a sharp object

Hardening – Growing hardness by appropriate treatment.

Macrostructure – The structure of the metals as exposed by macroscopic inspection of the etched surface of a polished sample.

Mechanical properties – The belongings of a material that disclose its elastic or inelastic performance when force is applied, signifying the appropriate mechanical applications.

Microstructure – The structure of an arranged surface of a metal, as exposed by a microscope at a particular magnification.

Metallurgy – The science and technology of metals and their alloys counting approaches of extraction and use.

Modulus of Elasticity – A measure of materials stiffness which is distinct as the ratio of stress to strain when the distortion is elastic.

Martensite – Is most commonly refers to a very hard form of steel crystalline structure, but it can also refer to any crystal structure that is formed by diffusion less transformation.

Parameter – The minimum and maximum parameters that will describe the operating range of a variable.

Parent material – A material in its as manufactured form or as supplied.

Plastic deformation – This is the distortion of material constantly and permanently in any direction.

Polished surface – A surface that reflects a large proportion of the incident light in a peculiar manner.

Tensile strength – The maximum tensile stress which a material is capable of sustaining. Tensile strength is calculated from the maximum load during a tension test carried out to rupture, and the original cross-sectional area of the specimen.

Tensile test – Measures the response of a material to a slowly applied axial force.

Ultimate Tensile Strength – Is the maximum stress that a material can endure while being stretched or pulled prior failing or infringement.

Vickers hardness – A number related to the applied load and the surface area of the permanent impression made by a square-based pyramid diamond indenter.

Void – The space that exists between particles or grains.

Nomenclature

Symbol		Description	Units
AL	-	Cross sectional Area	(m ²)
d	-	Diameter of specimen	(m)
E	-	Young's modulus of elasticity	(GPa)
%EL	-	Percentage elongation	(%)
G	-	Modulus of rigidity	(GPa)
n	-	Strain hardness coefficient	No units
T	-	Torque	(Nm)
Ti	-	Titanium	(none)
ΔT	-	Change in Temperature	(°C)
UTS	-	Ultimate Tensile Strength	(MPa)
YTS	-	Yield Tensile Strength	(MPa)

CHAPTER 1: INTRODUCTION

1.1 OVERVIEW OF TITANIUM

Titanium is generally used within titanium alloys with a wide scope of application in the aviation, medical, and automotive industry. Some of the titanium alloys are magnificent materials for biomedical use, particularly as orthopedic composites. The most significant properties of these biomedical titanium combinations are high quality, low thickness, amazing corrosion resistance, and the best biocompatibility among the metallic biomaterials [Pinke., 2014].

The fundamental issue is the assembling of vehicles and aircraft that are overweight, with lighter and more appropriate materials, without compromising toughness and integrity. It was ordinary in the past to encounter hard-core pickup trucks because of the materials that were utilized at the times. These vehicles exert huge burdens and strains on their assembled structure, damage road infrastructure, and contribute to the large fuel consumption. The advantages of a lighter-weight vehicle would be less expensive to assemble and also in the assembly infrastructure. Eliminating heavy materials like steel to make a lighter vehicle is really a noteworthy objective among most auto manufacturers.

According to Khorasani (2015), a large amount of about 230 000 of hip arthroplasty procedures (orthopedic medical procedures where the articular surface of a musculoskeletal joint was supplanted, rebuilt, or realigned) have been completed yearly in the USA and will increase in the next couple of decades due to the normal degeneration in human joints. The embedded materials utilized in orthopedic medical procedures ought to be kept away from contagious disease and contamination, yet additionally give long term biocompatibility and sturdiness (i.e., high quality, long lifetime, high-wear opposition, high protection from erosion in the human body, no lethality to the human body, and so forth. The titanium-based alloy has a moderately low flexible modulus and is the favored material for implants. The regularly utilized Titanium-based implant materials in orthopedic medical procedures are Ti-6Al-4V and unadulterated Titanium (Ti). Current uses of Ti-6Al-4V ELI (additional low interstitial) compound incorporate hip and knee joints prosthesis, injury, and dental inserts [Venkatesh., 2008].

Titanium (Ti) is a lightweight metal (around 60% of the density of steel) with remarkable erosion resistance. Its exquisite quality and high melting point (more than 1650 °C), makes it an indisputable material of choice for the airplane and motorsports fraternities. A large portion of the titanium produced is for aviation alone [Cheng-feng et al., 2017].

1.2 PROBLEM STATEMENT

Titanium is seen as a good material for application in many fields due to its compatibility with different environments. The problem is that it remains unclear what is this material's response when it is exposed to certain temperatures for a long time. This study investigated and analyses the mechanical properties of this material post-exposure to high temperatures for different durations.

1.3 BACKGROUND

Titanium together with its alloys has a profound impact in a variety of areas. In the chemical, petrochemical, and maritime fields, Ti alloys remained to a large extent invulnerable to corrosion. The biocompatibility of Ti alloy remains appreciated in therapeutic practice, in the form of various types of prosthetic implants. Ti alloy application in manufacturing includes knives, spoons, cameras, watches, and sports gear. The principle explanation behind the large utilization of Ti composites in the aerospace industry is its excellent quality. Figure 1.1 shows the tensile strength of various materials versus temperature. It is clear from figure 1.1 that Ti alloys have higher tensile strength compared to most metallic materials to a maximum temperature scope of 400-500°C [Pederson., 2004].

Even though polymer lattice composites display a larger tensile strength in comparison with most metallic materials, they are inappropriate in aviation applications; for example, in jet engine parts due to their poor strength and malleability and constrained by relatively low-temperature capabilities. A key objective of the jet engine industry is to elevate the operational temperature conditions in the engine to increase the effectiveness of the fuel-burning procedure. The working temperature improvement of the titanium compound over the last 70 years has almost doubled as shown in table 1.1 and figure 1 [Prasad et al., 2010].

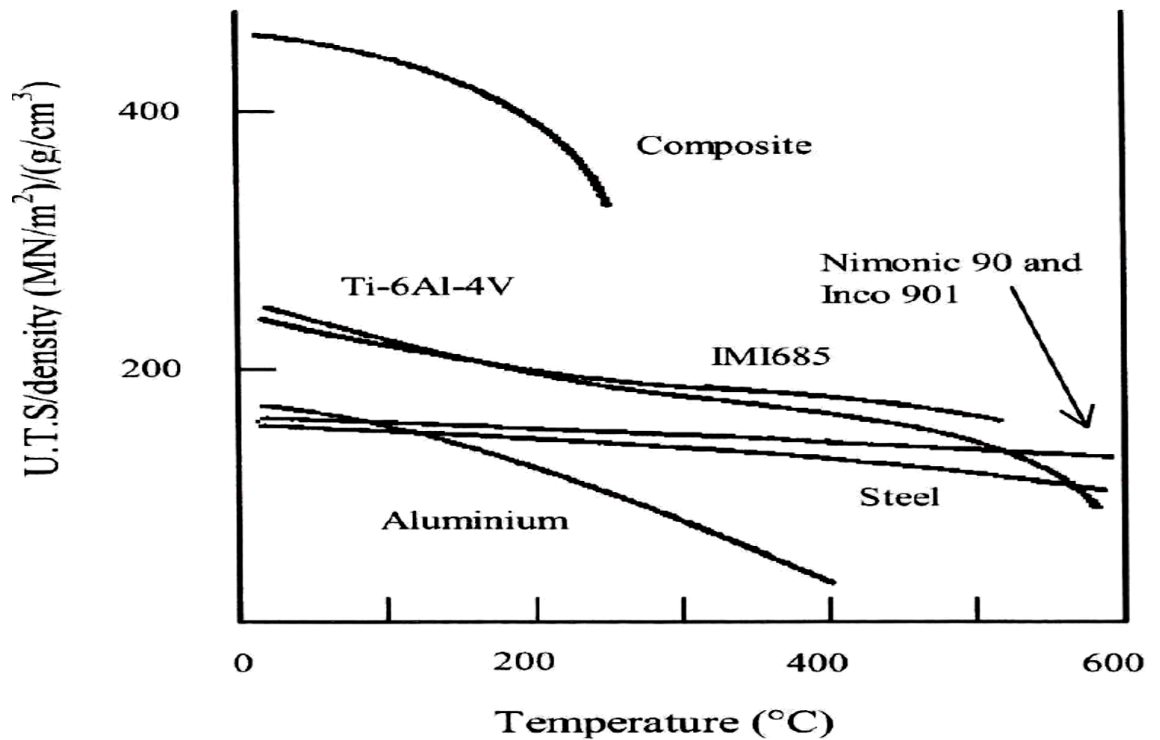


Figure 1.1 Tensile strength vs. temperature for various materials.
[Pederson et al., 2004]

Table 1.1 Maximum working temperature for several Ti alloys (The IMI designations);
[Pederson et al., 2004]

Name	Composition (wt %)	Introduction Year	Max.Working Temperature (°C)
Ti-64	6Al,4V	1954	300
IMI-550	4Al,2Sn,4Mo,0.5Si	1956	425
Ti-811	8Al,1Mo,IV	1961	400
IMI-679	2Al,11Sn,5Zr,1Mo,0.2Si	1961	450
Ti-6246	6Al,2Sn,4Zr,6Mo	1966	450
Ti-6242	6Al,2Sn,4Zr,2Mo	1967	450
IMI-685	6Al,5Zr,0.5Mo,0.25Si	1969	520
Ti-11	6Al,2Sn,1.5Zr,1Mo,0.1Si,0.3Bi	1972	540
Ti-17	5Al,2Sn,2Zr,4Mo,4Cr	1973	350
Ti-6242S	6Al,2Sn,4Zr,2Mo,0.1Si	1974	520
IMI-829	5.5Al,3.5Sn,3Zr,0.3Mo,INb,0.3Si	1976	580
IMI-834	5.5Al,4Sn,4Zr,0.3Mo,INb,0.5Si,0.06C	1984	590

The most popular Ti alloy, titanium-6Al-4V was developed during the 1950s with the highest operating temperature of about 300°C. However, the largest temperature that

a modern Ti alloy can safely withstand today is about 600 oC. The most extreme working temperature definition is to some degree a relative articulation and higher temperature working conditions can be utilized for short time periods while longer periods are possible for lower working temperatures. [Coelho et al., 1999].

The Cp Ti alloy is generally utilized for industrialized applications because of the weight implication, larger corrosion resistance, and higher safe operational temperature. Pure Ti varies from its amalgam partners due to its biocompatibility with the human skeleton and body. As indicated by the American Society of Testing Materials F67, commercially pure titanium is separated into 4 groups, G1s to G4s. Intermittently, Cp Ti is used in conditions of extreme pressure. Negative aspects of commercially pure titanium and its compounds are the lower young's modulus, poor mechanical quality, and weak wear resistance. Mechanical properties of commercially pure titanium depend on the weight quantity of oxygen (O₂) nitrogen (N), and carbon (C), and lower concentrations are needed if a large sturdiness is compulsory [Catherin et al., 2018].

1.3.1 Commercially Pure Titanium and Physical Metallurgy

Pure Ti (essential Ti additionally named CP Ti) is an allotropic metal that can be compared to two different rocks identified by temperature and weight. After heating titanium at atmospheric pressure, it experiences a strong solid-state phase at 882.5 °C, known as the transus temperature, whereby the alpha (α) stage, Hexagonal Close-Pack (HCP) precious stone form changes to a beta (β) stage body-focused cubic (BCC) crystal form. Ti liquefies at 1725 °C and solidifies at 1668 °C (solidus) (Khorasani et al., 2015; Warchomicka, 2010). The mechanical properties for commercially pure grade 2 Ti have an estimated fatigue rate of R = 0.1 – 274.9-344.9 Mpa (40-50 Ksi) [Veiga et al., 2012].

Table 1. 2 Mechanical properties of CP Ti grade 2
[Okabe., 1995]

Material	Modulus (GPa)	Ultimate Tensile Strength (MPa)	Yield Strength (MPa)	Elongation (%)	Density (g/cc)	Type of Alloy
Cp Ti grade 1	102	240	170	24	4.5	α
Cp Ti grade 2	102	345	275	20	4.5	α
Cp Ti grade 3	102	450	380	18	4.5	α

Cp Ti grade 4	104	550	483	15	4.5	α
Ti-6Al-4V-ELI	113	860	795	10	4.4	$\alpha + \beta$
Ti-6Al-4V	113	930	860	10	4.4	$\alpha + \beta$
Ti-6Al-7Nb	114	900-1050	880-950	8-15	4.4	$\alpha + \beta$
Ti-5Al-2.5Fe	112	1020	895	15	4.4	$\alpha + \beta$
Ti-15Zr-4Nb-2Ta-0.2Pd	94-99	715-919	693-806	18-28	4.4	$\alpha + \beta$
Ti-29Nb-13Ta-4.6Zr	80	911	864	13.2	4.4	$\alpha + \beta$

1.3.2 Alpha (α)/Beta (β) Titanium

According to Nady et al. (2017), the titanium alloys, alpha, or beta (α/β) Ti are the most commonly used for commercial applications. They represented the largest portion of titanium used in the United States during 1998, of which 56% was Ti-6Al-4V. As a result of the closeness of use between the alpha and beta (α & β) variations of titanium, the larger volume of the small (although only incrementally larger) because the α stage is the standard form at room temperature but the β stage needs temperature treatment, which improves its properties. The blend of the qualities of each stage gives these alloys an appealing suite of properties, including a helpful mix of strength, pliability, resistance to wear, and crack properties. The microstructure could be changed through exposing the material to maturing temperatures and times just at room temperature rates from over the beta transus. Additional commercial combinations are shown in Table 1.3 below.

Table 1. 3 Commercial alpha and beta (α/β) alloys list [Nady et al., 2017].

Grade or Alloy A + β Alloys	O (max) Fe (Max.) Other Additions	Stress (MPa)
Ti-811	Ti-8Al-1V-1Mo	1040
IMI 685	Ti-6Al-5Zr-0.5Mo-0.25Si	1020
IMI 834	Ti-5.8Al-4Sn-3.5Zr-0.5Mo-0.7 Nb-0.35Si-0.06C	1045
Ti-6242	Ti-6Al-2Sn-4Zr-2Mo-0.1Si	995
Ti-6-4	Ti-6Al-4V (0.200)	995
Ti-6-4 ELI	Ti-6Al-4V (0.130)	975
Ti-662	Ti-6Al-6V-2Sn	945
IMI 550	Ti-4Al-2Sn-4Mo-0.5Si	975

1.3.3 Crystal Construction of Titanium (Ti)

Ti experiences an allotropic stage variation at 882.5 °C, and transfers from the alpha stage below this temperature, into the beta stage above this temperature. The positive alteration is influenced by interstitial and substitutional components, producing a high-quality metal. The hexagonal closed pack element cell of the low-temperature stage is shown in figure 1.2 a, together with the three optimum grid packing parameters when the material is cold. The proportion $c/a = 1.587$ for unadulterated alpha-titanium is smaller when compared to the cubic shape proportion of $c/a = 1.633$. Figure. 1.2 b below shows the unit cell of the bcc or beta (β)-phase and the cross-section parameter of unadulterated titanium at 900 °C, [Vatsayan et al., 2014].

The natural anisotropic behavior of the hexagonal crystal structure of the stage has significant ramifications for flexibility, then plastic deformation behavior, and its different combinations on top of all the various other physical properties. Although such differences are smaller in polycrystalline alpha (α) titanium and its alloys, there can presently be different varieties of the finished material [Nakagawa et al., 2006].

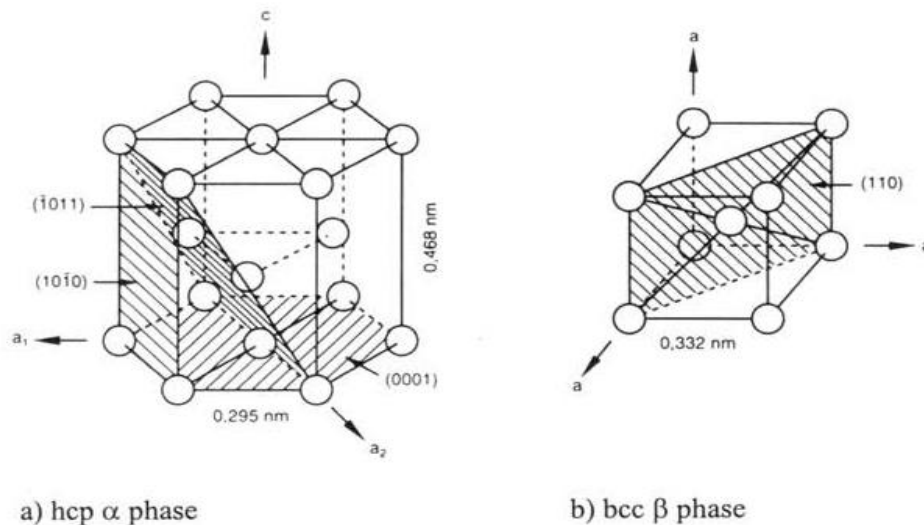


Figure 1.2 Component cell of alpha (α) and beta (β) phases of Ti [Vatsayan et al., 2014]

1.3.4 Effects of Alloying Elements of Titanium (Ti)

A broad variety of mechanical and physical properties is observed over a specific range of alloying components and Ti. The fundamental impacts of various alloying components are discussed below:

- Some alloying augmentations, such as aluminum (Al), Oxygen, Nitrogen, and Carbon, normally stabilizes the α stage and increases the strength, even at elevated temperatures. It can however change totally to the β stage if the temperature is not controlled (Figure 1.3).
- Different alloying concentrations stabilize the β stage by lowering the β – transus temperature from (α to β).
- Components within Ti such as tin and zirconium are α and β phase strengthener which improves creep resistance and has a slight influence on a temperature change. Different titanium amalgam combination microstructures typically have various compound concentrations and preparations as shown in figure 1.3 [Ahmed et al., 2014].

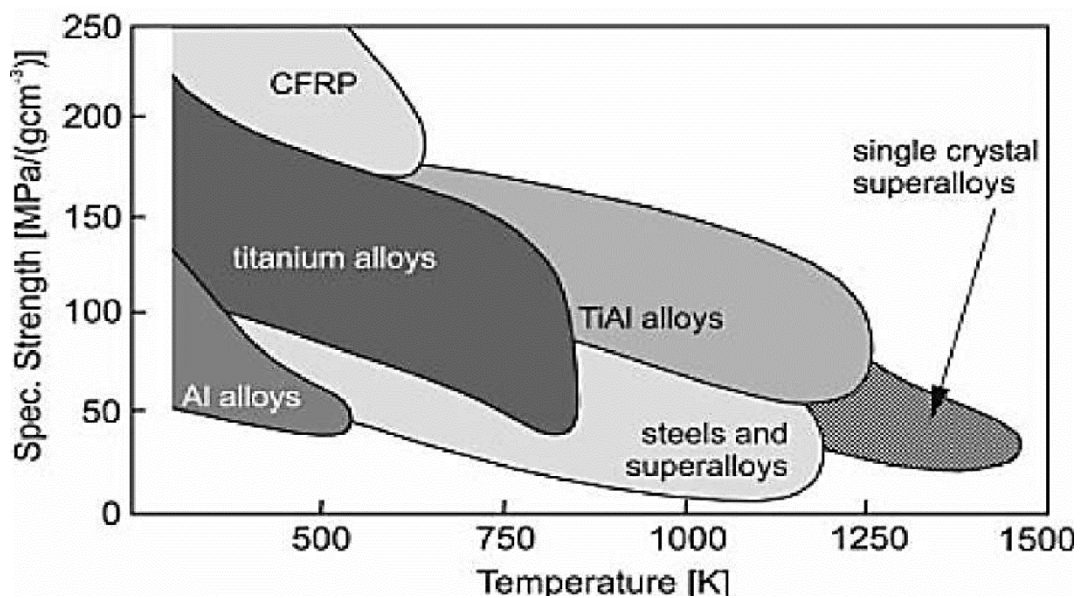


Figure 1.3 “Precise strength vs use temperature (K)
[Ahmed et al., 2014].

1.3.5 Titanium Alloys Classification

Characterization of Titanium and its alloys depends on the amount of alpha and beta phases retained at room temperature during its formation and includes the alpha, near alpha, alpha-beta, and metastable beta phases. Basically, Cp and the α alloy have all-alpha microstructures. The beta compounds essentially contain beta microstructures after the air-cooling procedure resulted in the arrangement of treating temperature over the beta (β) transus. Alpha-Beta (α – β) combinations display a blend of α and β stages at room temperature [Ahmed et al., 2014].

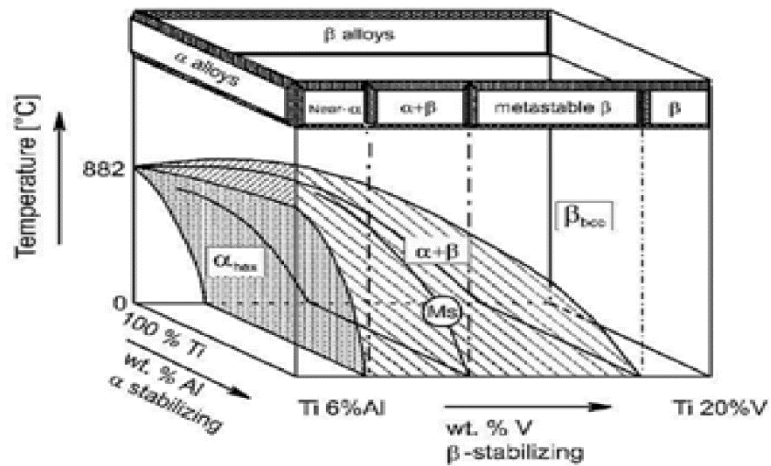


Figure 1.4 3-D phase diagram to classifying Titanium (Ti) alloys [Ahmed et al., 2014].

1.3.6 β -stabilizers

The structure changes from alpha to beta structure at a temperature of 884.9 °C as shown in figure 1.5. This phase changing temperature can be raised or lowered depending on the type and concentration of impurities or the alloying augmentations. Beta stabilizers are progress metals and they can be classified into two groups, namely the beta (β)-isomorphous and beta (β)-eutectoid stabilizers. Beta-isomorphous stabilizers have strong solvency within beta (β) Titanium [Gurao et al., 2011].

Beta (β) isomorphous components introduced into Ti compounds are vanadium (V), niobium (Nb), and molybdenum (Mo). These components settle the beta (β) stage into standard conditions as shown in figure 1.5(b). Tantalum and tungsten are only sometimes utilized because of weight issues. Beta eutectoid stabilizers ordinarily utilized for alloying with titanium are chromium, iron, and silicon while tungsten, copper, nickel, manganese, and bismuth are known to have a limited utilization [Halevy et al., 2010].

A schematic stage outline appears in figure 1.5(c). The large diffusivity of hydrogen makes it an unusual material of microstructure refinement as an ephemeral alloying component. Cr is limited up to 5 wt% because it will shape the intermetallic compound Ti-Cr₂ which is unwanted. Additionally, iron is constrained to 5.5 wt%. Silicon is a typical addition to Ti composites for extreme temperature resilience and also reduces creep [Ahmed et al., 2014].

1.3.7 α –Stabilizers

Pure Ti at standard temperature conditions consists of alpha hexagonal closely packed structure. Replacement alpha stabilizers are aluminum (Al), gallium (Ga), germanium (Ge), and interstitial alpha stabilizers are oxygen, nitrogen, and carbon. Amongst the replacement alloying components, Aluminium acts as most broadly utilized because it has good solvency in both alpha and beta stages and it reduces the alloy's weight. For titanium alloy, Aluminium expansion is restricted to approximately 5-6 wt% due to the titanium-3aluminium stage framed with the expanding aluminum content [Krakhmalev et al., 2016].

The double stage area alpha + titanium -3 aluminum starts at about 5 wt% of aluminium. The development of the Ti-3Al (α_2) stage results in fragile combinations. The proportional aluminium content in the multi-part titanium alloy appears in figure 1.5(a). A schematic stage outline with the alpha (α) stabilizing component is shown in figure 1.5. Other substitutional alloying components are gallium, germanium, and uncommon earth components though they are much lower than aluminium and oxygen. Oxygen, nitrogen, carbon altogether are solid alpha-stabilizers. These alloying components additionally bring down the malleability of titanium alloys. At room temperature, Cp Ti comprises the alpha (α)-stage. As alloying components are added to Ti, they will in general modify the properties of each stage that is available and the β progress temperature [Halevy et al., 2010].

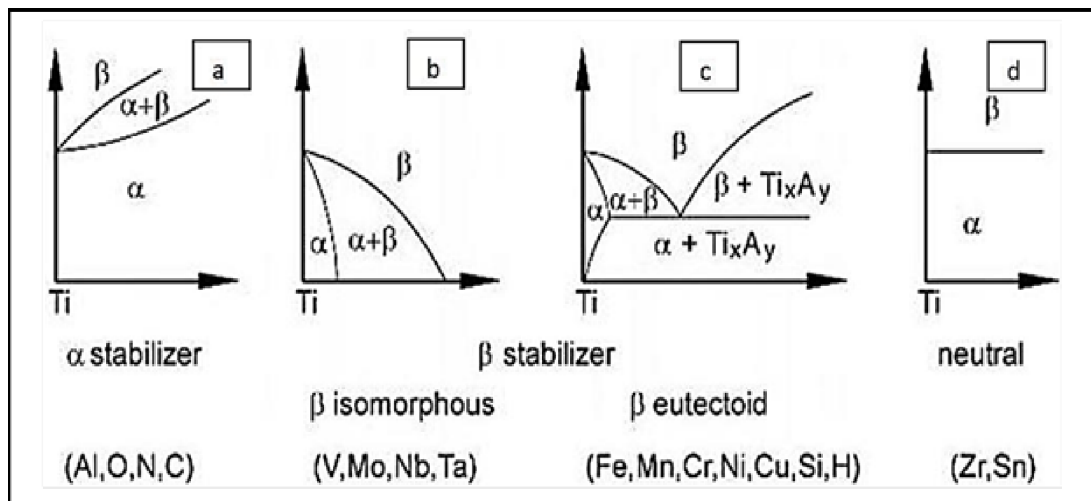


Figure 1. 5 Displays diverse kinds of stages illustrations of Titanium.

[Ahmed et al., 2014]

1.3.8 Impartial fundamentals of Ti

Tin, zirconium, and hafnium are viewed as nonpartisan additions since they lessen the alpha/beta (α/β) change temperature just marginally and later they change temperature again at considerably higher values. Zirconium and Hafnium both demonstrate the equivalent beta to alpha allotropic stage change and are isomorphous with the two stages of Ti. The type and quantity of these alloying components in the normal stages lower the temperatures. Because of the stages, Ti combinations are grouped into four fundamental classes which are alpha, close alpha, $\alpha + \beta$, and β alloys [Of, 2017; Hecht et al., 2007].

1.3.9 Microstructure of CP Ti grade 2

A microstructure example of Cp Ti grade 2 is shown in figure 1.6. The microstructure comprises of equiaxed alpha grains with a normal grain width of 83.4 μm [Fidder et al., 2013].

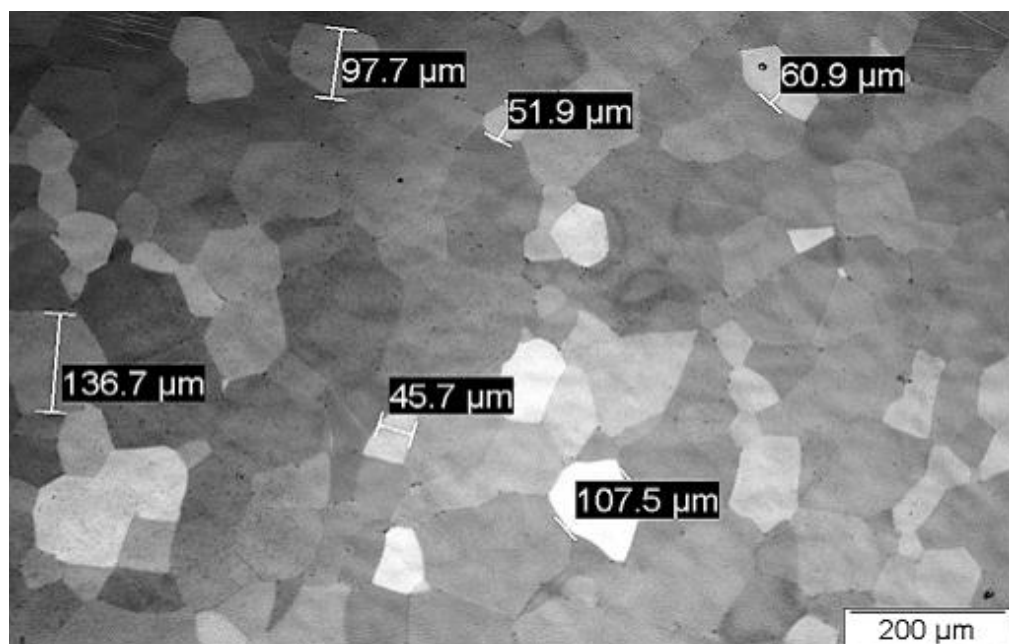


Figure 1.6 As received microstructure of commercially pure titanium grade 2. [Fidder, et al., 2013]

1.4 AIM AND OBJECTIVES

The key purpose of this research was to analyze the impact of exposing commercially pure grade 2 titanium to different constant temperatures. The aim was accomplished over these three research objectives:

- To compare the tensile properties of the heat-treated specimens against the untreated specimens;
- To compare the microstructures of the specimens which are heat-treated against the untreated specimens; and
- Analyze the hardness of the treated specimens against the untreated specimens.

1.5 THESIS OVERVIEW

Chapter 1: Presents the problem statement, background , and the detailed summary on titanium and its alloys.

Chapter 2: Detailed literature review that is related to this study.

Chapter 3: Presents the experimental setup and experimental performance.

Chapter 4: The examination and discussion of the results are presented in this chapter.

Chapter 5: Conclusion on accumulated results from this research and recommendations for future work.

CHAPTER 2: LITERATURE REVIEW

From the literature, studies were done to understand the mechanical properties of titanium. This literature review aimed to study and report findings by previous researchers about the analysis of titanium and its alloy materials. This clarified known facts about the topic and also assisted in what is unknown about the topic. The focus of this study was on the impact of thermal treatment on the tensile properties of the material.

2.1 Heat treatment on tensile properties

Catherine et al. (2018) studied the behavior of the tensile strength and ductility of pure Ti grade 2 after heat treatment. The analysis was performed on three specimens. The first specimen was not treated (symbolized by T1) while the other two were treated using two different temperatures (symbolized by T2 and T3) with T2 being 699.9°C and T3 being 899.9°C. The two samples were kept at the previously mentioned temperature for 59.9 minutes. An elevated amount of oxidation at T3 compared with T2 was observed, due to the development of acicular martensite at the higher temperature that was larger than the beta transus temperature. The final tensile strength of the material (T2) after heat treatment was reduced and recovery of strength was observed at (T3). However, after heat treatment, all treated samples displayed a high percentage of elongation compared to the parent sample (T1). The area and pattern of the necking behavior were similar for all the samples.

Zheng et al. (2015) examined the impact on material distortion for thin foils in micro forming during heat treatment or exposure to heat. The specimens used for the analysis had dimensions of 15.9 x 4 mm. All samples were cleaned to expel significant burrs at unanticipated areas. These samples have been hardened at an isothermal condition temperature of 649.9 °C in a measured climate of argon gas. The annealing times were 19.9 minutes, 29.9 minutes, and 59.9 minutes. The average grain sizes of the annealed samples were approximately 14.69, 24.49, and 42.39 μm , for tempering periods of 9.9, 29.9, and 59.9 minutes, respectively. The findings showed that the flow stress diminishes by the increase of grain size at a similar tensile temperature and that on the inner area of the sample larger flow stresses were found compared to the surface area where fewer flow stresses were found. The increase in grain size was due to the influence of heat treatment. The surface area increased as well, but the flow stress diminished. The size of the grain increases together with the surface area, therefore, the movement stress decreased.

Kunieda. (2014) investigated the outcome of heat treatment on the mechanical properties of extreme forte titanium alloy super-TIXTM 523AFM. The primary emphasis was:

- On the principal materials required for appropriate control of a wide scope of mechanical properties of a high quality β rich $\alpha+\beta$ type titanium composite,
- The impacts on the state of heat treatment on the materials and,
- On the mechanical properties depending on their cooling stage.

Samples were exposed to solution treatment (ST) and aging (A). Solution treatment was performed at 849.9, 899.9, and 929.9°C all in the $\alpha+\beta$ high-temperature range up to 60 minutes pursued by Air-Cooling (AC) and water quenching (WQ). Aging treatment was done at 499.9 and 549.9°C for 240 minutes pursued by air-cooling. Results showed that the S-S bends on the samples that were solution treated and air-cooled did not vary the same as at the solution treatment temperature. The S-S bends were fundamentally the same as those of typical $\alpha+\beta$ type titanium alloys. Aging the samples at 849.9°C with water quenching demonstrated that the S-S bend is fundamentally the same as those of the solution treatment with air-cooling. The 899.9°C and 929.9°C solution treatments followed by water quenching and the samples displayed two phases of work hardening. Both the 849.9°C solution treatment and AC procedures resulted in an extension of the samples between (16% to 23%). The samples exposed to the 899.9°C and 929.9°C solution treatments followed by air-cooling demonstrated a low evidence pressure, and their elasticity was high.

Seshacharyulu et al. (2000) investigated hot deformation and the microstructural damage mechanisms of extra-low interstitial (ELI) grade Ti-6Al-4V. The temperature profile was measured through the use of a thermocouple. A furnace was utilized to surround the plate samples. Compression testing was performed on the samples which were exposed to the temperature range of 749.9 to 1099.9 °C at temperature increments of 49.9 °C. Results showed that the bends displayed consistent stream relaxing conduct at lower strain rates while the movement was seen at extreme strain rates and this was illustrative of the material reaction in the $\alpha - \beta$ stage field. The pressure strain bends in the β stage field showed that the material displayed an enduring state stream.

Palumbo et al. (2012) did an exploratory study on the single point gradual framing of a titanium alloy part by combining static warming with high apparatus pivot speed. Their focus was on the solitary point incremental forming (SPIF) procedure of a scaled vehicle door shell made by a titanium combination (Ti6Al4V). SPIF analysis was done

assuming turning speeds between 799.9–1599.9 rpm, while concurrently varying the pitch values in the series between 0.49–0.99 mm. The impact of a temperature increment due to electric static warming and instrument turn speed was examined. The blend of the two approaches was utilized (warming both groups and extreme device pivot speed). The equipment utilized for the experiment was CNC machining, where the pyrometer was placed to persistently monitor the temperature advancement in the focal region of the blank during SPIF examinations. Heated samples were appropriately thermally segregated from the outer conditions. That was done utilizing high fibrous insulation sheets made from polycrystalline alumina fiber and extraordinary inorganic strand covers, though the top section was detached from the support utilizing a marble ring component. Samples acquired from SPIF tests were studied utilizing the digital image correlation (DIC) framework. From the examination of tests completed utilizing speed of 799.9 RPM, it was conceivable to take note that the parameter inadequately influenced the clear twisting. Strain values along the studied profile presented insignificant contrasts when the estimation of parameter variations from 0.49 mm to 0.99 mm was considered. The analysis portrayed by turning speeds of $S = 799.9$ rpm, $S = 1199.9$ rpm, and $S = 1599.9$ rpm gave significant data about the prevalent impact of the turn parameter of the specific equipment. The real strains pursue a similar pattern as that of the temperature, being described by most extreme qualities expanding persistently as indicated by rotational speed.

Kumar et al. (2014) investigated the impact on the tensile behavior of Ti-6Al-4V alloy at high-temperature conditions. The impact of temperature on the elastic conduct of Ti-6Al-4V was assessed over the temperature range from 25 to 500 °C at a consistent strain pace of 10^{-3} s⁻¹. During the analysis, the treatment arrangement was at 950 °C for 60 minutes in an argon environment, trailed by air-conditioning at ambient temperature. It was noted that the yield quality (0.2% counterbalance) seamlessly diminished from 906.9 to 484.9 MPa at room temperature to 499.9 °C. Between room temperature and 499.9 °C, uniform and all outstretching were affected by the temperature. There was an absolute increase of elongation on the samples at 499.9 °C. It was noted that the strength of the samples diminished with temperature increase. The quality coefficient constantly expanded with an increment in temperature.

Moletsane et al. (2016) investigated the tensile properties of direct metal laser-sintered (DMSL) Ti6Al4V (ELI) alloy. In experimenting, the as-received (AR) and stress-relieved (SR) level samples had been verified for the analysis of the features of yield stress, ultimate stress, young's modulus, elongation, and area reduction. The pre-stained SR samples were scanned to verify porosity. The blocks were scanned using

a zig-zag scan procedure, towards and after manufacturing. The chemical composition of both substrate and the powder materials were considered before use. Out of the two series, rectangular shaped bars were cut from the substrate of the first one. This didn't completely eliminate the specimens from the substrate and this led to a heat-treatment in an argon atmosphere at 649.50°C for 180 minutes for stress-relieving purposes. Part of the findings was that when compared to annealed Ti6Al4V (ELI) samples both AS and SR specimens have the maximum tensile stress and higher yield stress. The variances in the mechanical properties of the horizontal samples for all categories remained low, and there wasn't much difference in their coefficients.

Aliprandi et al (2019) investigated the tensile and creep property development of Ti-6Al-4V alloy samples formed through the additive manufacturing of electron beam powder bed fusion. The procedure started by warming the start plate prior to adding the initial layer of powder and the temperature used was determined by the type of powder and the quantity. The first layer of the powder was pre-warmed through strong, and the very fast electronic beam passes that had no additives. After the initial layer had melted, the base was reduced by the size of a single layer to survive the addition of more powder layers and processing. The arrangement recurred until the entire component was formed. The study discovered that the variation in tensile strength varied by as much as fifteen percent for ductility and seven percent for yield strength and ultimate strength. It was also observed that with the increase of testing temperature, ductility also increased reaching a value equal to thirty percent at a temperature of 800 °C, although mechanical strength was decreased with the temperature increase. The smoothed samples demonstrated better mechanical strength and better yielding than the AR samples. In both cases, the yield strength grades were about 90% percent of the maximum strength.

Balasubrahmanyam et al (2002) did a study on the change of form of beta titanium alloy Ti-10V-4.5Fe-1.5Al in a very hot upset forging. In experimenting, tensile samples used were 5 mm thick and had a gauge length of 10mm. The initial breakdown of the as-received β zone was around 899.9 °C then followed by hot rolling in the $\alpha + \beta$ zone at approximately 649.9 °C. The samples were heated at 764.9 °C for 0.5 hours and water quenched. Hot compression analysis was done on the samples at a temperature ranging between 649.9–899.9 °C and a strain rate ranging between 0.001 to 100 s⁻¹. Balasubrahmanyam et al (2002) had also alluded that samples had been flattened to their semi-height and that, the information on the load–stroke had been documented. Subsequently, these samples had been cooled in air and arranged parallel to the solidity axis. The tensile analysis was carried out in the temperature range between

749.9–899.9 °C, at intervals of 50 °C. Highlights of the study are the accurate stress and correct plastic strain curves at 649.9 and 849.9 °C were obtained for various stress degrees, and these show the typical behavior below and exceeding the transus temperature (749.9 °C). Moreover, the curves at 649.9 °C display continuous flow softening at strain degrees above 0.1 s⁻¹ while at lower strain degrees, the streamflow stress causes a stable state at big strains. At 849.9 °C, there is varied ultimate flow stress in the initial zone of distortion tailed through a stable state at higher stress. The peak stress increased with strain rate and reductions with temperature. It was also noted that the percentage elongation increased between 150% at 700 °C, 275 % at 850 °C and the ultimate effectiveness was 48%.

2.2 Heat treatment on microstructure

This subsection presents the previous work in quantifying the impact of thermal treatment on the microstructure of different materials.

Pinke et al. (2014), explored the impact of heat treatment on the mechanical properties of casted Ti6Al4V Ti alloy. Solution treatments at 1049.9 °C, 949.9 °C, and 799.9 °C pursued by water and air-cooling, and then maturation treatment at 549.9 °C was performed. The arrangement treatment at temperatures of 1049.9 °C and 949.9 °C, trailed by water cooling led to the development of α martensite. Under different instances of treatment, a lamellar structure of $\alpha + \beta$ stages was shaped. The results showed that the microstructure of the cast Ti6Al4V model composite indicated a microstructure comprising of α and β strong arrangements. The α stage demonstrated a lamellar structure which is moderately standard and between these lamellae are slight zones of the β stage. Also, the microstructure caused by the distinctive applied solution treatment and water-cooling from 1049.9 °C prompted a circular α' martensite structure. Arrangement treatment at 1049.9 °C pursued by air-cooling prompted the more common lamellar $\alpha + \beta$ structure with grain limit α in the earlier β grains. The metallographic examination demonstrated that no α' martensite stage was shaped after the treatment at 799.9 °C. The grain limit α stage was available in the structure after arrangement treatment at 799.9 oC after both water and air-cooling.

Najdahmadi et al. (2014) have investigated changes in the mechanical properties of titanium–29 niobium–13 tantaium–4.6 zirconium (Ti-29Nb-13Ta-4.6Zr) compounds through heat treatment. The focus was on the microstructural advancement and mechanical property improvement on another titanium built titanium–niobium–tantaium–zirconium mixture by applying an appropriate heat treatment technique. The

titanium–niobium–tantalum–zirconium alloy was exposed to arrangement treatment and cooling methodology through various techniques involving liquid N (nitrogen), H₂O (water), O (oil), static air, and a furnace heater. The as-manufactured solid was exposed to solution treatment at 844.9 °C, which exceeds the β transus temperature for about 44.9 minutes to remove the homogeneities within the alloying components specifically tantalum and zirconium. Arrangement treatment was completed by an immediate drive oiled fixed dissemination vacuum siphon under a vacuum pressure of 1×10^{-5} megabar. After this, a quick water quenching (WQ), oil quenching (OQ), liquid nitrogen quenching (NQ), static air-cooling (SAC), and homogenous furnace cooling (FC) followed. It was found that the microstructural qualities were altogether influenced by the cooling strategy. The heat-treated samples contained equiaxed beta grains, all samples quenched in the liquid nitrogen produced the smaller grain sizes, and the samples cooled in the heater produced the larger grain sizes. This was identified in the grain development impact of the cooling technique.

Warchomic. (2010) did an investigation on the annealing treatment of the Ti6Al4V alloy underneath the β transus temperature pursued through various chilling degrees conveyed to hot, twisted samples in the $\alpha + \beta$ field. All the prepared samples were heat-treated, this aided with studying of the microstructure evolution exposed to the non-factual parameters. Treatment was done in all eight prepared samples through the furnace oven. The heat treatment happened in the $\alpha + \beta$ range at the temperatures of 929.9, 949.9, and 969.9°C for 29.9 minutes then trailed by oil and air-cooling. After the analysis of metallurgy, ageing had been done at 719.9°C for 120 minutes, trailed by air-cooling. The results showed that the mature specimen's microstructure is more dependent on the cooling temperature. In oil cooled tests, α martensite changes into α needles and β stage as a result of the spreading of vanadium. The α martensite was supersaturated in β stabilizers vanadium during the tempering in $\alpha + \beta$ field. The impact of the stress on the microstructure of alpha needles was not observed in such conditions.

Lario et al. (2018) studied the impact of heat behavior from UV X-ray radiation for the wettability of the Titanium₃₅Nb₁₀Ta tubular molecules. The study concentrated on analyzing the impact of certain factors (voltage, heat treatment, and brightness illumination) on the wettability execution of a titanium compound. Beta titanium compound with ostensible composition Ti₃₅Nb₁₀Ta was set up by a powder metallurgy procedure by mixing natural powder. The ternary titanium compound was warmed in a vacuum sintering heater to 799.6 °C at 15 °C/min and was held at that temperature for 0.5 hours, and was finally heated to 1349.9 °C at an increment of 9.9 °C/min and was

held for 3 hours and cooled at increments of 10 °C/min. The microstructure demonstrated an organized heterogeneous stage, which consisted overwhelmingly of β equiaxial grain with a remaining $\alpha + \beta$ stage because of poor diffusion during the sintering procedure. The $\alpha + \beta$ regions with the lower substance of obstinate components exhibited high chemical heterogeneity.

Paulina et al. (2017) studied the results of heat-treated Ti6Al4V Alloy on the fibroblastic cell response. Samples of Ti6Al4V800 and Ti6Al4V1050 were both heat-treated and this was accomplished under and exceeding Ti6Al4V beta-stage transformation temperature. These titanium alloy samples were seeded with fibroblast cells and submerged for seven days in the cell culture at 36.9 °C with a pH of 7.40, 5% CO₂, and 100% relative moisture content. Analysis of the results indicated that the parent material showed beta-stage equiaxed grains scattered in the alpha-stage lattice. In the Ti6Al4V800, the alpha-stage acted as an obstruction, as it thickened and this had prevented the quick expansion of the smaller size of the beta-stage. A mixture of a widmanstätten or lamellar-like microstructure experimented in Ti6Al4V1050, whereby, both alpha and beta-stages were spread on the entire surface. The β stage endured the heat treatment at 1049.9 °C, this was proven by the stability of the compound.

Dgurlwvhy et al. (2016) studied the precipitation process during heating and aging of the β -metastable stage in the close β Ti-5553 compound. Heat treatment was first completed at room temperature, which permitted controlled warming rates to 10°C/s. The sample temperature was estimated to utilize an S thermocouple spot-welded surface. The electrical resistivity variation of the samples was recorded during the heat treatment. Thermal heat treatment was done on the samples above the β transus temperature of 889.9 °C for 29.9 minutes before exposure to rapid cooling at room temperature. The microstructure results indicated that depending upon the heating rate, the alpha (α) grains presented a huge contrast in size and morphology. The lower the heating rate the better the microstructure. Utilizing a heating increment of 0.14°C/s, exceptionally small semi equiaxed grains were obtained circulated homogeneously in the grain. Precipitation along grain limits of the parent beta (β) stage was observed as well, encompassed by a free zone.

Khan. (2008) did a study on the effect of the quenching medium on the wear behavior of a Ti-6Al-4V alloy. The study focus was to heat the Ti-6Al-4V alloy samples over and under the β transus temperature and to vary the surface wear bearing of the samples when quenched by either oil, water, and liquid nitrogen. Each sample was prepared from a copied Ti-6Al-4V plate, with sizes 20mm x 10mm x 10mm. The

solution treatment at 749.9 °C and at 999.99 °C was collated and the results of a combination of water with oil and liquid nitrogen for quenching were examined. After the quenching action, a typical $\alpha+\beta$ zone structure was noticeable in both samples as the results showed that there's no major variation in the microstructure of the samples. The treatment at 749.9 °C for 29.9 minutes was far below the β -transus temperature and in the alpha (α) zone; hence, change in α zone was not projected in the quenching process. During the solution-treatment at 999.9 °C (above the β -transus 979.9 °C) for 29.9 minutes, followed by quenching in liquid nitrogen, water, and/or oil, a clear variation in microstructure was found.

Luo et al. (2015) studied the effect of the alpha grain size on the distortion behavior in isothermal solidity of Ti–6Al–4V alloy. A round bar of Ti–6Al–4V that is 3 cm in diameter was utilized. To find four diverse alpha grain sizes, heat treatments were used through the heating procedures at 929.9 °C for 120 minutes, 840 minutes, 2160 minutes, and 3600 minutes respectively and furnace-cooling at room temperature was done after the process. Also, heat treatment was done at 599.99 °C for 120 minutes, and then air-cooling at room temperature. Furthermore, four specimens with dissimilar α ounce sizes were heated at 859.9 °C, 889.9 °C, 919.9 °C, and 959.9 °C, and soaked for 5 minutes. The results showed that at 859.9 °C the flow curves nearly coincided and the curves were within a few percent of each other. It was also noted that at 919.9 °C, the flow stress values tended to show a minor reduction with increasing alpha grain size; and the variation was approximately 5 to 12 %. At greater strain rates, the flow strain rates decreased with the growth of alpha grain size. The flow strain rate significantly reduced during the decrease of the growth of alpha grain size at a smaller strain rate.

Milner et al. (2013) studied the grain refinement and mechanical properties of Cp-Ti treated by hot accumulative roll bonding. The main focus was to study the accumulative roll bonding (ARB), as the serious plastic distortion method, had been utilized to produce commercially pure titanium (Cp-Ti) at 450 °C. The commercially pure titanium parent samples were prepared from 0.5mm thickness sheets, under an annealed state. A variation of hot accumulative roll bonding tests was done. The bonding surface for all sheets was wire brushed and degreased with acetone in order to certify a correct bonding amid the sample layers prior to being loaded and held with Cp-Ti wire around the corners of the specimen. The accumulative roll bonding procedure was performed on a two-high roll mill with a 20 cm roll diameter. Before the roll-bonding, the accumulative roll bonding samples were pre-heated to 450 °C for 5 minutes to ensure a constant temperature throughout the procedure and also increase the workability of the samples and the bonding in-between the layers. The results obtained showed the

impact of hot ARB on the microstructural development of Cp –Ti. The samples submitted to two cycles showed a structure comprising of mainly lamellar grains extended in the rolling direction. About seven percent of the sample was almost equal to the grains. The equiaxed grains were engaged as grains with an aspect ratio of less than 1.5, as determined utilizing the grain span and thickness along the rolling direction and normal direction, correspondingly.

2.3 Heat treatment on micro hardness

Abdalla et al. (2017) did a study on the effect of heat treatment parameters on the microstructure and microhardness of Ti-6Al-4V Alloy. The main focus of the study was on the impact of altering the heat treatment parameters on the microstructure and microhardness of Ti-6Al-4V alloy to describe the behavior of the alloys based on mechanical property relations. Samples were prepared from a 0.2 cm rod of Cp Ti-6Al-4V. Three different types of heat treatment were carried out in the samples. The first treatment was recrystallization annealing (RA) grouped as T1, heat-treated at 925 °C for 240 minutes, and air-cooled. The second treatment was solution treatment and aging (STA) grouped as T2 treated at 900 °C for 60 minutes trailed by air-cooling, then again followed by re-heating at 600 °C for 240 minutes and air-cooled again. Last was the β -Annealing (BA) grouped as T3 heat-treated at 100 °C for 60 minutes then air-cooled and after the completion of heat treatment, all treated samples were compared with the parent sample represented as T0. The results showed the group of T0 and T1 having fine and coarse equiaxed microstructures, also a marginal difference between their microhardness was also noticed. There was a major increase in microhardness values of the lamellar microstructure related to equiaxed structure.

Kang et al. (2019) studied the influence of heat treatment on the microstructure and hardness of the SLMed TC4 alloy samples. Samples were prepared and heat-treated in a shaft furnace. There were two diverse heat treatments conducted on these samples, annealing at 799.9°C, 969.9°C, 999.9°C, and 1099.9°C and cooled inside the furnace, thereafter, solution treatment at 939.9°C followed by water quenching and then aging at variance temperature stages of 449.9 °C, 499.9 °C and 649.9 °C. The microhardness results showed all heat-treated samples displayed a larger micro rigidity than the fabricated state. The increase in the microhardness of these samples was influenced by annealing. The increase in annealing temperature, the greater the microhardness results obtained. The rigidity had been related to the rate and scope of α and β zones.

A study by Martino et al. (2016) on the impact on hardness and mechanical properties by heat treatment of medium carbon steel was investigated. The rigidity and microstructure properties of the medium carbon steel had been treated at numerous heat treatment arrangements. Three types of heat-treatment procedures were conducted, namely; annealing, quenching, and tempering. During the tempering procedure, the samples were heated to 899.9 °C over a period of 60 minutes in the oven. The samples were then quenched in the water. The treatment was trailed by tempering, which was performed at 299.9 °C, 449.9 °C, and 599.9 °C with a heating time of 120 minutes for every temperature. After the heat treatment procedure was complete, Rockwell hardness tests were performed. The results showed that the hardness of medium carbon steel after quenching in water was higher than the quenched samples at room temperature.

Semiatin et al. (2003) studied hardness development in the alpha-beta heat treatment of Ti-6Al-4V. The heat treatment comprised of heating and soaking at a pinnacle temperature of $T_p = 954.9$ °C, trailed by controlled preservation at a fixed increment of 11 °C/min, 41.9 °C/min, and 194 °C/min. Lastly, water quenching was performed. After heat-treatment metallography and measurable picture scrutiny were used to indicate the volume fraction of essential alpha phase present and the nucleation area as well as the shape development of the alpha fraction during cooling. The hardness results showed proof of the development of the essential alpha phase during cooling.

The impacts of heat treatment and aging on hardness and microstructural composition of the α and β stage in Ti-6Al-4V wire were investigated [Zeng et al.,2005]. In experimenting, wire samples were firstly cold worked by extrusion, then heat-treated in the $\alpha + \beta$ stage field, water quenched, and after that aged. After solution treatment and quenching, an optional fiber with the basal plane normal lined up with the wire pivot design to the underlying surface, demonstrated that a definite variation happened during quenching. The treatment of samples from the center of the coil was at 919.9 °C trailed by a quenching stage in room temperature water. Aging treatment was done in an oven at 499.9 °C. The results showed the crystal structures of α and β stages were comparative and they fall into various crystallographic classifications. The microstructural investigation demonstrated that α martensitic plates were shaped after heat treatment and quenching of α and β . However, after aging, α and β changed back to the β stage.

Nady et al. (2017) investigated the influence of heat treatment on the mechanical properties of Ti-6Al-4V. The study focused on several heat treatments that were

completed below and above the beta-change temperature of the Ti-6Al-4V composite trailed by aging at 549.9 °C for 6 hours. The experimental setup was achieved by placing 8 mm flat bar titanium alloy specimens in a 499.9 kg vacuum heater, trailed by forging and machining. The heat treatment utilized differential examining calorimetry (DSC) in argon gas at the β -transus temperature. The heat treatment temperatures were chosen based on the DSC estimations. The results of the solution treated samples displayed an increase in the hardness in the acicular martensite in the β -stage. The widmanstatten microstructure of the air-cooled samples also displayed the same hardness to some extent. The annealed samples also displayed an improvement in rigidity; however, the aged samples didn't show any noteworthy alteration.

Adabo et al. (2006) studied the impact of heat treatment on the hardness of CP titanium and Ti-6Al-4V. The CP titanium and Ti-6Al-4V alloy samples were randomly set into 3 groups and received heat treatment, annealing, and aging. The first heat treatment was at 749.9 °C for 120 minutes, and the second treatment was annealing at 954.9 °C for 60 minutes and aging at 619.9 °C for 120 minutes. After heat treatment, the samples were entrenched in acrylic resin, and their surface was ground and cleaned, and rigidity was measured. The analysis of the results showed that the CP Ti Vicker's hardness for the T2 grouping was fundamentally higher than those of the different groupings. There was not much difference in Vicker's hardness of the control and T1 grouping.

Morita et al. (2005) investigated the effect of short-time duplex heat treatment on the mechanical properties of the Ti-6Al-4V alloy. Samples were heat-treated at 1203 K for 60 seconds and water-quenched, and then aged at 752.9–952.9 K for 40 seconds for the purpose of the solution. After the heat treatment, the tested segments were thoroughly cleaned with emery papers and alumina powders. The surface oxide layer that formed during the heat treatment was eliminated by the cleaning. The results showed that the hardness was fundamentally improved by the short-time duplex treatment. It was believed that this improvement of hardness was mostly due to the quenching. The results of aging for only 40 seconds showed that the rigidity was better than the value at the short-time duplex conditioning aside from the aging at 952.9 K. The time expected to arrive at the optimum rigidity had been reduced by an increase in the aging temperature which decreased the hardness started before. In cases of aging at 952.9 K, the hardness constantly declined from 40 seconds.

Ke et al. (2017) studied the effect of a salt bath of Cp titanium grade 2 and Ti-6AL-4V grade 5. The main focus of the study was on investigating galling by linking the morphology of the nitride case molded in commercially pure grade 2 titanium and the

nitride formations formed in the titanium Ti6Al4V alloy through the nitride salt bath. Samples were cut into sizes of 4cm x 2.5cm x 0.5cm and all the ends of the material were cleaned and polished to remove impurities on the sample surface. The prepared samples were then loaded into the nitride chamber. The machine utilized for the analysis was an enclosed chamber of a salt. Inside the chamber, salts of ammonia or cyanide were introduced before the nitride procedure. The samples were then placed on a fixture, which was positioned inside the molten salt bath comprising the nitride salts. During the procedure, single samples were not to be in contact with each other. The general procedure temperature was kept between 559.9 and 579.9 °C for a duration of 24 hours. The results showed that the regular value of the rigidity increased significantly in liquid nitride samples of cp grade 2 titanium and the grade 5 titanium alloy. The pre-hardening of these titanium grades enhanced the hardness values to a clear grade and water quenching after the nitride in salt bath furnace improved the hardness of the material. Following the same procedure again on grade 5, hardness and roughness were achieved at the material surface texture.

Kim et al. (2009) studied surface hardening treatment for titanium materials utilizing Ar-5 % CO gas in combination with post-heat treatment under vacuum. The study focused on the two steps of surface hardening using Ar-5 % CO gas for a short time period which was followed by heat treatment under vacuum. The experiments were done on a titanium plate with a thickness of 0.4 cm, and it was cold-rolled to a thickness of 0.2 cm to make samples that were 1 cm x 1 cm x 0.2 cm. The samples of SP-700 and Ti-15-53 alloys had been exposed to recrystallization annealing and solution treatment at 1073 K for 120 minutes and 15 minutes, correspondingly, followed by air-cooling. The cp titanium samples were then exposed to the surface hardening treatment without prior annealing. The samples were then wet-polished using emery papers and were also buff-polished utilizing alumina powder, and cleansed by acetone. Moreover, the acid-pickled procedure was followed prior to surface hardening treatment and the surface was cleaned ultrasonically in ethanol. The results showed that the maximum surface hardness improved from 419.9 to 829.9 in hardness with an increased heating period from 30 minutes to 360 minutes; also, an increase in the hardening layer thickness from 30 μm to 100 μm was observed. The results also showed that the maximum surface rigidity and the toughening layer thickness improved in the heating period.

Ka et al. (2005) studied the hardness variation of α and β pure titanium with different grain sizes. Commercial pure grade 2 titanium round bar, 1.6 cm in diameter and 10 cm in length, was used for this investigation. The parent material of pure titanium was

heat-treated to attain α and β titanium. The α titanium samples were exposed to heat treatment at 749.9 °C in a furnace at different time periods, ranging between 60 minutes to 14400 minutes, and was trailed by quenching in a 24.9°C water bath. Similarly, the β titanium samples were exposed to heat treatment at 999.9 °C ranging between 60 minutes to 1440 minutes and quenched in water. The outcomes displayed that the rigidity of α titanium samples declined sharply and then gradually with the increase in heating time at 749.9 °C. It was also noticed that the α titanium samples with larger grain sizes had a low hardness compared to the samples with small grain size. Conflicting to the hardness of α titanium samples, the hardness of the β titanium samples increased with an increasing heating period at 999.9 °C. Though grain sizes of β titanium samples were much larger than those of the α titanium sample, the hardness of β titanium samples remained much higher than that of α titanium samples.

2.4 Heat treatment on Scanning Electron Microscope (SEM)

Singh et al. (2019) have investigated the effect of heat treatment on the mechanical properties and the fracture behavior of Ti-6Al-4V alloy produced by powder compact extrusion. The study focused on the development of a connection between fracturing, microstructure, and formed properties of the analyzed samples. The blended powder mixture was heated at 219.9 °C in a 55.9 mm diameter of heat-treated steel die below a weight of 312.9 MPa for about 8 minutes holding time in order to reach a relative powder compaction density of 79.9 % or beyond. Before heat pressed sintering was done to the compacts at 1325 °C in a furnace at a heating increment of 10 °C /min. The fracture surface and crack propagation of all treated and tested samples had been analyzed, following the heat treatment. The fracture surface for both β annealed and aged treatments were very coarse with shiny surfaces and small shear lips, while around the edges large shear lips and smooth fracture surfaces on treated samples were constant. Rough and frequent crack shapes were found on the first half of the fracture profile, but after reaching the middle of the sample, the crack propagation mechanism changed on the annealed and aged sample.

Srivatsan et al. (2010) studied the tensile deformation and fracture behavior of commercially pure titanium and titanium alloys. The specimens of Cp titanium and the Ti-6Al-4V alloy had been set on parallel and slanting directions. A scanning electron microscope (SEM) was conducted on the tensile neck area, after doing a tensile test on the set samples. The SEM outcomes displayed the morphology appearing to be coarse and layered. Fine microscopic cracks linked with population dimples of diverse shapes and sizes, covering a transgranular fracture surface were also shown. Also,

high magnification, the population of fine microscopic voids, and shallow dimples were displayed covering the region of tensile overload.

An investigation on the impact of heat treatment on the surface fracture of explosively welded commercially pure titanium grade 1 with carbon steel plates was conducted [Wachowski et al., 2017]. The plates were welded and joined and samples were cut in the direction parallel to the joining surface. The heat treatment was conducted on the samples at a temperature of 599.9 °C for 90 minutes then trailed by cooling in the furnace to 299.9 °C, and then cooled in the air to room temperature. The morphology results showed the fracture surface of the titanium plate being exposed to fatigue under a bending moment before and after heat treatment. There were also noticeable cracks identified on the surface and stable crack growth and unstable cracking with dislocation slips and accompanied by twinning.

Filip et al. (2003) did a study on the impact of microstructure on the mechanical properties of two-phase titanium alloys. The study focused on the mechanical properties of two-phase $\alpha+\beta$ titanium alloys after numerous heat-treatments. Ti-6Al-4V and Ti-6Al-2Mo-2Cr samples were used in the study. The samples were vacuum melted and rolled in the $\alpha+\beta \rightarrow \beta$ heating region to achieve the fine grains and equal microstructure. The prepared samples were also treated in a furnace at a temperature of 1054.9 K for 60 and 120 minutes, thereafter, oil quenched for 1.5 h followed by water preservation and aging at a temperature of 622.9, 722.9 K for 300 minutes and 1200 minutes. Toughness fracture bending tests were conducted on the samples according to ASTM E 399 standards. Results displayed an improvement in the fracture toughness and an increase in the amount of lamellar α stage. Moreover, there was an obvious variance in orientation crack development on the colonies of the α -phase lamella. The borders between colonies displayed crack direction changes and this caused branching and secondary crack formation.

Giudice et al (2019) investigated the tensile property development of Ti-6Al-4V alloy samples formed by electron beam additive powder bed fusion manufacturing. The heating procedure of the start plate began prior to the deposition of the initial powder layer, at a temperature selected based on the powder material. Moreover, after adding each layer, the powder bed was then pre-heated through a non-concentrated, high-power, and high-speed electronic beam. The initial base was halved in order to allow the deposition of another layer. The procedure was repeated until the component was completely formed. The samples were scanned on the electron microscope in order to analyze the surface fractures. The results on morphology measured yield strength

together with ductility depending on the alpha (α) lath thickness. The yield strength and ductility both decreased when morphology increased.

Huang et al. (2014) did an investigation on the impact of microstructures on the notch tensile fracture feature of heat-treated Ti-6Al-6V-2Sn alloy. Samples were prepared from a 4 mm thick titanium alloy sheet. Samples were correspondingly solution treated at 964.9 °C and 899.9 °C trailed by water quenching and aged at precise temperatures of 481.9 °C, 592.9 °C, and 703.9 °C. After performing the heat treatment, scanning electron microstructure analysis was done to determine the fracture surfaces. There were various findings; there was a specific zone of both slant fractures also known as shear lips and a wide flat fracture zone on the surface. The appearance of the fracture showed a yielding dimple fracture for all samples.

Albiter et al. (2000) did an investigation on the microstructure and heat-treatment response of Al-2024: Ti/C composites. The samples of Al-2024 and Ti/C composites were formed by pressureless melt infiltration of a 2024-aluminum alloy into TiC. After the process, all samples had been treated for a solution at 529.9 °C for about 150 minutes and then trailed by cold water quenching. Aging was done at 189.9 °C for 720 minutes in an argon environment. The outcomes of the as-fabricated Al-2024: Ti/C showed trans granular fractures on the exterior during the intermetallic CuAl₂ stage. Construction of the fracture advocated that in regions of the matrix the CuAl₂ enriched rapidly rich, as the process took place before the damage spread.

2.5 Chapter Summary

The literature study focussed on comparable investigations of heat treatment on titanium. Most of the attention has been on the treatment of titanium alloy $\alpha+\beta$ and β phases. It was additionally seen that the basic mechanical properties examined incorporated the tensile testing, microstructure analysis, and microhardness testing. It was also noticeable that the selection of the material for these studies was done on round bar material. The chapter also reviewed relevant literature on using a 3 mm commercially pure titanium grade 2 plate as a post preparation strategy of heat-treatment. The mechanical properties of the heated commercially pure titanium grade 2 are studied and associated with untreated material. The following chapter focuses on the assessment and performance of the grade 2 plate.

CHAPTER 3: EXPERIMENTAL SETUP AND PERFORMANCE

This chapter presents the laboratory evaluation conducted on the commercially pure titanium grade 2 samples. A full and thorough explanation of the equipment used for testing and the test measures that were employed in this research is also presented. The experimental and analysis preparation process is also given with details.

3.1 LIST OF EQUIPMENT USED DURING HEAT-TREATMENT

The following is the list of equipment used in conducting heat treatment of Cp Ti grade 2:

- Vulcan Furnace 3-1750 (120V 50/60Hz) Oven;
- Digital thermometer; and
- Stopwatch.

3.2 EQUIPMENT DESCRIPTION

3.2.1 Vulcan Furnace Oven

The Vulcan model 3-1750 (120V 50/60Hz) is a digital, multi-stage programmable furnace see figure 3.1. It is a 3-phase numerical controllable oven with changeable temperature escalations within 1 degree, a 9 multi-phase line-ups, a grip temperature line-up, and an adjournment switch option that permits line-ups to switch time to be approximately seven (7) days.

The Vulcan 3-1750 can reach a maximum temperature of 1100 °C. It includes recital hybrid muffle technology unique to Vulcan benchtop heaters for quicker warming and cooling than full firebrick heaters. It is built with a substantial check steel bureau completed with a sturdy heated lacquer covering.

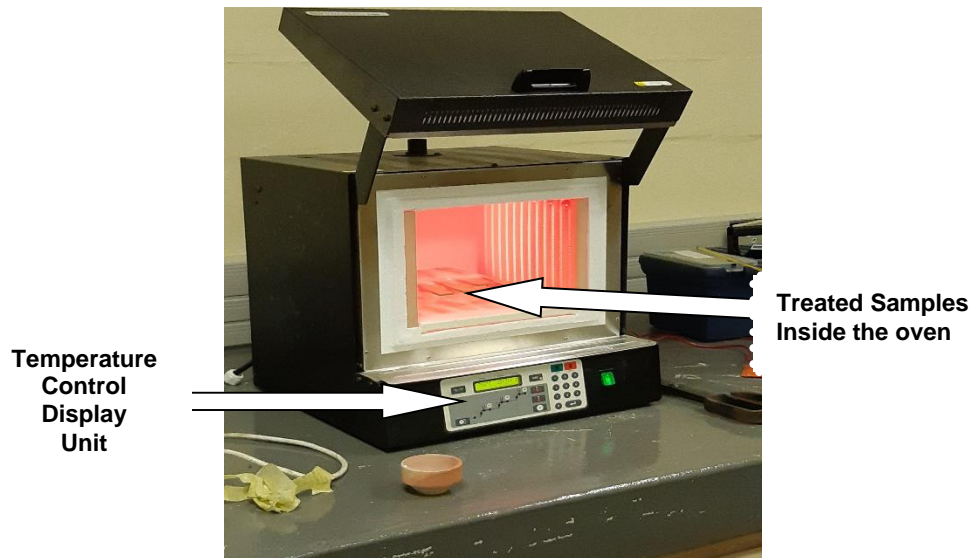


Figure 3.1: Vulcan Furnace 3 – 1750 Oven

3.2.2 Thermometer

The Thomas traceable kangaroo thermometer was used to monitor the room temperature see figure 3.2. The Thomas traceable kangaroo thermometer has a 7.5 Probe Length and can measure between -50 to 300 °C .



Figure 3.2: Thomas Traceable Kangaroo Thermometer

3.2.3 Stop watch

A Civvio stopwatch was used, Press the Start button to begin the measuring of elapsed time; then press the stop button to stop measuring elapsed time see figure 3.3.



Figure 3.3: Civvio stop watch

3.2.4 Performance of Heat Treatment

The heat treatment procedure started by inserting the prepared samples into the furnace oven at room temperature. The temperature was monitored through the Vulcan oven display (built-in digital thermometer) and another two digital thermometers that were placed outside the oven at different positions to monitor the room temperature during the process. The temperature in the slagging chamber was set and maintained at 900 °C allowing Cp titanium grade 2 to change through allotropic transformation from the hexagonal-close packed (HCP) alpha phase to the body-centered cubic (BCC) beta phase at a temperature of 882,5 °C.

Each period of heat treatment contained three tensile samples, one micro hardness sample, and one microstructure sample see figure 3.4, and judgments were done among the as-received sample and the heat-treated samples. For all heating periods, samples were placed inside the furnace at room temperature and the furnace was switched on to reach the desired temperature of 900 °C, the counting for each period would start when the temperature reaches 900 °C. After reaching the desired heating period, the furnace was then switched off, the samples were taken out of the oven immediately to allow them to cool at room temperature, and this procedure was followed for all heating periods.

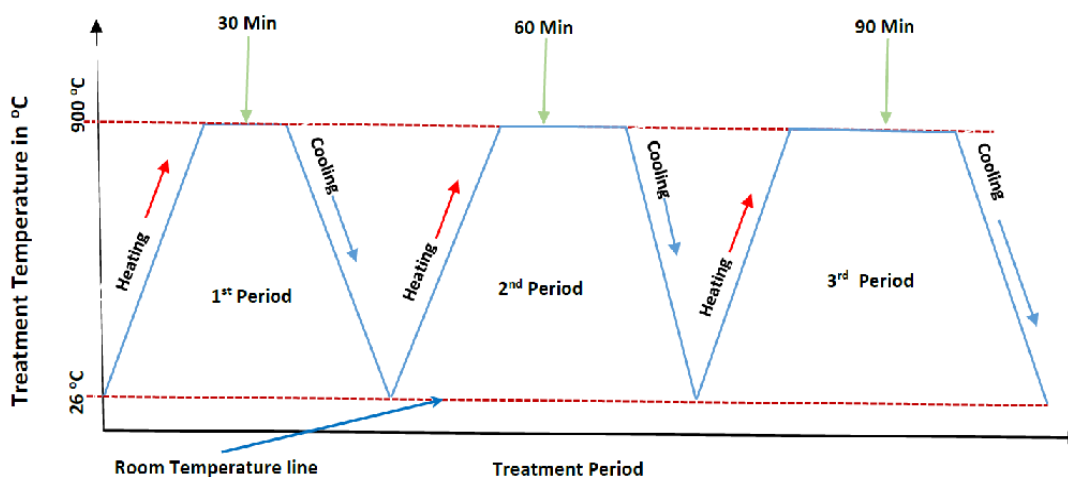


Figure 3.4: Heat Treatment process diagram

The following steps were followed during heat treatment:

First period

During the first period of 30 minutes, all samples were loaded into the oven at a room and oven temperature of 26 °C and the oven was closed. The oven was then turned on and the heating temperature was set to 900 °C. It took the oven 82 minutes to reach

900 °C and it took a total of 112 minutes to finish the heat treatment for the first period (stopwatch was used to monitor the heating period). For the cooling, after reaching the desired time for each period all samples were removed from the furnace and air-cooled at room temperature of 26 °C.

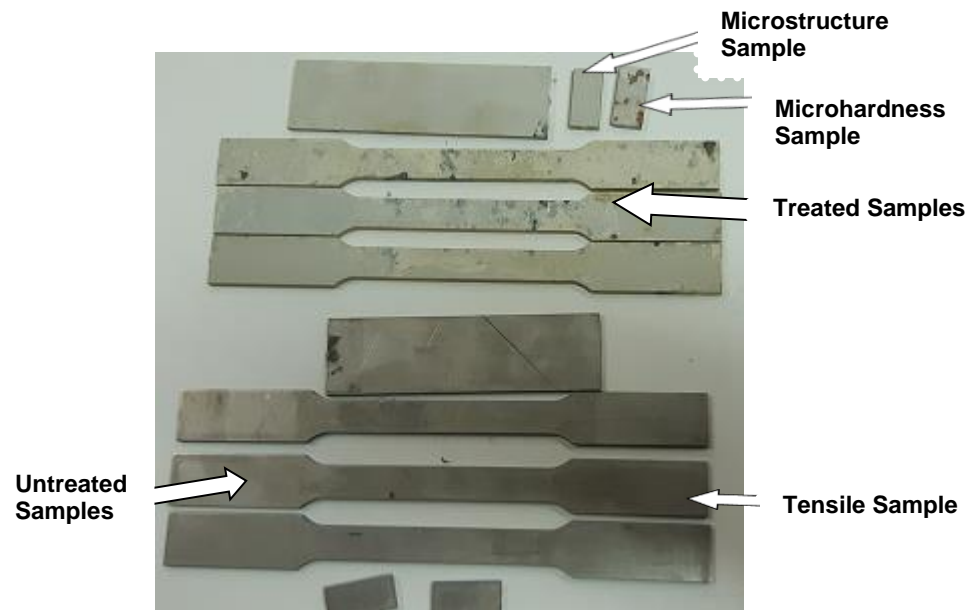


Figure 3.5: Treated and untreated samples

Second Period

For the second treatment period of 60 minutes, all the samples were loaded into the oven at room temperature of 26 °C and the oven was closed. The furnace was switched on and the heating temperature was set to 900 °C. It took the oven 82 minutes to reach 900 °C and it took a total of 142 minutes to finish the heat treatment for the second period. All samples were taken out of the oven and air-cooled at room temperature of 26 °C.

Third Period

For the third treatment period of 90 minutes, the samples were loaded into the oven at room temperature of 26 °C and the oven was closed. The furnace was switched on and the heating temperature was set to 900 °C. It took the oven 82 minutes to reach 900 °C and it took a total of 172 minutes to finish heat treatment for the third period. All samples were air-cooled at room temperature of 26 °C.

3.3 EQUIPMENT USED FOR THE ANALYSIS OF THE RESULTS

The following is the list of equipment used in conducting analyzing Cp Ti grade 2 samples:

- Motic AE2000MET inverted Microscopy coupled with Image Viewing Monitor;
- InstronTensile apparatus;
- Tescan Mira 3 Scanning Electron Microscopy
- Innova Test Falcon 500 Microhardness machine.

3.4 EQUIPMENT DESCRIPTION

3.4.1 Motic AE2000MET inverted microscope

The Motic inverted microscope is an inverted microstructural microscope that allows for the viewing of a large scale or irregular specimen that could not be fitted under an upright microscope. Microscopy enables the study of an object that is too small to see with the eye by optical amplification of lenses without degrading the light reflections from the sample, which includes the contrast between the emitted, absorbed, and reflected light [Diaspro et al., 2006].

3.4.2 Instron tensile testing machine

Tensile testing is an important material science and engineering test in which a tensile specimen is exposed to a measured force or pressure until it breaks, therefore a tensile machine is utilized to complete the testing [Systems., 2015].

The Instron equipment comprises of two grip jaws, an upper jaw, and lower jaw used for the holding and gripping the inserted specimen. The lower jaw is fixed on the Instron bed and the upper jaw moves up and down to allow stretching and compression. A computer system connected to the equipment calculates and displays the tensile data during the operation of the machine.

3.4.3 MIRA Scanning Electron Microscope

The Mira Scanning Electron Microscope (SEM) employs a concentrated beam of electrons to scan over a specimen to produce a picture or to modify the specimen surface in nano-metric resolution. The specimen picture is generated by distinguishing between secondary and backscattered electrons released from the influenced zone of the beam. The e-beam lithography is the preferred tool, where the resistant-coated specimen is selectively exposed to the electron beam, allowing the preparation of very small patterns in the resistant surface. An interferometric stage can also be used to achieve the ultimate resolution of the electron beam lithography over a large area and to join more fields together [Horak et al., 2018].

3.4.4 Microhardness Tester machine

Microhardness is widely utilized in testing of materials by utilizing small applied loads. Vickers and Knoop hardness tests are the most well know and used in microhardness testing. The exclusive force actuator system employs an electronic closed-loop system and controls and sensor to measure accurate, reliable, and repeatable, on all the forces employed during testing [Obianyo, 2019].

3.5 PERFORMANCE OF ANALYSIS

3.5.1 Microstructure

Prior to the microstructural analysis, the treated and untreated samples were cut into dimensions suitable for the test. The samples were cut into a rectangular size of 25mm x 12mm and 3 mm thick using the waterjet technology. The prepared samples were mounted, grinded, polished, and etched.

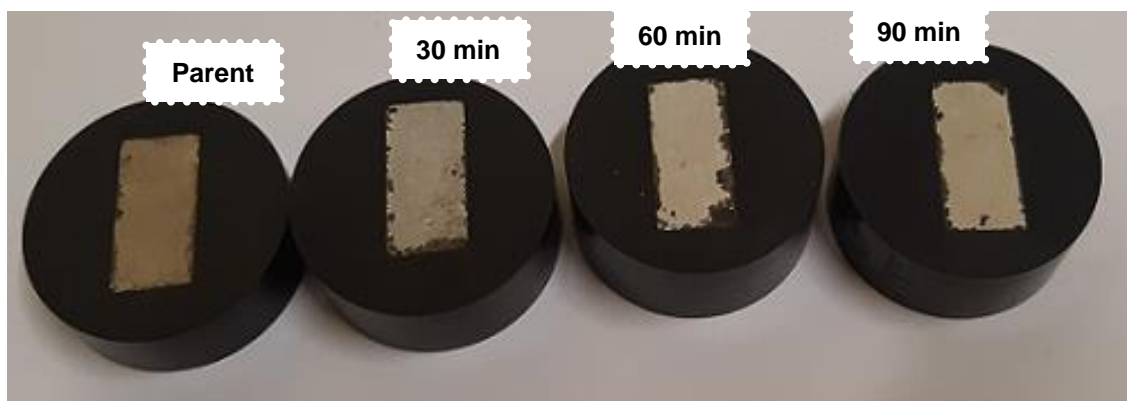


Figure 3.6: Hot mounted microstructure samples

3.5.1.1 Hot Mounting

The basic role of mounting is making the handling of metallographic samples of different shapes possible and easier. It also assists by shielding and saving extraordinary ends or surface imperfections throughout metallographic arrangement [Mondal et al., 2016].



Figure 3.7: Mounting machines

The mounting is performed preparing hot black Bakelite mounting powder and a mounting press for the hot mounting of the samples. The microstructure samples were placed in a mounting chamber and the hot black Bakelite mounting powder was added into the chamber. A temperature of around 180 °C and a force of around 250 bar was applied during the mounting of the sample. The hot mounted samples were taken out of the chamber and air-cooled.

3.5.1.2 Polishing

Polishing is the final step in making a level, scratch-free and mirror-like surface. It is vital for the accurate metallographic elucidation of the quantitative and qualitative description of the sample [Mondal et al., 2016]. In performing the polishing, Water, a 2000 grit sic pad, a Nap pad, and Op solution were prepared for the polishing and rinsing. A solution of 3 ml nitric acid (NA), 1.5 ml hydrofluoric acid (HF), 100 ml distilled water, and ethanol were prepared for etching. A firm pressure is applied, as evenly as possible, during the active oxide Polishing (AOP), and especially during the application of the polishing and rinsing steps as shown in figure 3.11. The following steps were followed: Fine grinding using a 2000 grit SiC paper pad with water for 10 minutes,

followed by polishing using a nap pad with Op solution for 20 minutes, and Rinsing was also done with a nap pad with water for 10 minutes.



Figure 3. 8: Polisher machine used in preparation of microscope samples

3.5.1.3 Etching

The metallographic etching is utilized to uncover specific basic attributes of steel. This is crucial because these basic qualities are not obvious in the cleaned mirror-like surface in the metal. It may very well be utilized for stage distinguishing and for dislocation density calculation [Lopes et al., 2007]. In performing the etching, the etchant used was Kroll's Reagent and is made by mixing 3ml nitric acid, 1.5ml HF, and 46.5ml of purified water. The specimens were immersed in the etchant for thirty (30) seconds and then thoroughly rinsed with distilled water. Afterward ethanol was used to clean the surface which is then dried using hot air.

3.5.1.4 Microscope Analysis

The American Society of Testing Materials E112 evaluation procedure was followed to determine the typical grain size and this test method relates typically to the single-stage grain size grain structure to the multi-stage or multi-constituent samples.

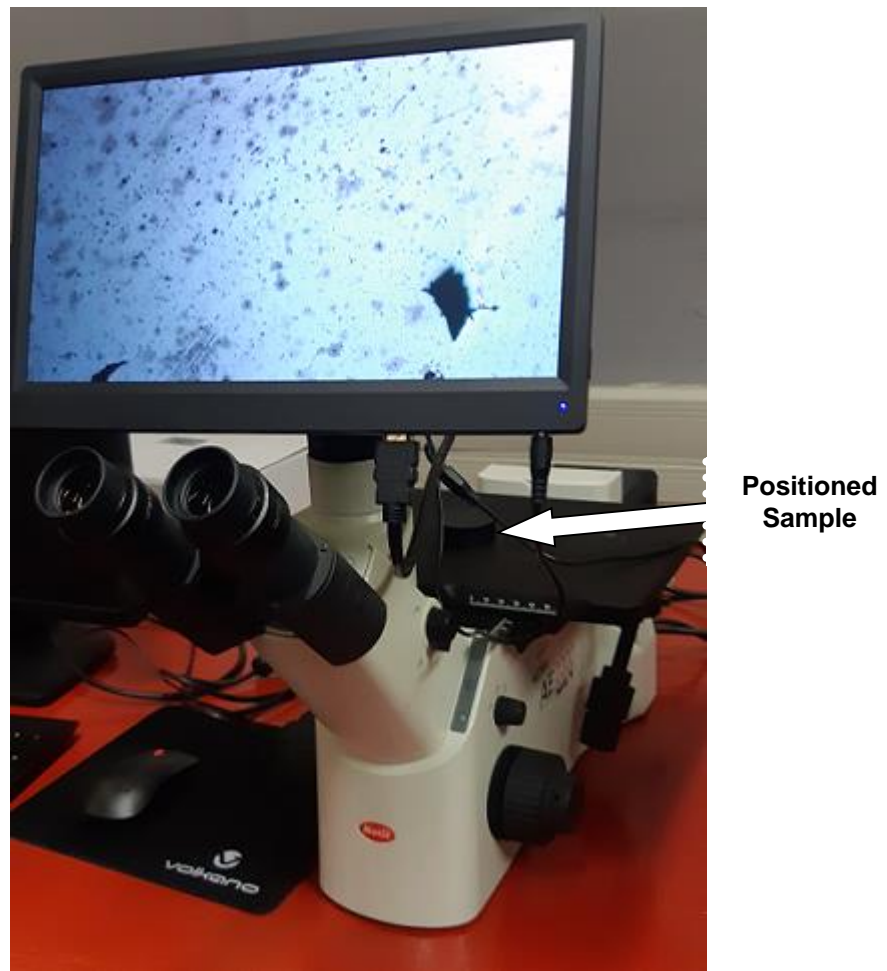


Figure 3.9: Motic AE2000MET inverted microscope

3.5.2 Tensile

Prior to the performance of the tensile test, the treated and untreated samples were cut to a bone shape following the ASTM-646-98 standard using the waterjet technology see figure 3.10.



Figure 3.10: Prepared tensile sample

In performing the Analysis, the treated and untreated tensile samples were loaded and positioned in the grip jaws (both upper and lower) of the Instron tensile machine. After securing the samples in the jaws, the computerized system connected to the machine initialized the test by allowing the upper jaw of the Instron machine to stretch the sample at a continuous ratio though gauging the load and the extension of the specimen (figure 3.11) below. The data was then recorded and a stress-strain curve was plotted.

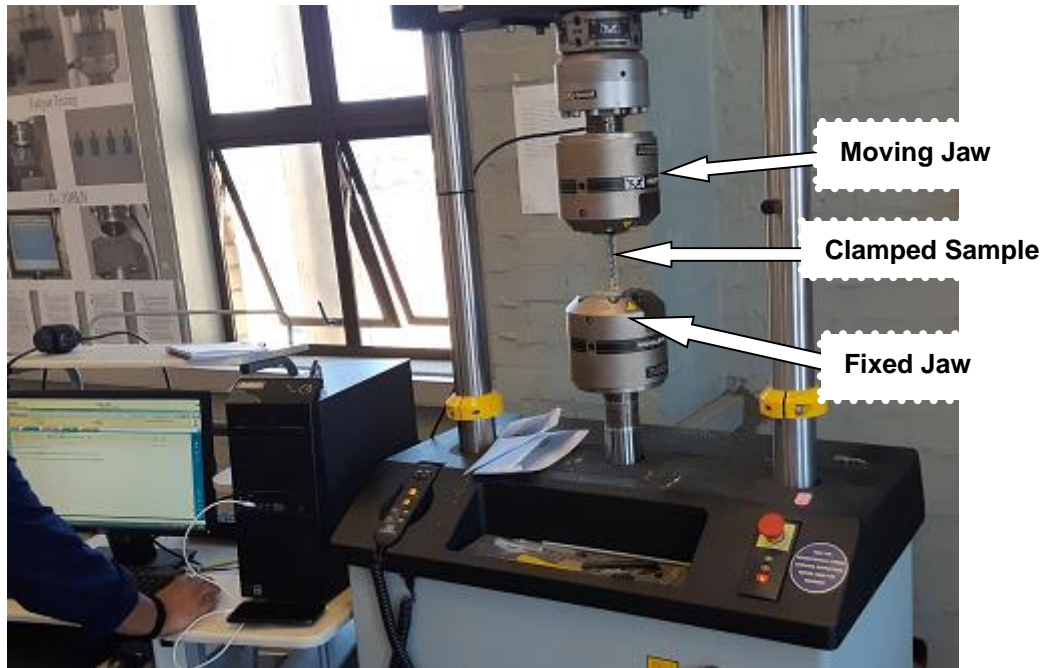


Figure 3.11: Instron Tensile Machine

3.5.3 Scanning Electron Microscope (SEM)

Prior to the performance of scanning electron microscope (SEM) analysis, all treated and untreated fractured tensile samples were cut around the necking areas and grouped in preparation of the SEM see figure 3.12. SEM analysis was then conducted in two samples of each group to check surface fracture morphology.

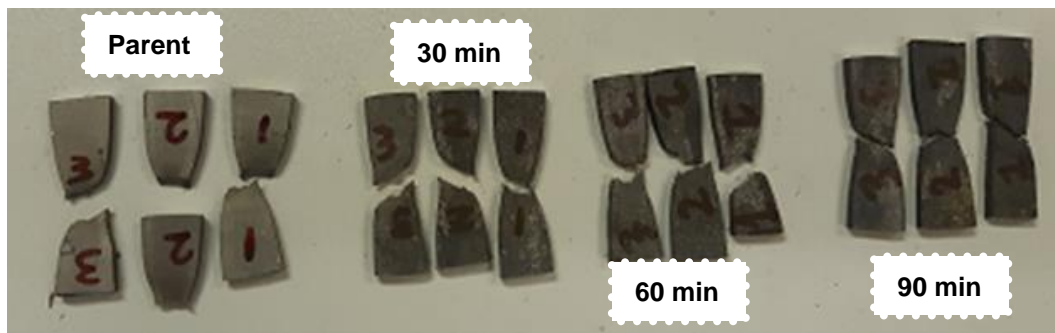


Figure 3.12: Prepare SEM samples

In conducting the analysis, prepared samples were loaded into the MIRA stage inside the chamber. Tensile fractured surfaces were positioned facing upwards toward the

Mira infra-red camera. Images of the fractured surface samples were taken in all prepared samples.

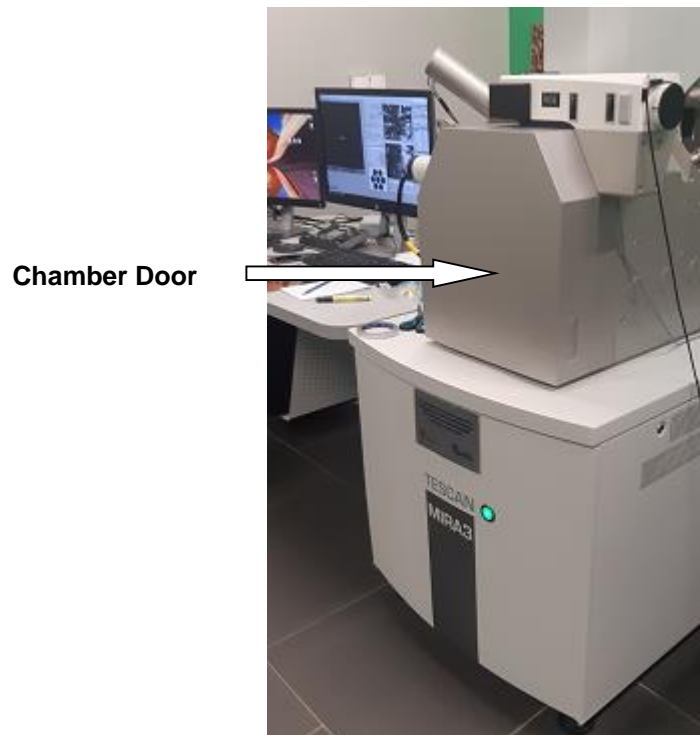


Figure 3.13: Tescan Mira 3 machine

3.5.4 Microhardness

Prior to the performance of microhardness testing all treated and untreated samples were cut into dimensions of 25mm by 12mm by 3mm. The prepared samples were then hot mounted, grinded, polished exactly by the same procedure mentioned in section 3.5.1.1 and 3.5.1.2, and the prepared samples were the same as the microstructure prepared samples to refer to figure 3.14 below.

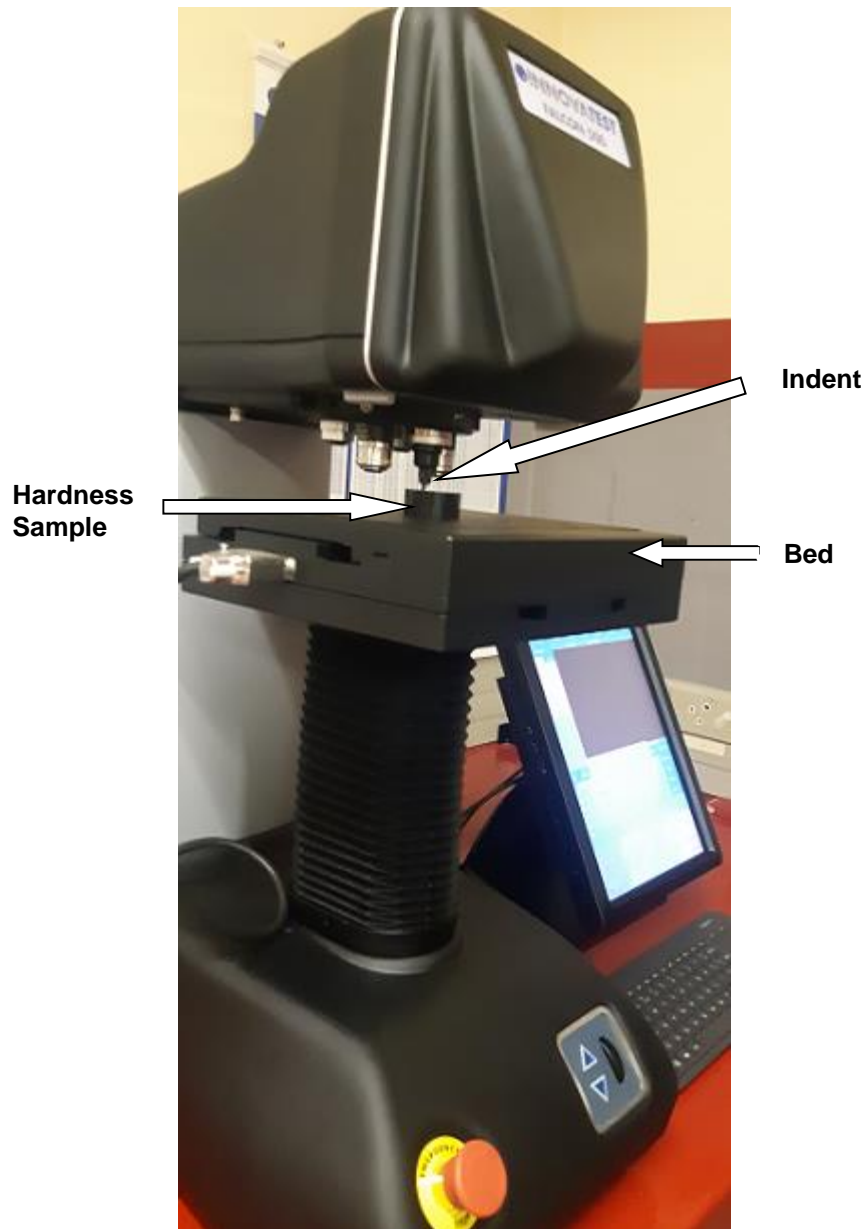


Figure 3.14: Innova Test Falcon 500 Microhardness Machine

In performing the Analysis, the machine was first programmed to follow the method to measure the hardness scale, the dwelling time, and the pattern the Vickers indenter was to follow when taking the hardness measurements. The dimensions for the Vickers pattern were 5mm in-between hardness testing points, 4mm in between the lines, and the middle line passing through the center of the sample. It must be noted that points were selected as follows: -Points 1 to 5 and points 11 to 15 were measured close to the edge of the sample and points 6 to 10 were passing through the centerline of the sample as shown in figure 3.15. Below table 3.1 shows the program that was loaded onto the machine for all hardness samples. A start button was pressed and the Vickers indenter started to move toward the sample and started measuring the hardness in all points that were selected from points 1 to 15.

Table 3.1 Microhardness information entered loaded on the machine

Method selected	Vickers
Hardness scale	HV0.5
Dwelling Time	10 Seconds

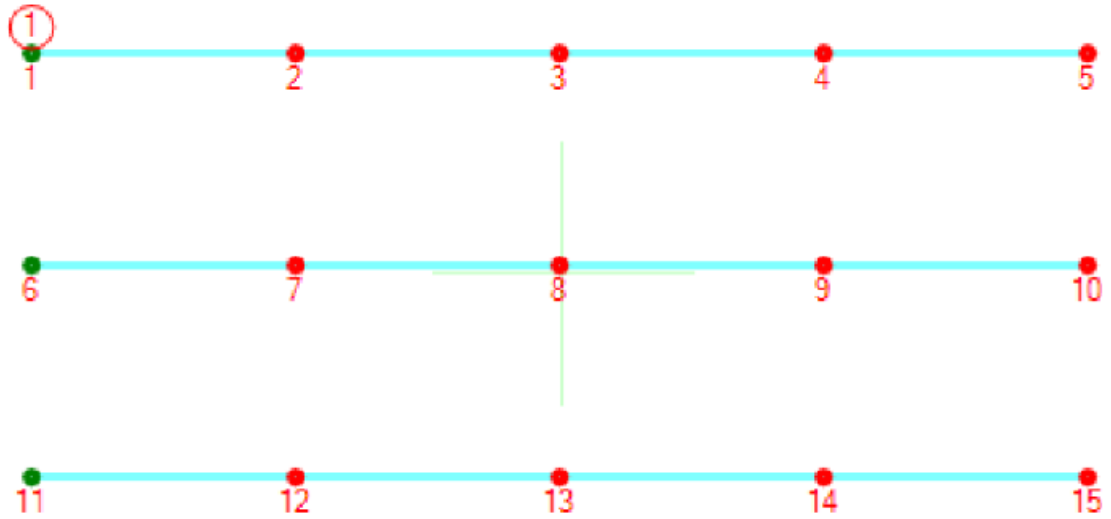


Figure 3.15: Microhardness test pattern followed

CHAPTER 4: RESULTS AND DISCUSSIONS

This chapter presents and discusses the outcomes that were attained in the previous chapter. The outcomes are discussed comparatively and correlatively.

4.1 TENSILE STRESS TEST

4.1.1 Parent vs 30 minute-soaked results

Table 4.1 presents the results for the ultimate tensile stress, strain, and percentage elongation yield at the breaking point of the parent material versus the heat-treated sample that was treated for 30 minutes. Figure 4.1 shows the stress-strain curve of the parent sample and figure 4.2 shows the stress-strain curve for the sample that was 30 minutes heat treated.

Table 4.1: 30 Minutes results compared with parent material results at the yield point.

Sample	Stress(UTS) (MPa)	Strain (Dimensionless)	% Elongation (Yield Point)	% Elongation (Maximum)
Parent	545,21	0,052	5,22	15,88
30 Minutes	378.52	0.12	11.95	27.55

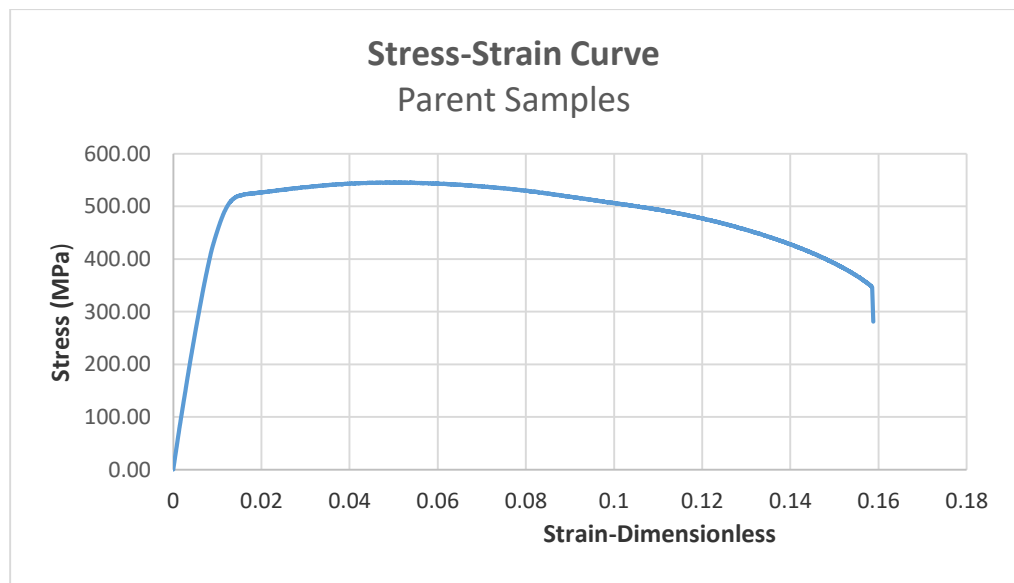


Figure 4.1: Parent Sample Stress-strain curve graph

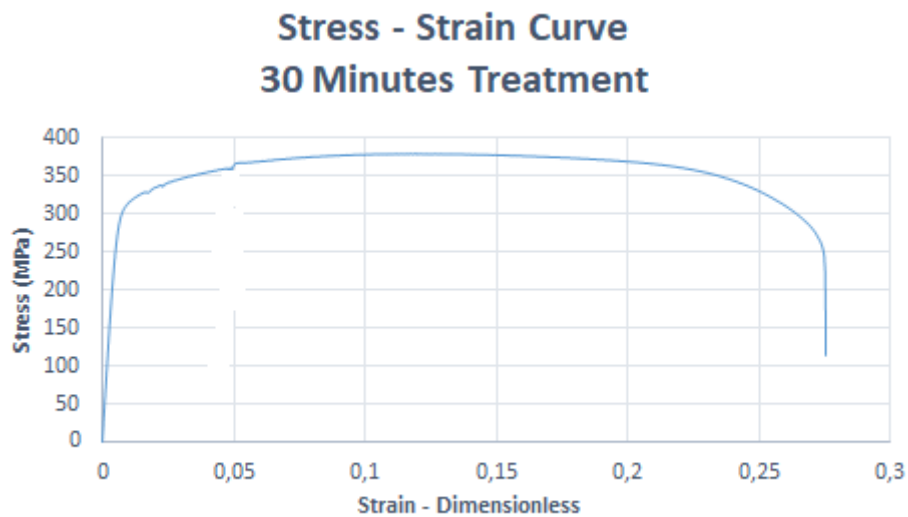


Figure 4.2: 30 Minutes Heat Treatment Stress-strain curve graph

There had been a notable reduction in the ultimate tensile strength of the samples that were heat-treated for 30 minutes in comparison to the parent sample results that had led to the heat treatment beyond transus temperature. The application of heat in the Cp titanium grade 2 sample caused the grains to expand and that resulted in the strength decrease [Herring, 2005].

There was a noticeable increment in percentage elongation on the 30 minutes heat-treated sample compared to the parent as it elongated more by 74%. The microstructure after plastic disfigurement in the α , $\alpha+\beta$, and β phases, comprised of elongated and distorted grains. Higher levels of initial deformation prompt fine microstructure containing increasingly elongated α grains [Motyka, 2010].

The necking (sample breaking during a tensile test) of the parent sample was not close to the middle of the gauge length, Instead, it appeared close to the edges of the gauge length of the sample (figure 4.3 (A)). In a thin sheet, an unusual type of deformation may occur at the crack edge and the height of the necking area in the specimen is commonly approximately equal to the sheet thickness [Silva et al., 2016].

In all heat-treated samples the area and pattern of the necking were also not the same (figure 4.3 (B)). In some cases, the necking appeared close to the center of the gauge length of the sample and in some samples, necking was displaced from the center. When conducting tensile testing, forces on the samples are symmetric. Therefore, it is instinctive that necking should begin at the center or close to the middle of the tensile gauge length sample [Roylance, 2001].

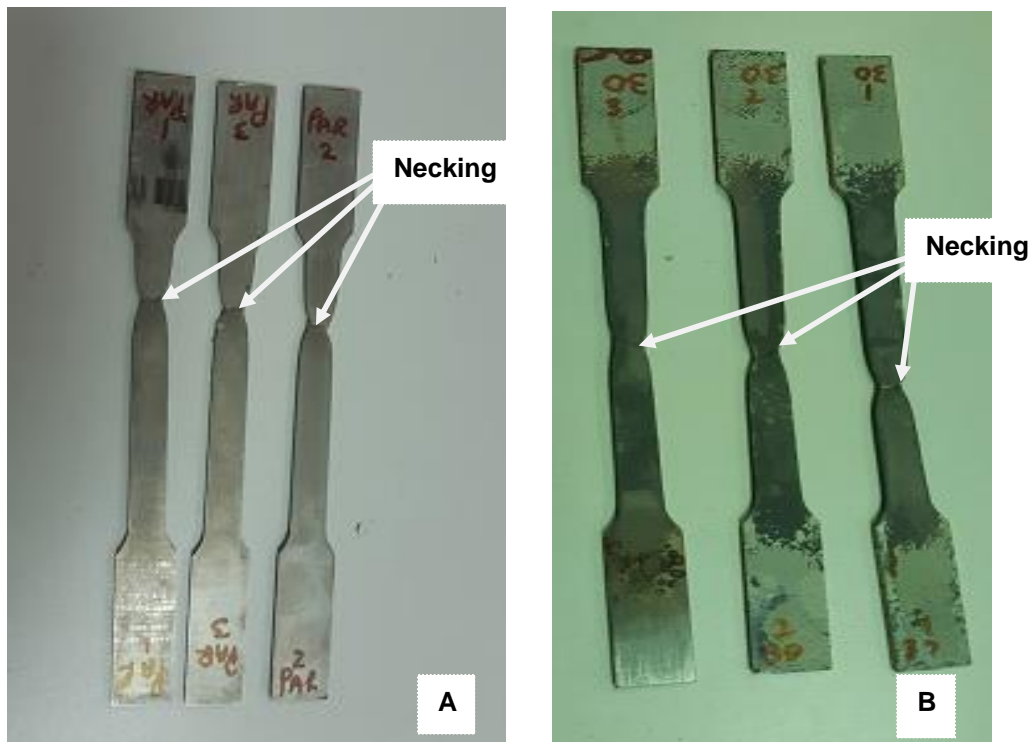


Figure 4.3: Fractured tensile samples, (A) Parent, (B) 30 Minutes

4.1.2 Parent vs 60-minute heat treatment results

Table 4.2 presents the results of the ultimate stress, strain, and percentage elongation yield point at the breaking point. Figure 4.4 shows the stress-strain curve diagram for the 60 minutes of heat treatment.

Table 4.2: 60 minutes of results compared with parent material at yield point.

Sample	Stress(UTS) (MPa)	Strain (Dimensionless)	% Elongation (Yield Point)	% Elongation (Maximum)
Parent	545,21	0,052	5,22	15,88
60 Minutes	372.56	0.13	12.56	27.88

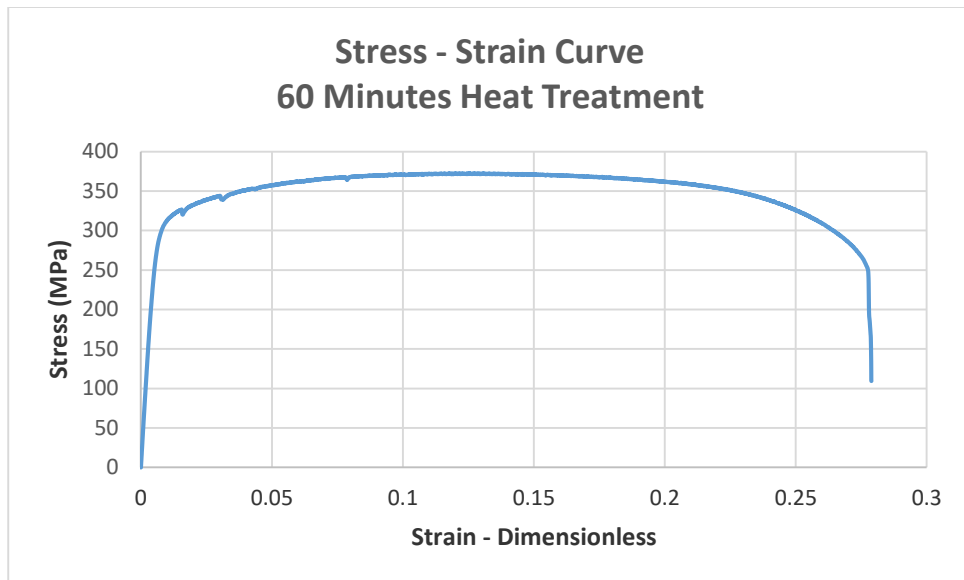


Figure 4.4: 60 minutes soaking Stress-strain curve

There was a notable decrease in the ultimate tensile strength compared with the parent samples, and also slightly lower than the 30-minute heat-treatment results. The reduction in strength on the treated samples compared to the parent and the 30-minute heat-treatment sample was attributed to the heating above the transus temperature, which increases the dislocation density of grain that plays a major role in the strength changes [Kamachali., 2012].

An increment in percentage elongation was also noted in the 60-minute heat-treated samples compared to the parent samples, as it increased by 76 %. During yield and the plastic-stream system the following yield, the material streams with an immaterial change in volume; increment in length are counterbalanced by diminishes in the cross-sectional region [Roylance., 2001].

The observation of the necking in the 60 minutes treated sample showed that the necking appeared not far from the center of the sample but in different zones (figure 4.5.(B)). Once a ductile material is used in a tensile test, necking commences and vacuums are created starting close to the midpoint of the specimen [Kumar et al., 2014].



Figure 4.5: Fractured tensile samples, (A) Parent, (B) 60 Minutes

4.1.3 Parent vs 90 minutes-soaked results

Table 4.3 presents the parent test results compared with the 90-minute heat-treated results, which include the ultimate stress, strain, percentage elongation, and yield point at the point of fracture. Figure 4.7 shows the stress-strain curve diagram of 90-minute heat treatment.

Table 4.3: 90 minutes results compared with parent material at yield point.

Sample	Stress(UTS) (MPa)	Strain (Dimensionless)	% Elongation (Yield Point)	% Elongation (Maximum)
Parent	545,21	0,052	5,22	15,88
90 Minutes	375.57	0.15	14.96	35.03

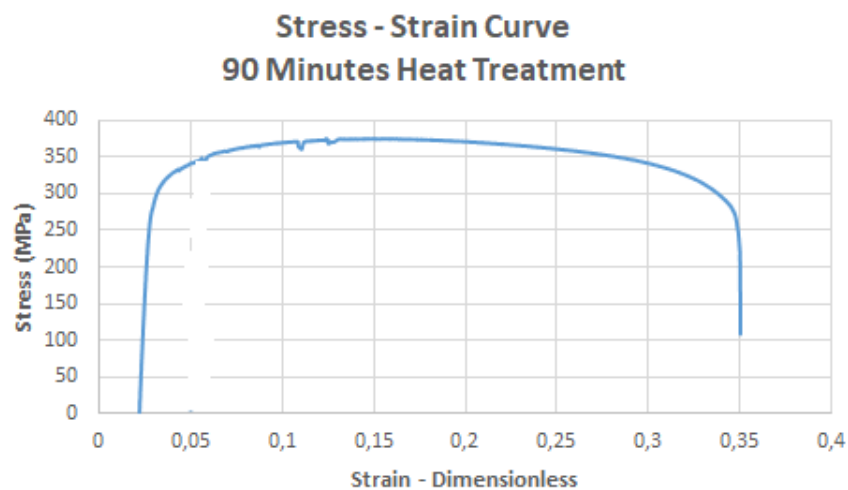


Figure 4.6: Parent compared with 90 minutes soaking Stress-strain curve

The results of the 90 minute treatment also showed a decrease in the tensile strength values compared with parent samples results. The flow stress diminishes with the expansion of the grain size at the similar tensile temperature and on the inner area of the sample larger flow stress are found compared to the surface area, where less flow stress were found [Zheng et al., 2015].

There was also a noticeable increment in percentage elongation on the 90-minute treatment samples compared to the parent sample as it displays a 121 % increment. During the air-cooling of the heat-treated material, the hardness will diminish and the toughness will improve, and the ductility of the materials increase [Martino et al., 2015]. The ductility of the heated sample grows with expanding of the α grain size [Jiang et al., 2015].

The necking for the 90-minute treatment is presented in figure 4.7. It was noted that the necking did not appear close to the center for all the samples. The area of the neck fluctuates from the center point of the sample to the affected or inverse side. It is worth noting that the increase in the strain of structural failure increases with the weight loaded and is reduced through the sample length. For shorter samples, the neck is created at its middle, while for longer samples the neck is obviously incepted near the contrary side [Osovski et al., 2013].

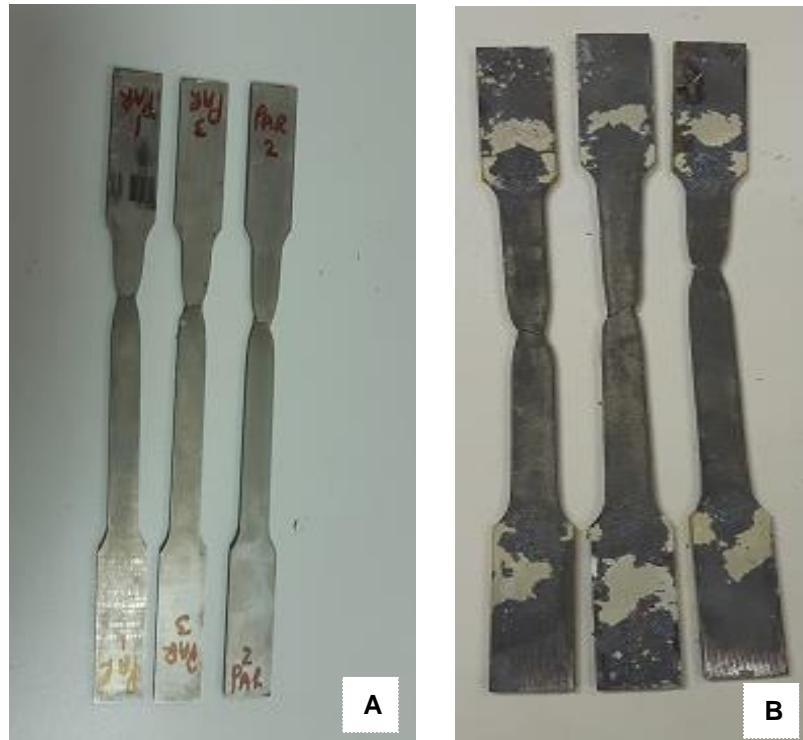


Figure 4.7: Fractured tensile Samples, (A) Parent, (B) 90 Minutes

4.2 Summary of Tensile Behaviour

Tensile testing gives the data on the strength, the ductility of the metallic material, and the yield strength. It quantifies the power needed for breaking a composite or plastic sample, and the maximum level to which the sample can stretch. In addition, tensile testing was able to allow the analysis of strains on the treated and untreated samples from the stress-strain diagram. All treated samples showed a low tensile strength and modulus of elasticity than the parent sample. It was also noted that the breaking of all treated samples was more elastic as it was observed that the curves after the elastic region remained linear until the treated samples broke or fractured. Subsequently, after breaking there was a permanent change in the original form.

4.3 Scanning Electron Microscope (SEM)

Observations of fracture surfaces were done in all heat-treated and non-treated tensile fracture samples to evaluate the impact of the heat treatment and compared it with the non-treated samples. Figure 4.8 below shows the SEM images of the fracture surface for the heat-treated and non-treated samples. The fracture surface zone was observed by means of scanning electron microscopy techniques in secondary electron imaging mode. SEM images were attained at the surface thickness of the fractured tensile samples in the necking area.

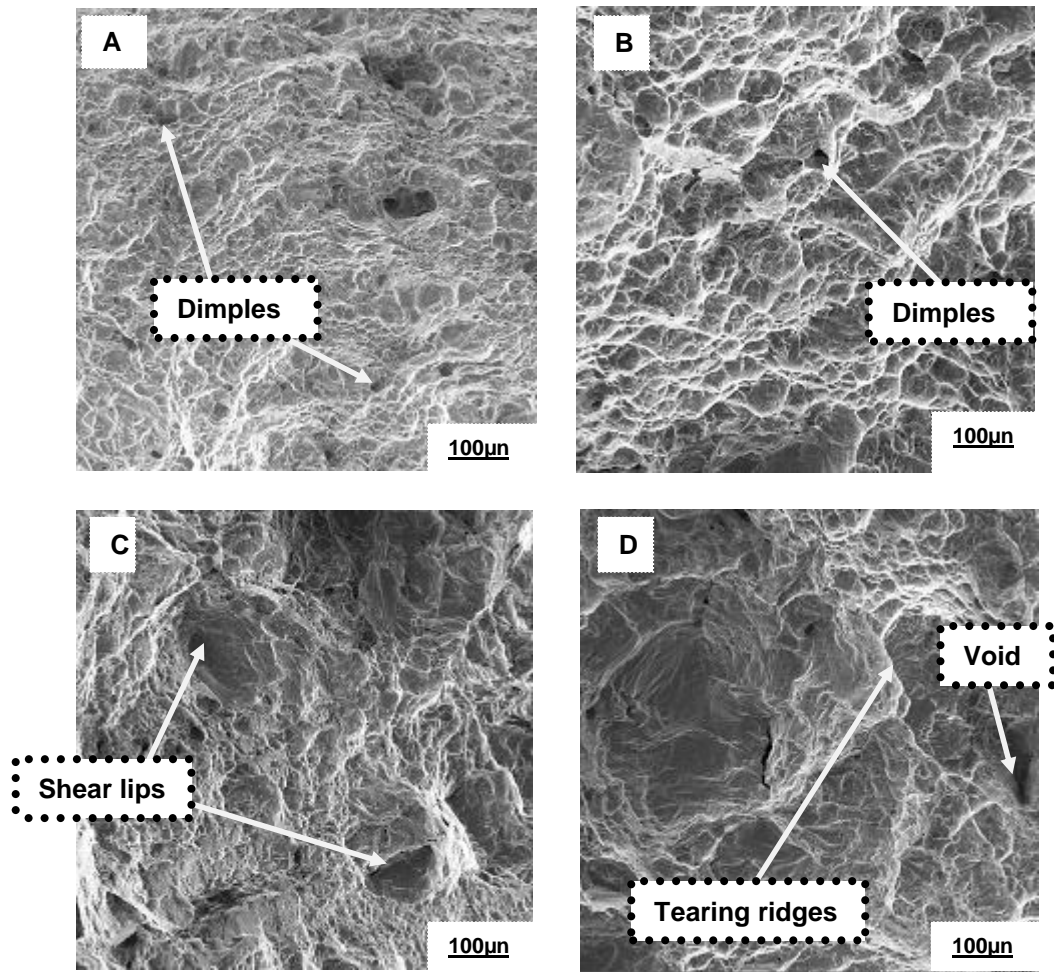


Figure 4.8: Fracture morphology of different samples after the tensile test (A) parent, (B) 30 Min, (C) 60 Min, (D) 90 Min

The morphology of a tensile fracture surface of the parent sample (A) appeared to be a bit rough but there were no obvious cracks detected. There were notable dimples and tiny shear lips on the surface. This then suggests that the fracture was semi-brittle and semi ductile. The morphology of the 30-minute tensile fracture surface (B) also showed dimples of different sizes with a large number of tearing ridges suggesting that the fracture was ductile. For the 60-minute sample morphology (C), it portrayed deep shear lips and also obvious ductile dimples, and also tiny cleavage facets were also noted. A clear indication of ductile fracture was noted. The morphology of the 90-minute sample (D) portrays deep shear lips, voids with different sizes, facets, and also tearing ridges that were noted, and that was a clear indication of ductile fracture.

4.4 Microstructure grain sizes investigation and Structure Analysis

The measured grain sizes for the treated and untreated samples (parent sample) are presented below see table 4.4. Grain measurement in all heat-treated and non-treated samples was attained by using imageJ.

Table 4.4: Average grain size measurement for Cp Ti grade 2 samples (μn)

Item	Sample	Grain Size
1	Parent	12.02
2	30 Minutes	53.08
3	60 Minutes	60.03
4	90 Minutes	66.09

The average grain size for the non-treated sample is approximately 12.02 μm while the heat-treated samples have an average grain size larger than the parent sample. There is a noticeable growth in grain size in all heat-treated samples. The samples heat-treated for 90 minutes appears to have the largest grain size compared to the other heat treatment periods. It is evident that the period of heating has an influence in grain growth, the longer period of heating the bigger the grain size. The development in grain size of a material is seen when heat treatment happens for a longer tempering period [Htun., 2015].

Evidence of high-temperature treatment recrystallization influence on the microstructure was noticeable in all heat-treated samples and was seen affecting the material properties as shown in figure 4.9, 4.10, 4.11, and 4.12, where there is a visible change in microstructure. The grains did not only expand due to the temperature rise but some grains became elongated following the rolling direction that was also noticeable in all heat-treated samples. The fine equiaxed grain is reflected as martensite and elongated grains concurrent to the rolling direction (RD) are referred to as delta ferrite, which stays unchanged without changing into gamma once the temperature is increased from normal conditions to high-temperature conditions [Archibald., 2005].

Since the heating happened above transus temperature, new grains began to grow and took over the original grain structure, causing a decrease in the number of original grains and affecting the grain boundary energy. The smaller the boundary energy, that favors the development of positive sub-grains and that also leads to the advancement of sturdy film texture [Barmak., 2005].

The microstructure images of commercially pure titanium grade 2 can be observed in figures 4.9, 4.10, 4.11, and 4.12 for heat-treated and non-treated samples.

The parent sample microstructure is shown in figure 4.9 and the microstructure shows a fine grain structure, an indication of strain, and clear indications of the rolling direction present in the microstructure. The grains are very fine as expected from the sheet or plate material. Fine grains are noticed when inhomogeneous deformation occurs between the outer and inner sheets because of the rolling procedure. This can be seen by the variance in contrast amongst the four layers; the darker layers (outer two sheets) show elevated levels of shear bands, while the lighter layers (inward two sheets) display little, assuming any, shear banding [Milner et al., 2013].

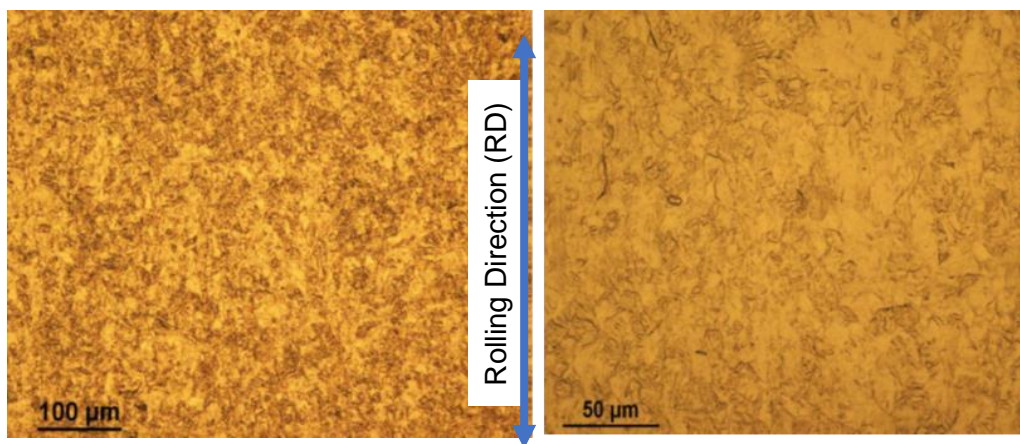


Figure 4.9: Microstructure of a parent material

The first-period heat-treatment microstructure appears in figure 4.10 and it shows signs of sub-grains formed within the larger grains due to the introduction of heat. Extreme heat-treatment prompts more dislocation accumulation and the creation of finer sub-grain structures [Forging et al., 2019].

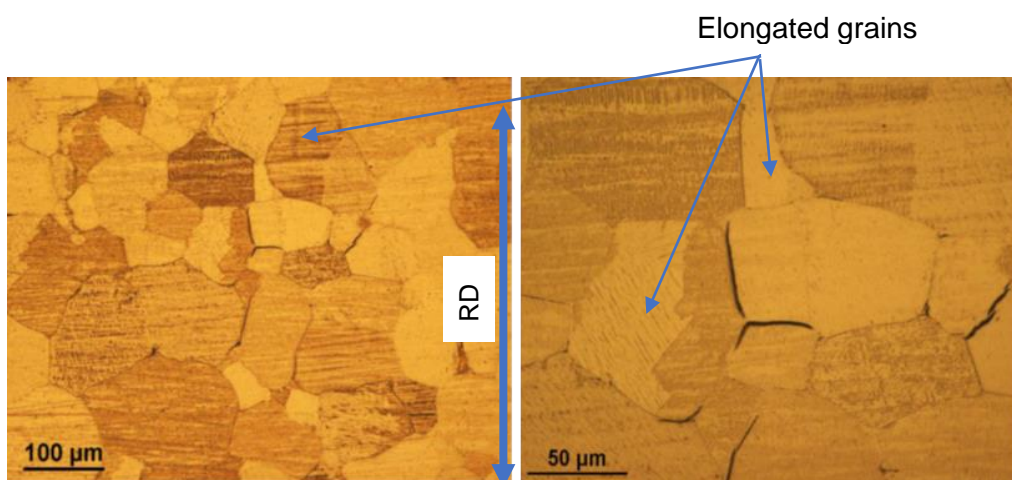


Figure 4.10: Microstructure of 30 minutes heat-treatment sample

The second-period heat-treatment microstructure is shown in figure 4.11 and it shows sub-grains started to disappear but some areas showed finer grains and this was due to the grain growth turning the sub-grains into new finer grains (due to recrystallization). This appears to be grain growth in some of the pre-existing grains. With the increase in the heating period, fine equiaxed grains, and dislocation densities are well characterized and a huge amount of dislocations, shear bands, and sub-grains appear [Sauvage et al., 2012].

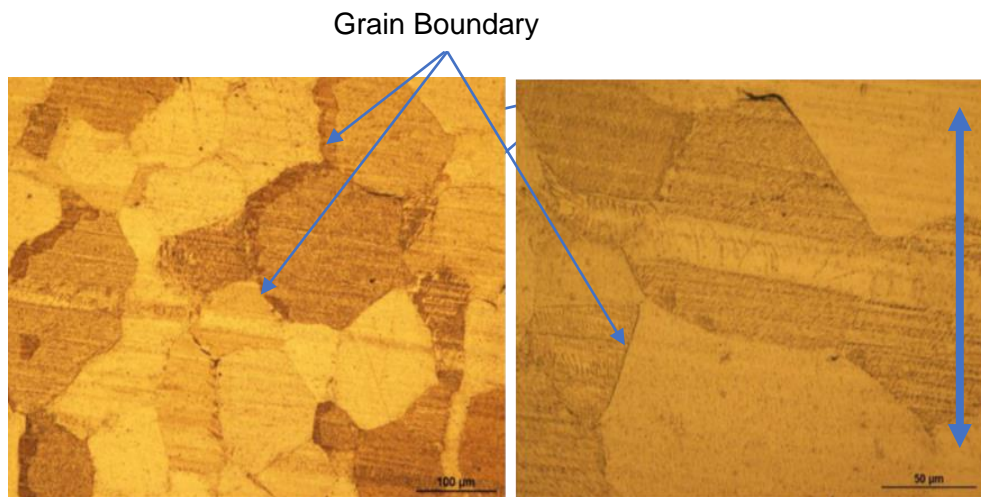


Figure 4.11: Microstructure of 60 minutes heat-treatment sample

The third-period heat-treatment microstructure is shown in figure 4.12 and it shows fine grains starting to disappear but introduces an ultra-fine grain structure that was influenced by the longer heating period. Depending upon the regimes of severe heating, various types of grain boundaries can be structured in the ultra-fine grain materials, which paves the way to grain boundary engineering of ultra-fine grain material [Wilde et al., 2012].

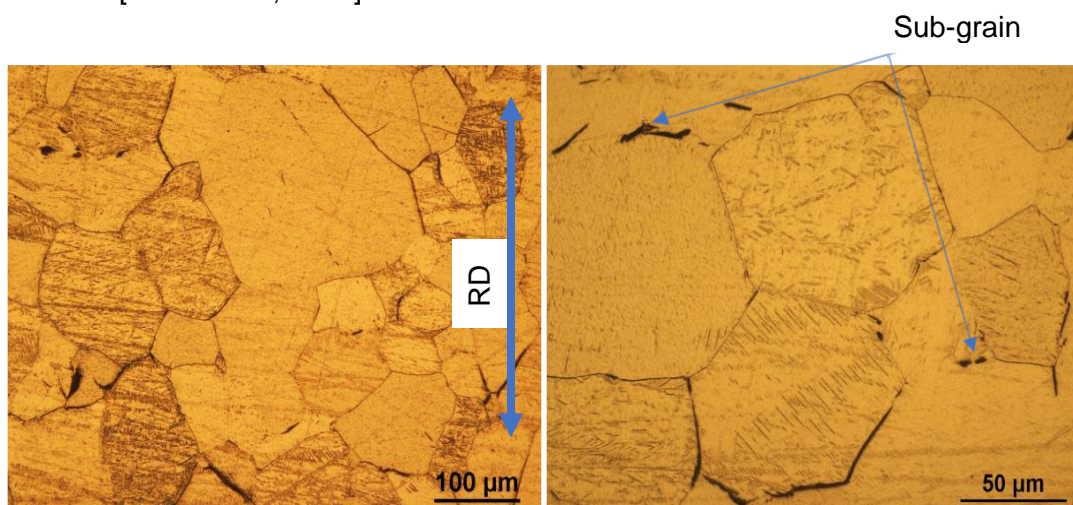


Figure 4.12: Microstructure of 90 minutes heat-treated sample

4.5 Microhardness

4.5.1 Parent

Prior to the hardness analysis of the samples, the variation in the physical appearance of all heat-treated samples was observed (figures 4.9, 4.10, and 4.11). The difference in appearance compared to the parent samples was attributed to the titanium oxide layer which also influence the surface hardness. The oxide layer on the titanium surface is in charge of the titanium biocompatibility since it shields the underlining metal from consumption and represses the arrival of any metal particles that could be lethal. [Khalaf et al., 2017]. The average microhardness results are presented in Table 4.5, where samples of the 90 Minute treatments show the largest microhardness value compared to the parent and other treatments.

Table 4.5: Average micro hardness results

Sample	Micro hardness
Parent	195
30 Minutes	186
60 Minutes	170
90 Minutes	305

The microhardness results for the parent sample are presented in table 4.6. In all treated and untreated samples, the microhardness was measured from point 1 to point 15 as illustrated in figure 4.13.

Table 4.6: Microhardness results measured at a different point

Measurement point	Hardness Results (HV0,5)
1	185.52
2	189.3
3	185.66
4	194.0
5	185.74
6	183.46
7	182.21
8	185.22
9	191.09
10	215.64
11	204.52
12	205.76
13	210.0
14	215.66
15	192.94

There was a noticeable variation in microhardness points for all heat-treated and non-treated samples. The variation in microhardness values was attributed to the fact that all 15 points for hardness measurement were selected randomly on the surface of the samples and therefore some points were in the center of the grain, some were next to the grain boundary, some were exactly on the grain boundary. Grain boundaries hinder the dislocation motion and they are also looked at as a basis of dislocation, hence, the dislocation collides or dislocation forestry is created in zone nearby to the grain boundaries [Jung et al., 2013].

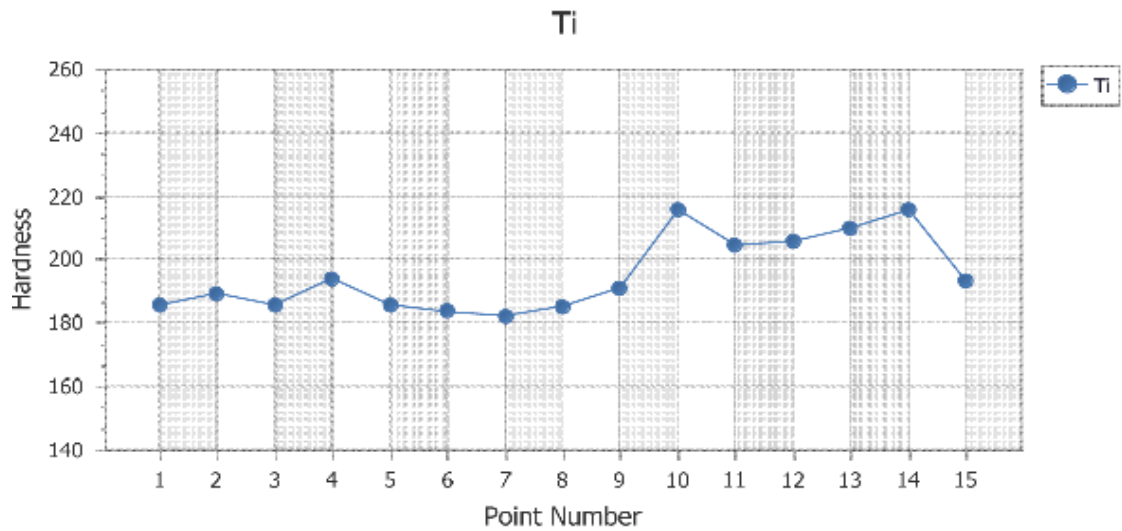


Figure 4.13: Hardness (HV) vs hardness points

4.5.2 30 Minute Heat Treatment

30-minute heat-treatment results for hardness are presented in table 4.7.

Table 4.7: Microhardness results for 30 minutes sample

Measurement point	Hardness Results (HV0,5)
1	183,98
2	188.21
3	186.83
4	177.9
5	200.56
6	237.74
7	177,93
8	154.41
9	171.55
10	185.5
11	224.46
12	164.58

13	162.64
14	191.73
15	191.73

There was a noticeable decline in rigidity values in comparison to the original sample. The decline in rigidity was attributed to the increase in grain size due to the application of heat above the transus temperature of 882.5 °C. The strength coefficient, yielding stress, and hardness declined through the increase in grain size. The hardness diminishes with expanding of grain size when the sample is α stage structure. [Jiang et al., 2015].

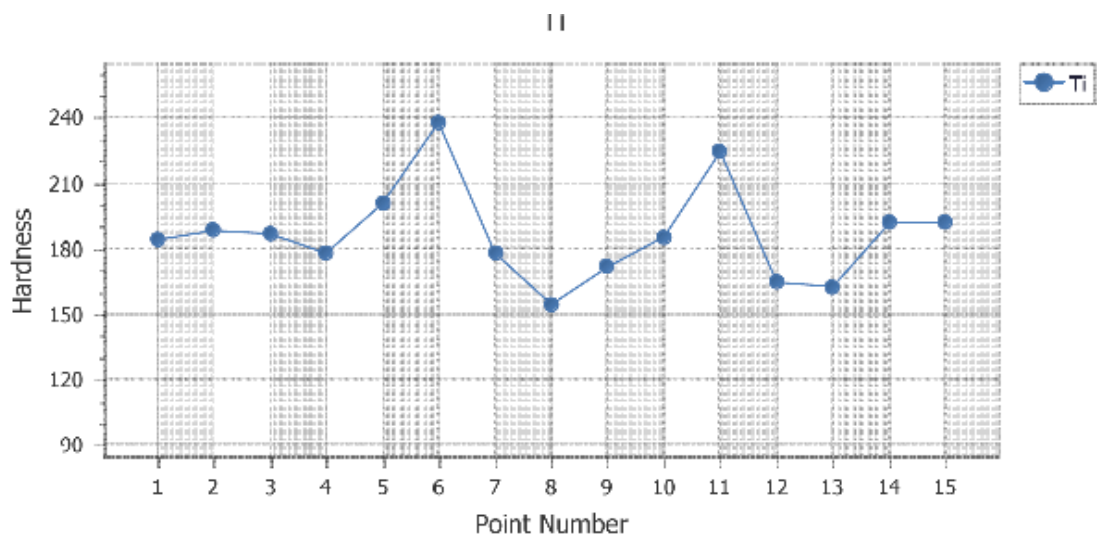


Figure 4.14: 30 minutes heat-treatment Hardness (HV) vs hardness points graph

4.5.3 60 Minute Heat Treatment

60 minute heat treatment results for hardness are presented in Table 4.7

Table 4.8: 60-Minutes microhardness results

Measurement point	Hardness Results (HV0,5)
1	172.32
2	196.05
3	163.3
4	151.75
5	178.98
6	152.43
7	154.34
8	158.02
9	167.48
10	166.53

11	170.37
12	149.28
13	184.65
14	192.97
15	190.54

There was a noticeable decline in rigidity values in comparison with the original and 30-minute samples. The grain growth led to a decrease in rigidity due to the application of heat above transus temperature. Recrystallization annealing is responsible for the development of equiaxed grains although retaining a similar pattern of the microstructure (equiaxed) that was existing before the treatment [Abdalla et al., 2017].

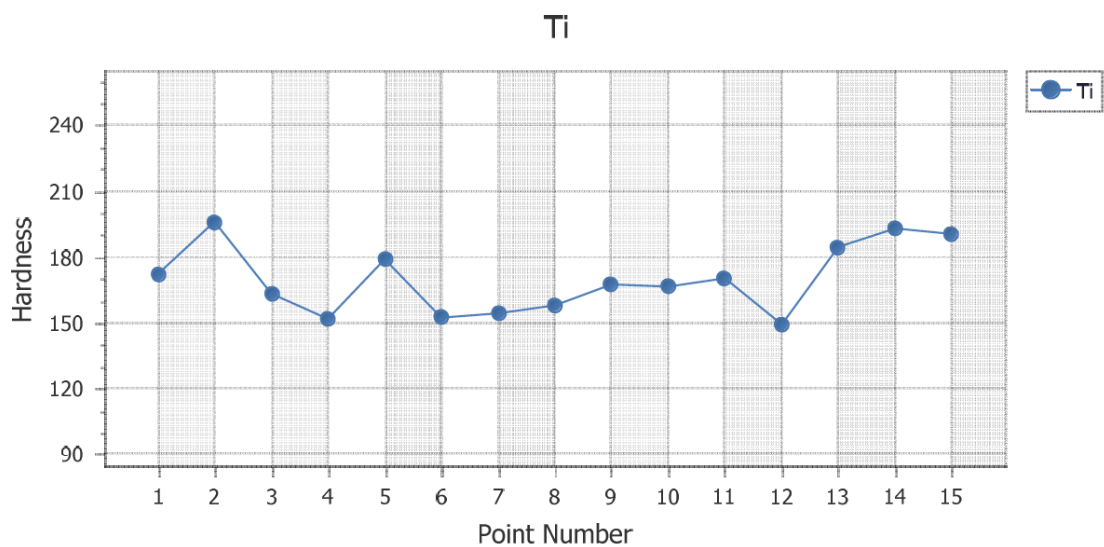


Figure 4.15: Hardness (HV) vs hardness points

4.5.4 90 Minute heat treatment

90-minute heat treatment results are presented in Table 4.8

Table 4.9: 90 Minutes microhardness results

Measurement point	Hardness Results (HV0,5)
1	312.56
2	235.89
3	197.97
4	182.34
5	220.07
6	422.24
7	347.38
8	199.23

9	253.42
10	369.18
11	359.56
12	372.22
13	283.55
14	407.81
15	404.02

With the 90-minute heat-treatment, there was a noticeable gain in hardness although the grain sizes are larger compared to the parent and the 30 and 60-minute heat treatments. The gain in hardness on the 90-minute sample was attributed to the heating period of the sample that had an effect on the grain structure and on the titanium oxide. Even though the grains of β titanium is much larger in size than those of the α titanium samples, the hardness of the β titanium samples is much larger than that of the α titanium samples. The development of numerous lengthy fine laths, that settled in the heating and chilling after above the transus temperature, is the cause of the hardness improvement [Kao et al., 2005]. The thickness of the oxide layer expands with an increase in the heating timeframe of the surface, also the largest surface hardness expands with an increase in the heating timeframe and the hardness layer depth additionally expands [Kim et al., 2009].

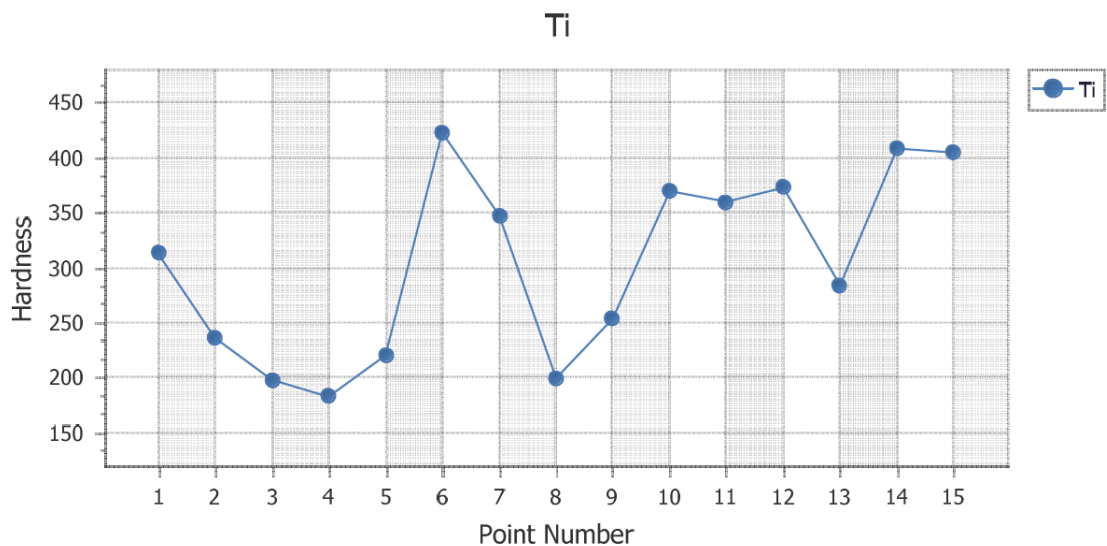


Figure 4.16: 90 Minutes Hardness (HV) vs hardness points graph

CHAPTER 5: CONCLUSION AND RECOMMENDATION

5.1. Conclusion

From this research, a conclusion is drawn that the primary objective of the study to investigate the effect of heat on commercially pure titanium grade 2 at a constant temperature of 900 °C at varying heating followed by air cooling times was fulfilled.

The microstructure of heat-treated samples was found to be influenced by the heat above the transus temperature of 882.5 °C, as transformation takes place from the hexagonal-close packed alpha stage to the body-centered cubic stage. When the transformation occurs the grains expanded and eventually, new grains started to develop through a process called recrystallization.

Heat treatment had an effect on the strength of commercially pure titanium, as the results of the heat-treated samples displayed a decrease in strength when compared to the parent sample but showed an increase in ductility. The strength of the treated samples decreased with the heating period and suggests that longer heating periods weakens the strength of the material.

The heating period had an effect on the hardness of commercially pure titanium as the results showed the longest heating period resulted in the largest hardness values. However, an increase in the hardness value was associated with the oxide layer that formed on the surface of the sample due to a longer heating period and it was confirmed by a physical appearance of an oxide layer in all treated samples.

Lastly, the investigation on commercially pure titanium showed that heat treatment and the heating period had effects on the plasticity of the treated samples which became elongated more than that of the parent sample, and the most elongated being the longer period treatment. This then means that the microstructure obtained after the heat treatment can provide good or poor mechanical properties depending on the nature of the application required. The mechanical properties can be referred to as poor because heat treatment reduces the strength, yet the properties can be referred to as good because brittleness is reduced due to the high ductility and surface hardness increased due to the titanium oxide layer.

5.2 Recommendations for future work

This research dealt with the heat-treatment of commercially pure grade 2 titanium above the transus temperature. The results obtained in this project will be advantageous to the engineering environment and the bio-medical applications such as bone replacement implantations. The outcomes from this research will add meaningfully to the information of refining the microstructure and mechanical properties of one of the greatest significant engineering metals for the automobile and aerospace industries. There is a necessity to discover the correct processing parameters that will exploit the utilization of this expensive material for the overall economy of the industries. Further work on the compressive study of the mechanical properties of these composites would improve the industrial potential of using these materials and processing routes to produce economically feasible titanium matrix composites.

REFERENCES

- Adabo, G. L., & Nobilo, M. (2006). Vickers Hardness of Cast Commercially Pure Titanium and Ti-6Al-4V Alloy Submitted to Heat Treatments, (May 2014).
<https://doi.org/10.1590/S0103-64402006000200008>
- Albiter, A., Leo, C. A., Drew, R. A. L., & Bedolla, E. (2000). Microstructure and heat-treatment response of Al-2024 / TiC composites, 289, 109–115.
- Aliprandi, P., Giudice, F., Guglielmino, E., & Sili, A. (2019). Tensile and Creep Properties Improvement of Ti-6Al-4V Alloy Specimens Produced by Electron Beam Powder Bed Fusion Additive Manufacturing, 1–22.
- Balasubrahmanyam, V. V., & Prasad, Y. V. R. K. (2002). Deformation behaviour of beta titanium alloy Ti – 10V – 4 . 5Fe – 1 . 5Al in hot upset forging, 336, 150–158.
- Barmak, K., Archibald, W., Kim, C., & Rollett, A. D. (2005). Grain Boundary Energy and Grain Growth in Highly-Textured Al Films and Foils : Experiment and Simulation Grain Boundary Energy and Grain Growth in Highly-Textured Al Films and Foils : Experiment and Simulation, (January).
<https://doi.org/10.4028/www.scientific.net/MSF.495-497.1255>
- Catherine, L. D. K., Bin, D., & Hamid, A. (2018). The effect of heat treatment on the tensile strength and ductility of pure titanium grade 2 The effect of heat treatment on the tensile strength and ductility of pure titanium grade 2.
<https://doi.org/10.1088/1757-899X/429/1/012014>
- Coelho, C., Ramos, A. S., Trindade, B., Vieira, M. T., Fernandes, J. V., & Vieira, M. (1999). Structure and properties of sputtered TiAl – M (M = Ag , Cr) thin films, 121, 297–302.
- Krakhmalev, P., Fredrikson, G., Yadroitsava, I., Kazantseva, N., Du Plessis, A., Yadroistev, I.(2016). Deformation behaviour and microstructure of Ti6Al4V manufactured by SLM, 83, 778-788 <https://doi.org/10.1016/j.phpro.2016.08.080>
- Diaspro, A., Usai, C., & National, I. (2006). Optical Microscopy, (April).
<https://doi.org/10.1002/9780471740360.ebs0869>
- Fidder, H., Botes, A., Woudberg, S., & McGrath, P. J. (2013). Characterization of microstructure and fatigue life of CP titanium grade 2 specimens subject to various bending processes. *WIT Transactions on Engineering Sciences*, 78(June), 25–33. <https://doi.org/10.2495/SECM130031>
- Filip, R., Kubiak, K., Ziaja, W., & Sieniawski, J. (2003). The effect of microstructure on the mechanical properties of two-phase titanium alloys, 133, 84–89.
- Forging, M. (2019). Changes of Microstructures and Mechanical Properties in Commercially Pure Titanium after. <https://doi.org/10.3390/met9020175>
- Halevy, I., Carmon, R., Halevy, I., & Salhov, S. (2010). Crystallographic structure of

- Ti-6Al-4V , Ti-HP and Ti-CP under high-pressure Crystallographic structure of Ti-6Al-4V , Ti-HP and Ti-CP under. <https://doi.org/10.1088/1742-6596/215/1/012013>
- Horák, M., Bukvišová, K., Švarc, V., Jaskowiec, J., & Křápek, V. (2018). Comparative study of plasmonic antennas fabricated by electron beam and focused ion beam lithography, (June), 1–8. <https://doi.org/10.1038/s41598-018-28037-1>
- Huang, R., Huang, W., Huang, R., & Tsay, L. (2014). Materials Science & Engineering A Effects of microstructures on the notch tensile fracture feature of heat-treated Ti – 6Al – 6V – 2Sn alloy. *Materials Science & Engineering A*, 595, 297–305. <https://doi.org/10.1016/j.msea.2013.12.024>
- Jiang, C., & Huang, Z. (2015). Grain Size Effect on Mechanical Properties of Titanium Alloy, 626, 548–552. <https://doi.org/10.4028/www.scientific.net/KEM.626.548>
- Journal, S. A., November, I. E., & Edition, S. (2016). Article details, 27(November), 110–121.
- Jung, B., Lee, H., & Park, H. (2013). International Journal of Solids and Structures Effect of grain size on the indentation hardness for polycrystalline materials by the modified strain gradient theory. *International Journal of Solids and Structures*, 50(18), 2719–2724. <https://doi.org/10.1016/j.ijsolstr.2013.05.002>
- Kamachali, D. (2012). Grain boundary motion in polycrystalline materials.
- Kao, Y. L., Tu, G. C., Huang, C. A., & Liu, T. T. (2005). A study on the hardness variation of α - and β -pure titanium with different grain sizes, 398, 93–98. <https://doi.org/10.1016/j.msea.2005.03.004>
- Ke, Z., Cheng-feng, L., & Zhen-, Z. (n.d.). *IOP Conference Series : Materials Science and Engineering Salt Bath Nitriding of CP Titanium Grade-2 and TI- SALT BATH NITRIDING OF CP TITANIUM GRADE-2 AND*. <https://doi.org/10.1088/1757-899X/197/1/012066>
- Khan, C. F. AE. T. I. (2008). The effect of quenching medium on the wear behaviour of a Ti – 6Al – 4V alloy, 788–792. <https://doi.org/10.1007/s10853-007-2298-y>
- Khorasani, A. M., Goldberg, M., Doeven, E. H., & Littlefair, G. (2015). *Titanium in Biomedical Applications - Properties and Fabrication : a Review*. <https://doi.org/10.1166/jbt.2015.1361>
- Kim, Y. Z., Konno, T., Murakami, T., Narushima, T., & Ouchi, C. (2009). Surface Hardening Treatment for Titanium Materials Using Ar-5 % CO Gas in Combination with Post Heat Treatment under Vacuum * 1, 50(12), 2763–2771. <https://doi.org/10.2320/matertrans.MA200911>
- Kumar, K., Pooleery, A., Madhusoodanan, K., Singh, R. N., & Chakravartty, J. K. (2014). Use of Miniature Tensile Specimen for Measurement of. *Procedia Engineering*, 86, 899–909. <https://doi.org/10.1016/j.proeng.2014.11.112>

- Kumar, S., Chattopadhyay, K., & Singh, V. (n.d.). Tensile Behavior of Ti-6Al-4V alloy at Elevated Temperatures, (Model 4206), 5–8.
- Kunieda, T. (2014). Effect of Heat Treatment Conditions on Mechanical Properties in High Strength Titanium Alloy Super-TIX TM 523AFM, (106).
- Lopes, G. C., Thys, D. G., & Oliveira, G. M. S. (2007). Enamel acid etching : A review, (February).
- Luo, J., Ye, P., Li, M. Q., & Liu, L. Y. (2015). Effect of the alpha grain size on the deformation behavior during isothermal compression of Ti – 6Al – 4V alloy, *88*, 32–40. <https://doi.org/10.1016/j.matdes.2015.08.130>
- Martino, S. F. Di, Faulkner, R. G., Gorham, D. A., Field, J. E., Ludwig, A., Holzmann, T., ... Mikhaylov, V. (n.d.). The effect of heat treatment on the hardness and impact properties of medium carbon steel. <https://doi.org/10.1088/1757-899X/114/1/012108>
- Milner, J. L., Abu-farha, F., Bunget, C., Kurfess, T., & Hammond, V. H. (2013). Materials Science & Engineering A Grain refinement and mechanical properties of CP-Ti processed by warm accumulative roll bonding. *Materials Science & Engineering A*, *561*, 109–117. <https://doi.org/10.1016/j.msea.2012.10.081>
- Mondal, K., & Verma, V. (2016). Physical Metallurgy Lab 2015-2016.
- Morita, T., Hatsuoka, K., Iizuka, T., & Kawasaki, K. (2005). Strengthening of Ti – 6Al – 4V Alloy by Short-Time Duplex Heat Treatment, *46(7)*, 1681–1686.
- Nady, M., Khalifa, W., & Shash, A. (2017). Influence of heat treatment conditions on the mechanical properties of Ti – 6Al – 4V alloy. *Canadian Metallurgical Quarterly*, *0(0)*, 1–8. <https://doi.org/10.1080/00084433.2017.1412557>
- Nakagawa, N., Hana, O. E., Otaki, M., & Ishizaki, K. (2006). Application of microbial risk assessment on a residentially-operated Bio-toilet. *Journal of Water and Health*, *4(4)*, 479–486. <https://doi.org/10.2166/wh.2006.028>
- Obiany, I. (2019). Laboratory manual for hardness test, (March).
- Okabe, T. (1995). The Use of Titanium in Dentistry, *5(2)*.
- Osovski, S., Rittel, D., Rodríguez-martínez, J. A., & Zaera, R. (2013). Dynamic tensile necking : Influence of specimen geometry and boundary conditions. *Mechanics of Materials*, *62*, 1–13. <https://doi.org/10.1016/j.mechmat.2013.03.002>
- Palumbo, G., & Brandizzi, M. (2012). Experimental investigations on the single point incremental forming of a titanium alloy component combining static heating with high tool rotation speed. *Materials and Design*, *40*, 43–51. <https://doi.org/10.1016/j.matdes.2012.03.031>
- Paper, C., Abdalla, A., Amrin, A., & Muhamad, S. (2017). Effect of heat treatment parameters on the microstructure and microhardness of Ti-6Al-4V alloy Effect of heat treatment parameters on the microstructure and microhardness of Ti-6Al-4V

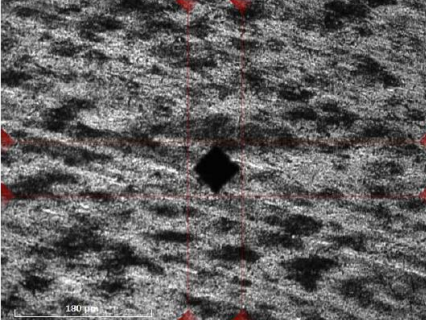
- alloy Ayad Omran Abdalla , Astuty Amrin , Sallehuddin Muhammad , and M . A . Azmah Hanim View online : <http://dx.doi.org/10.1063/1.4993335> View Table of Contents : <http://aip.scitation.org/toc/apc/1865/1> Published by the American Institute of Physics, (July). <https://doi.org/10.1063/1.4993335>
- Pederson, R., & Pederson, R. (2004). DOCTORAL THESIS The Microstructures of Ti-6Al-4V and Ti-6Al-2Sn-4Zr-6Mo and their Relationship to Processing and Properties.
- Pinke, P. (n.d.). THE INFLUENCE OF HEAT TREATMENT ON THE MICROSTRUCTURE OF THE THE INFLUENCE OF HEAT TREATMENT ON THE MICROSTRUCTURE OF THE CASTED Ti6Al4V TITANIUM ALLOY, (December 2014).
- Prasad, K., & Kamat, S. V. (2010). Dynamic fracture toughness of a near alpha titanium alloy Timetal 834, *491*, 237–241. <https://doi.org/10.1016/j.jallcom.2009.09.061>
- Roylance, D. (2001). STRESS-STRAIN CURVES, 1–14.
- Sauvage, X., Wilde, G., Divinski, S. V, Horita, Z., & Valiev, R. Z. (n.d.). Grain boundaries in ultrafine grained materials processed by severe plastic deformation and related phenomena, *540*(2012), 1–12. <https://doi.org/10.1016/j.msea.2012.01.080>
- Science, M., & Journal, E. I. (2019). Effect of heat treatment on the microstructure and hardness of the SLMed TC4 alloy specimens, *3*(3), 82–87. <https://doi.org/10.15406/mseij.2019.03.00096>
- Seshacharyulu, T., Medeiros, S. C., Morgan, J. T., Malas, J. C., Frazier, W. G., & Prasad, Y. V. R. K. (2000). Hot deformation and microstructural damage mechanisms in extra-low interstitial (ELI) grade Ti – 6Al – 4V, *279*, 289–299.
- Silva, M. B., Bay, N., & Martins, P. A. F. (2016). *Hole-flanging by single point incremental forming. Materials Forming and Machining*. Elsevier Ltd. <https://doi.org/10.1016/B978-0-85709-483-4.00002-8>
- Srivatsan, T. S., & Patnaik, A. (2010). A Study of the Tensile Deformation and Fracture Behavior of Commercially Pure Titanium and Titanium Alloy : Influence of Orientation and Microstructure, (August 2019). <https://doi.org/10.1007/s11665-010-9613-5>
- Steel, S., Htun, M. S., Kyaw, S. T., & Lwin, K. T. (2015). Effect of Heat Treatment on Microstructures and Mechanical Properties of Effect of Heat Treatment on Microstructures and Mechanical Properties of Spring Steel, (January 2008).
- Systems, M. (2015). AN ANALYSIS OF TENSILE TEST RESULTS TO ASSESS THE INNOVATION, *XXII*(1), 127–138. <https://doi.org/10.1515/mms-2015-0015.->
- Treatment, H., Properties, I., & Extrusion, C. (2019). Heat Treatment , Impact

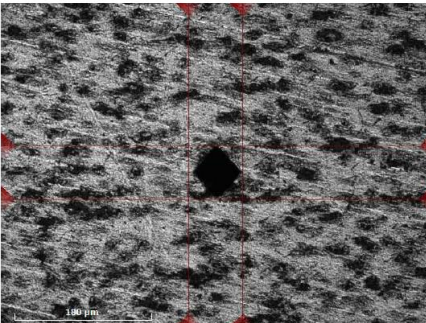
Properties , and Fracture.

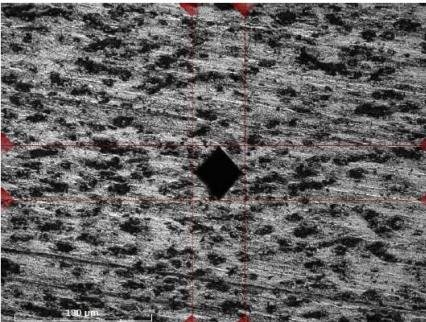
- Vatsayan, U., & Pandey, K. M. (2014). Effects of Heat Treatment on Materials Used In Automobiles : A Case Study, *11*(5), 90–95.
- Venkatesh, B. D. (2008). Effect of heat treatment on mechanical properties of bio-medical Ti-6Al-4V eli alloy.
- Wachowski, M., Wachowski, M., & Jan, K. (2017). The Effect of Heat Treatment on the Microstructure and Properties of Explosively Welded Titanium-Steel Plates, *26*(March), 945–954. <https://doi.org/10.1007/s11665-017-2520-2>
- Warchomicka, F. (2010). Effect of heat treatments on the microstructure of deformed Ti-6Al-4V, (September).
- Zheng, Q., Shimizu, T., & Yang, M. (2015). Effect of heat on tensile properties of thin pure titanium foils, (January 2016). <https://doi.org/10.1051/mfreview/2015005>

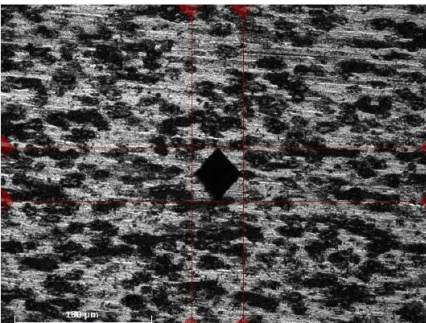
APPENDICES

Figure A1: Images around micro hardness points measured for Parent sample

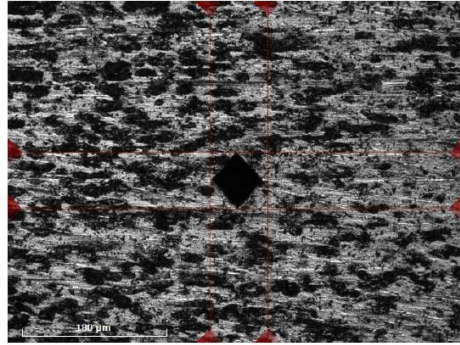
ID	1 (1/1)	
Hardness	185.52 HV0.5	
d1	0.0707 mm	
d2	0.0707 mm	
position	x: 51.05 mm y: 55.28 mm	
Conversions		
Time	12:24:46	

ID	2 (1/1)	
Hardness	189.3 HV0.5	
d1	0.0706 mm	
d2	0.0693 mm	
position	x: 56.05 mm y: 55.28 mm	
Conversions		
Time	12:25:28	

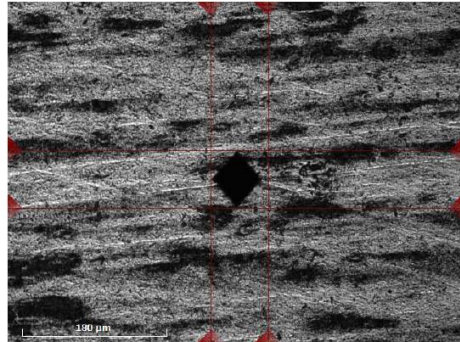
ID	3 (1/1)	
Hardness	185.66 HV0.5	
d1	0.0694 mm	
d2	0.0720 mm	
position	x: 61.05 mm y: 55.28 mm	
Conversions		
Time	12:26:09	

ID	4 (1/1)	
Hardness	194.0 HV0.5	
d1	0.0685 mm	
d2	0.0698 mm	
position	x: 66.05 mm y: 55.28 mm	
Conversions		
Time	12:26:51	

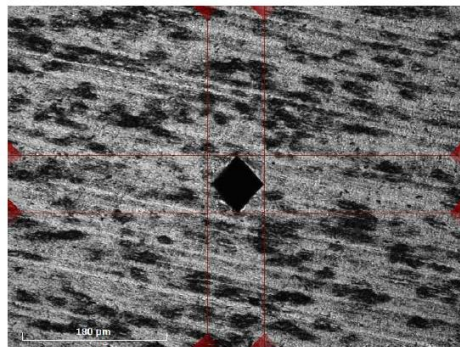
ID 5 (1/1)
Hardness 185.74 HV0.5
d1 0.0720 mm
d2 0.0693 mm
position x: 71.05 mm
y: 55.28 mm
Conversions
Time 12:27:34



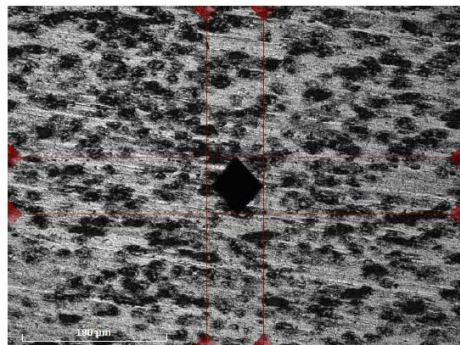
ID 6 (1/1)
Hardness 183.46 HV0.5
d1 0.0711 mm
d2 0.0711 mm
position x: 51.05 mm
y: 51.28 mm
Conversions
Time 12:28:17



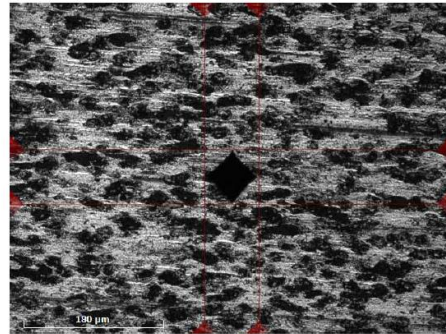
ID 7 (1/1)
Hardness 182.21 HV0.5
d1 0.0711 mm
d2 0.0715 mm
position x: 56.05 mm
y: 51.28 mm
Conversions
Time 12:28:59



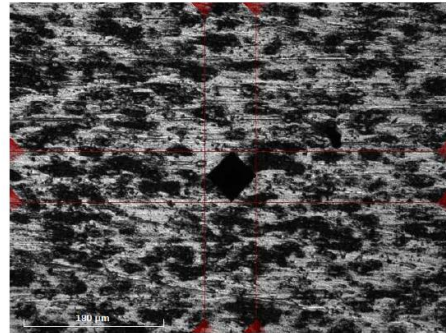
ID 8 (1/1)
Hardness 185.22 HV0.5
d1 0.0712 mm
d2 0.0703 mm
position x: 61.05 mm
y: 51.28 mm
Conversions
Time 12:29:40



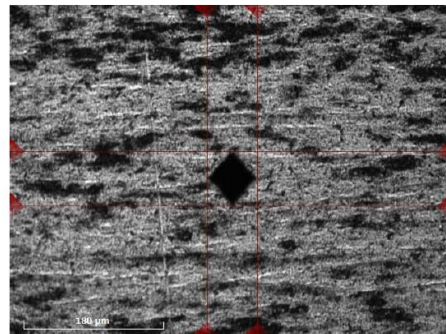
ID 9 (1/1)
Hardness 191.09 HV0.5
d1 0.0700 mm
d2 0.0693 mm
position x: 66.05 mm
y: 51.28 mm
Conversions
Time 12:35:01



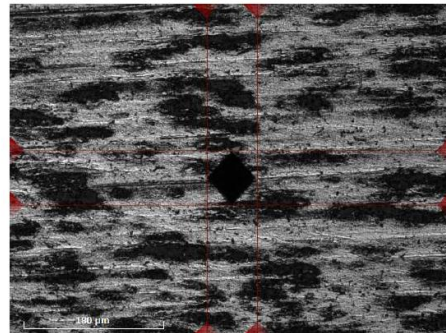
ID 10 (1/1)
Hardness 215.64 HV0.5
d1 0.0662 mm
d2 0.0649 mm
position x: 71.05 mm
y: 51.28 mm
Conversions
Time 12:31:04



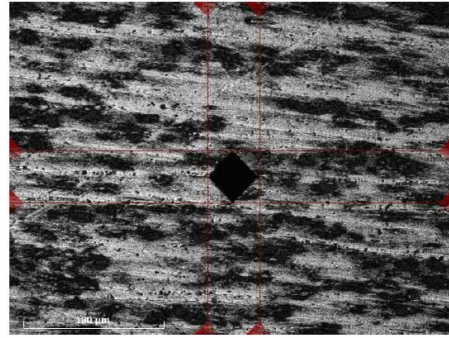
ID 11 (1/1)
Hardness 204.52 HV0.5
d1 0.0649 mm
d2 0.0698 mm
position x: 51.05 mm
y: 47.28 mm
Conversions
Time 12:31:47



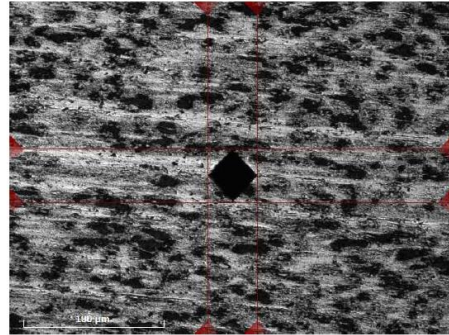
ID 12 (1/1)
Hardness 205.76 HV0.5
d1 0.0645 mm
d2 0.0698 mm
position x: 56.05 mm
y: 47.28 mm
Conversions
Time 12:32:29



ID 13 (1/1)
Hardness 210.0 HV0.5
d1 0.0662 mm
d2 0.0667 mm
position x: 61.05 mm
y: 47.28 mm
Conversions
Time 12:35:26



ID 14 (1/1)
Hardness 215.66 HV0.5
d1 0.0636 mm
d2 0.0676 mm
position x: 66.05 mm
y: 47.28 mm
Conversions
Time 12:33:52



ID 15 (1/1)
Hardness 192.94 HV0.5
d1 0.0684 mm
d2 0.0702 mm
position x: 71.05 mm
y: 47.28 mm
Conversions
Time 12:34:35

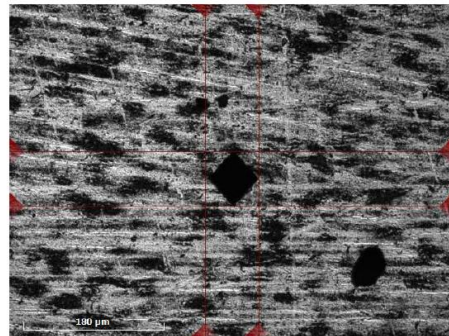
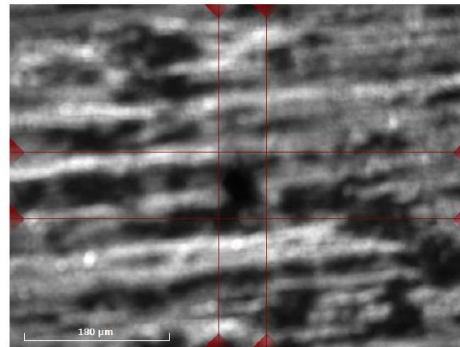
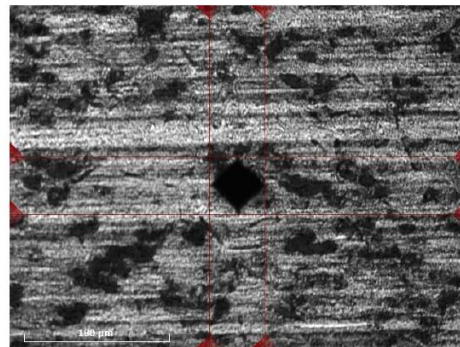


Figure A2: Images around micro hardness points measured for 30 minutes heat treated sample

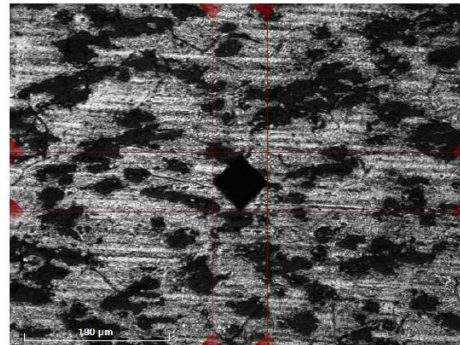
ID 1 (1/1)
Hardness 183.98 HV0.5
d1 0.0596 mm
d2 0.0824 mm
position x: 63.38 mm
y: 52.14 mm
Conversions
Time 11:37:08



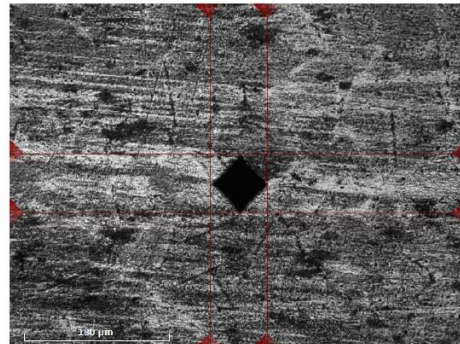
ID 2 (1/1)
Hardness 188.21 HV0.5
d1 0.0693 mm
d2 0.0711 mm
position x: 68.38 mm
y: 52.14 mm
Conversions
Time 11:26:29



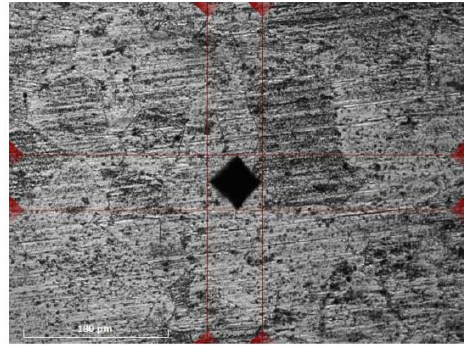
ID 3 (1/1)
Hardness 186.83 HV0.5
d1 0.0672 mm
d2 0.0737 mm
position x: 73.38 mm
y: 52.14 mm
Conversions
Time 11:27:12



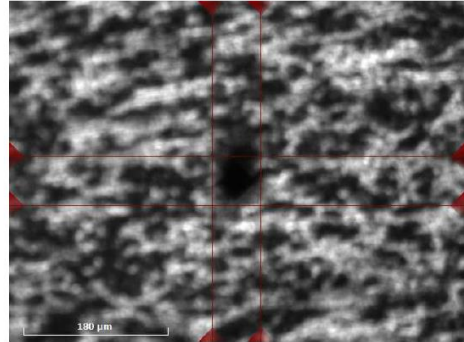
ID 4 (1/1)
Hardness 177.9 HV0.5
d1 0.0711 mm
d2 0.0733 mm
position x: 78.38 mm
y: 52.14 mm
Conversions
Time 11:27:55



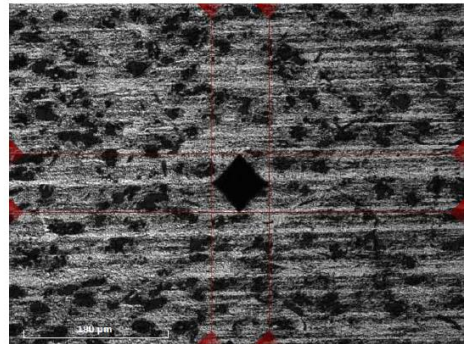
ID 5 (1/1)
Hardness 200.56 HV0.5
d1 0.0680 mm
d2 0.0680 mm
position x: 83.38 mm
y: 52.14 mm
Conversions
Time 11:28:39



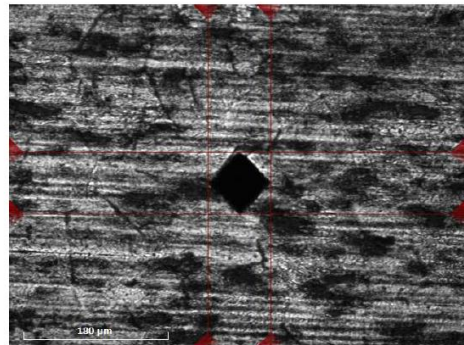
ID 6 (1/1)
Hardness 237.74 HV0.5
d1 0.0644 mm
d2 0.0605 mm
position x: 63.38 mm
y: 48.14 mm
Conversions
Time 11:38:30



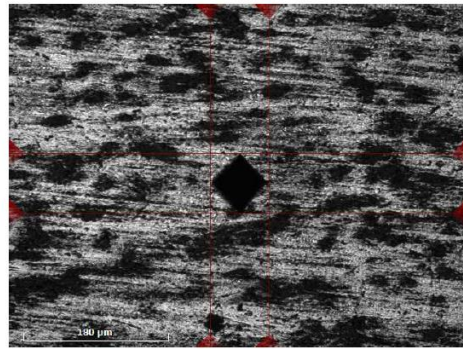
ID 7 (1/1)
Hardness 177.93 HV0.5
d1 0.0715 mm
d2 0.0728 mm
position x: 68.38 mm
y: 48.14 mm
Conversions
Time 11:30:08



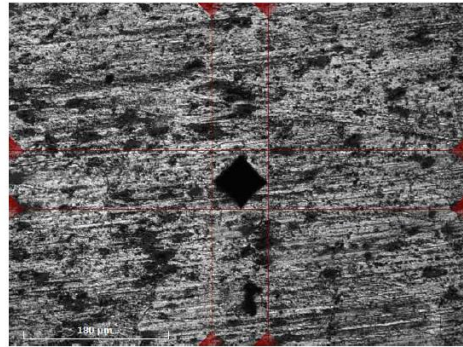
ID 8 (1/1)
Hardness 154.41 HV0.5
d1 0.0781 mm
d2 0.0768 mm
position x: 73.38 mm
y: 48.14 mm
Conversions
Time 11:30:51



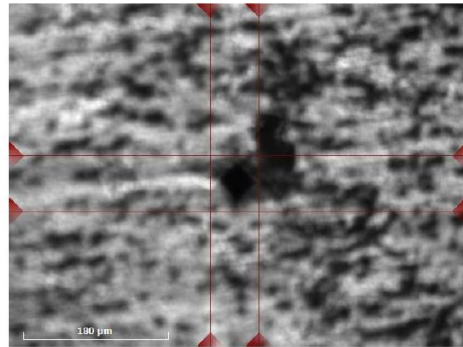
ID 9 (1/1)
Hardness 171.55 HV0.5
d1 0.0729 mm
d2 0.0742 mm
position x: 78.38 mm
y: 48.14 mm
Conversions
Time 11:31:34



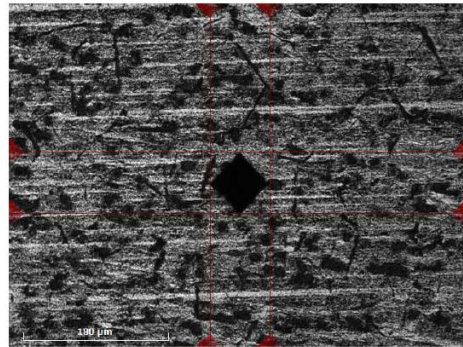
ID 10 (1/1)
Hardness 185.5 HV0.5
d1 0.0694 mm
d2 0.0720 mm
position x: 83.38 mm
y: 48.14 mm
Conversions
Time 11:32:16



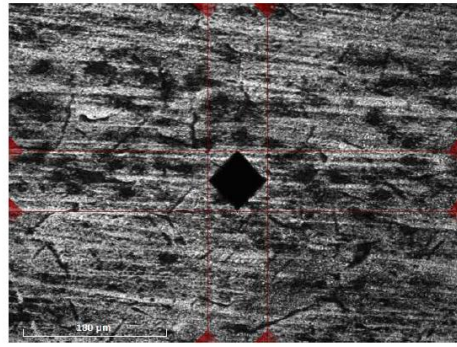
ID 11 (1/1)
Hardness 224.46 HV0.5
d1 0.0601 mm
d2 0.0685 mm
position x: 63.38 mm
y: 44.14 mm
Conversions
Time 11:39:24



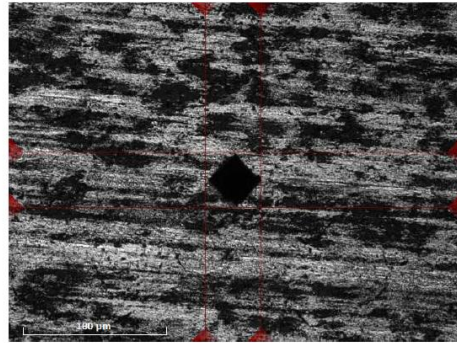
ID 12 (1/1)
Hardness 164.58 HV0.5
d1 0.0746 mm
d2 0.0755 mm
position x: 68.38 mm
y: 44.14 mm
Conversions
Time 11:33:46



ID 13 (1/1)
Hardness 162.64 HV0.5
d1 0.0751 mm
d2 0.0759 mm
position x: 73.38 mm
y: 44.14 mm
Conversions
Time 11:34:29



ID 14 (1/1)
Hardness 191.73 HV0.5
d1 0.0702 mm
d2 0.0689 mm
position x: 78.38 mm
y: 44.14 mm
Conversions
Time 11:35:11



ID 15 (1/1)
Hardness 191.73 HV0.5
d1 0.0671 mm
d2 0.0720 mm
position x: 83.38 mm
y: 44.14 mm
Conversions
Time 11:35:54

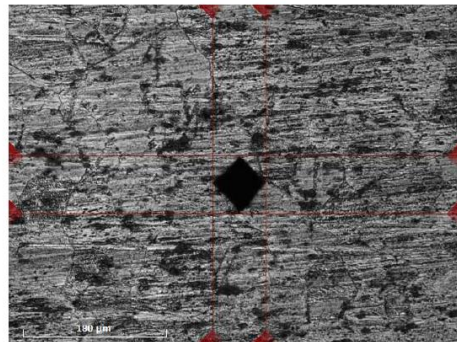
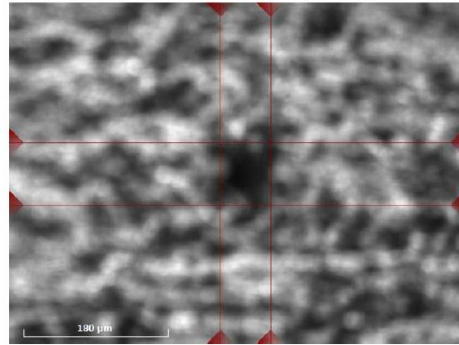
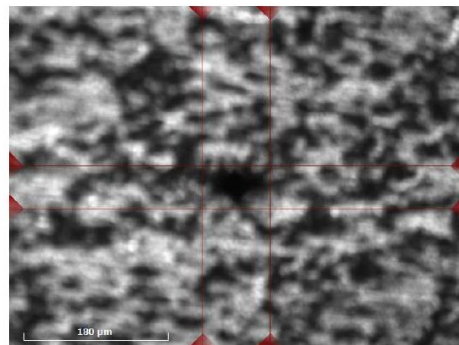


Figure A3: Images around micro hardness points measured for 60 minutes heat treated sample

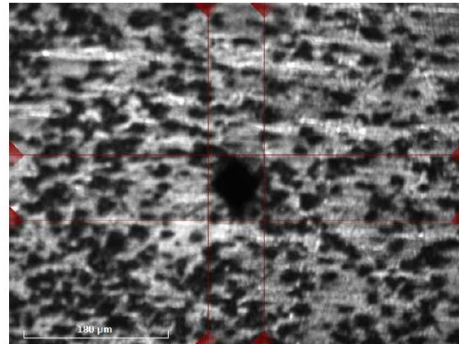
ID 1 (1/1)
Hardness 172.32 HV0.5
d1 0.0685 mm
d2 0.0782 mm
position x: 63.38 mm
y: 52.14 mm
Conversions
Time 11:17:23



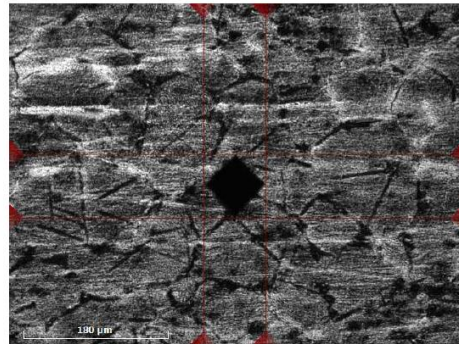
ID 2 (1/1)
Hardness 196.05 HV0.5
d1 0.0841 mm
d2 0.0534 mm
position x: 68.38 mm
y: 52.14 mm
Conversions
Time 11:17:52



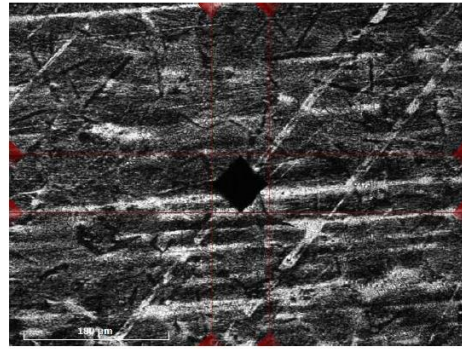
ID 3 (1/1)
Hardness 163.3 HV0.5
d1 0.0698 mm
d2 0.0809 mm
position x: 73.38 mm
y: 52.14 mm
Conversions
Time 11:19:37



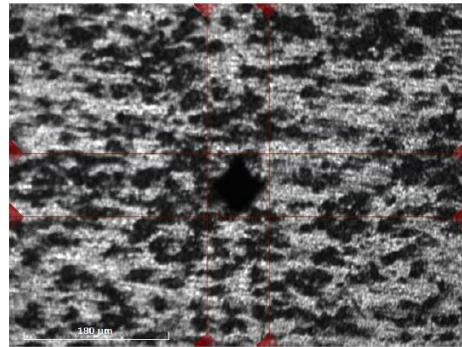
ID 4 (1/1)
Hardness 151.75 HV0.5
d1 0.0773 mm
d2 0.0790 mm
position x: 78.38 mm
y: 52.14 mm
Conversions
Time 11:08:37



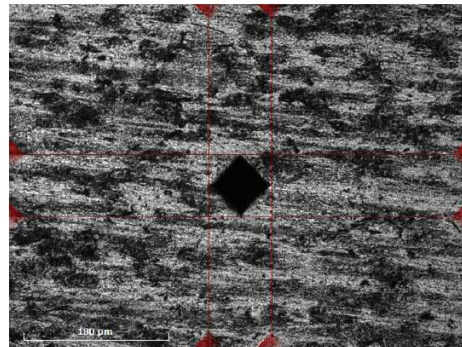
ID 5 (1/1)
Hardness 178.98 HV0.5
d1 0.0720 mm
d2 0.0720 mm
position x: 83.38 mm
y: 52.14 mm
Conversions
Time 11:09:19



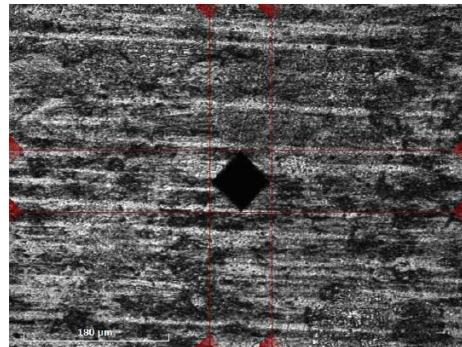
ID 6 (1/1)
Hardness 152.43 HV0.5
d1 0.0774 mm
d2 0.0786 mm
position x: 63.38 mm
y: 48.14 mm
Conversions
Time 11:18:36



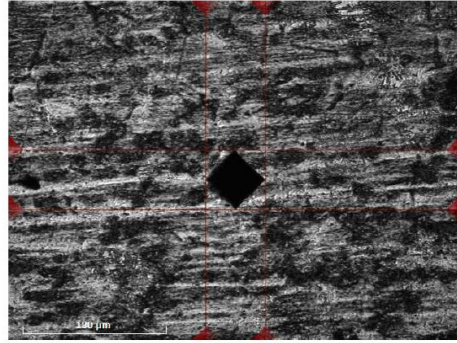
ID 7 (1/1)
Hardness 154.34 HV0.5
d1 0.0777 mm
d2 0.0773 mm
position x: 68.38 mm
y: 48.14 mm
Conversions
Time 11:10:47



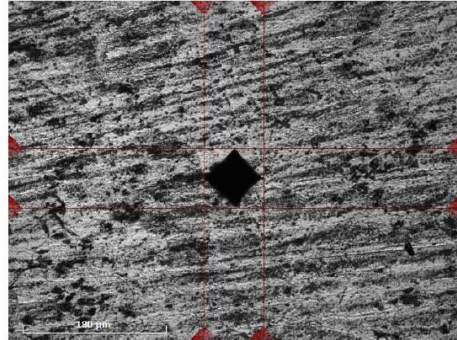
ID 8 (1/1)
Hardness 158.02 HV0.5
d1 0.0768 mm
d2 0.0764 mm
position x: 73.38 mm
y: 48.14 mm
Conversions
Time 11:11:29



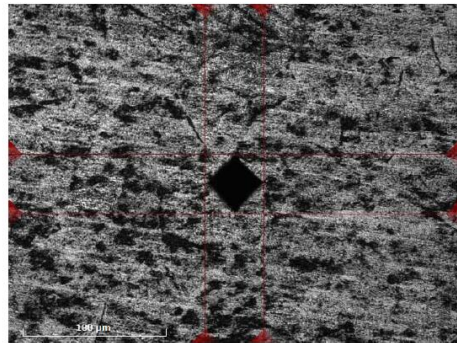
ID 9 (1/1)
Hardness 167.48 HV0.5
d1 0.0742 mm
d2 0.0746 mm
position x: 78.38 mm
y: 48.14 mm
Conversions
Time 11:12:11



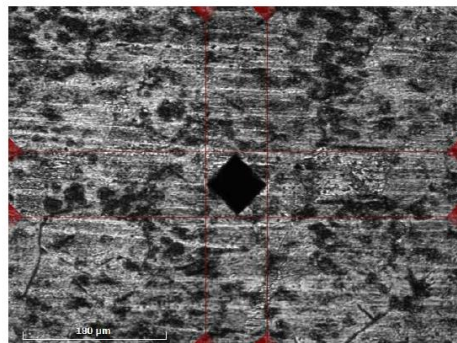
ID 10 (1/1)
Hardness 166.53 HV0.5
d1 0.0746 mm
d2 0.0746 mm
position x: 83.38 mm
y: 48.14 mm
Conversions
Time 11:12:53



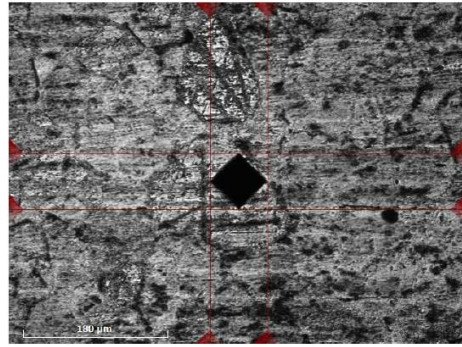
ID 11 (1/1)
Hardness 170.37 HV0.5
d1 0.0733 mm
d2 0.0742 mm
position x: 63.38 mm
y: 44.14 mm
Conversions
Time 11:13:39



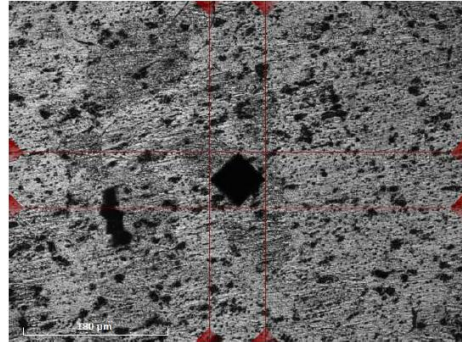
ID 12 (1/1)
Hardness 149.28 HV0.5
d1 0.0768 mm
d2 0.0808 mm
position x: 68.38 mm
y: 44.14 mm
Conversions
Time 11:14:21



ID 13 (1/1)
Hardness 184.65 HV0.5
d1 0.0715 mm
d2 0.0702 mm
position x: 73.38 mm
y: 44.14 mm
Conversions
Time 11:15:03



ID 14 (1/1)
Hardness 192.97 HV0.5
d1 0.0702 mm
d2 0.0684 mm
position x: 78.38 mm
y: 44.14 mm
Conversions
Time 11:15:46



ID 15 (1/1)
Hardness 190.54 HV0.5
d1 0.0684 mm
d2 0.0711 mm
position x: 83.38 mm
y: 44.14 mm
Conversions
Time 11:16:29

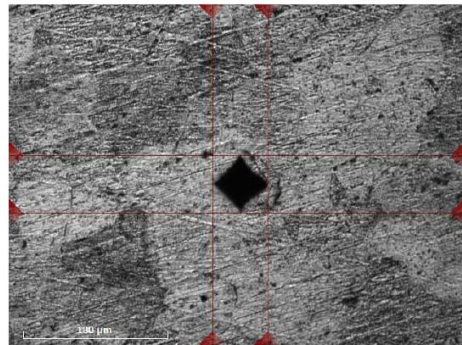
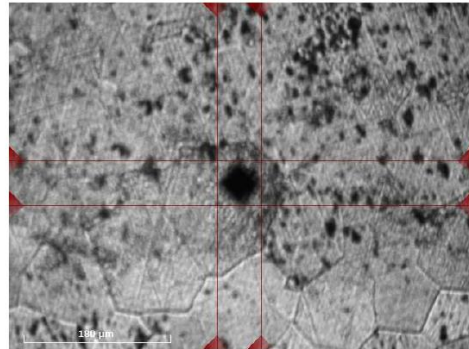
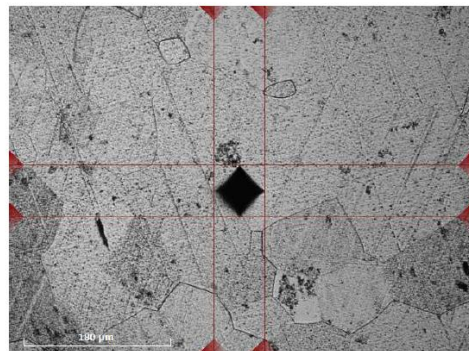


Figure A4: Images around micro hardness points measured for 90 minutes heat treated sample

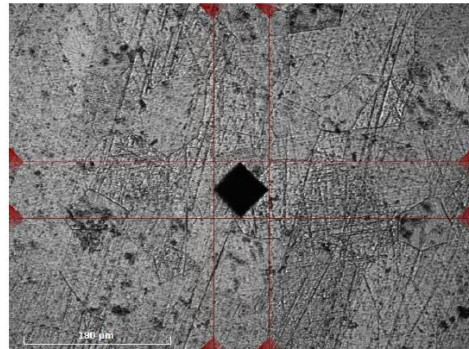
ID 1 (1/1)
Hardness 312.56 HV0.5
d1 0.0539 mm
d2 0.0550 mm
position x: 51.05 mm
y: 55.28 mm
Conversions
Time 10:34:39



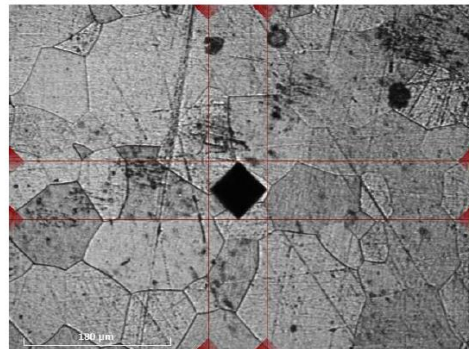
ID 2 (1/1)
Hardness 235.89 HV0.5
d1 0.0623 mm
d2 0.0631 mm
position x: 56.05 mm
y: 55.28 mm
Conversions
Time 10:24:33



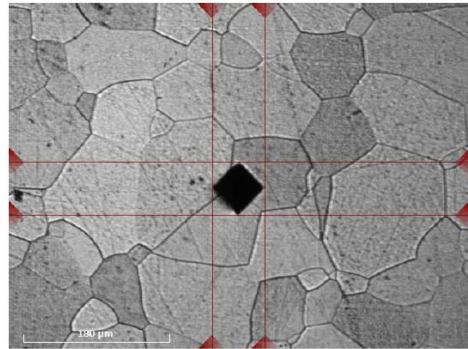
ID 3 (1/1)
Hardness 197.97 HV0.5
d1 0.0684 mm
d2 0.0684 mm
position x: 61.05 mm
y: 55.28 mm
Conversions
Time 10:25:16



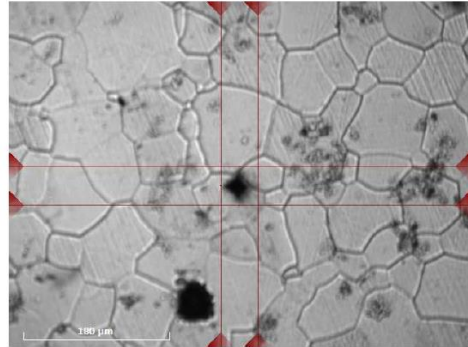
ID 4 (1/1)
Hardness 182.34 HV0.5
d1 0.0715 mm
d2 0.0711 mm
position x: 66.05 mm
y: 55.28 mm
Conversions
Time 10:25:58



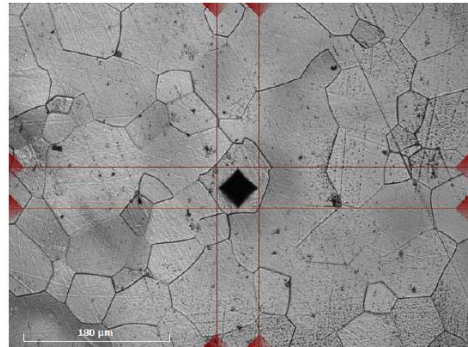
ID 5 (1/1)
Hardness 220.07 HV0.5
d1 0.0649 mm
d2 0.0649 mm
position x: 71.05 mm
y: 55.28 mm
Conversions
Time 10:26:40



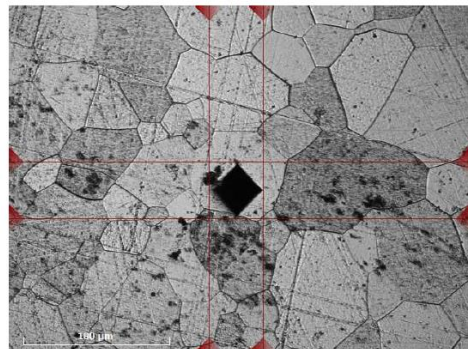
ID 6 (1/1)
Hardness 422.24 HV0.5
d1 0.0460 mm
d2 0.0477 mm
position x: 51.05 mm
y: 51.28 mm
Conversions
Time 10:35:37



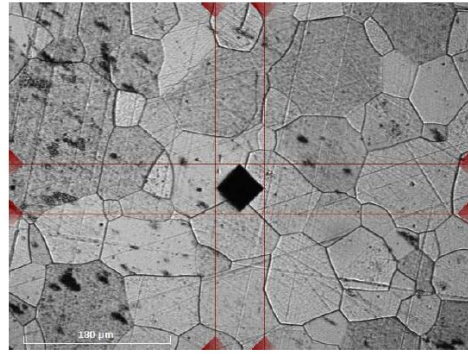
ID 7 (1/1)
Hardness 347.38 HV0.5
d1 0.0525 mm
d2 0.0508 mm
position x: 56.05 mm
y: 51.28 mm
Conversions
Time 10:36:07



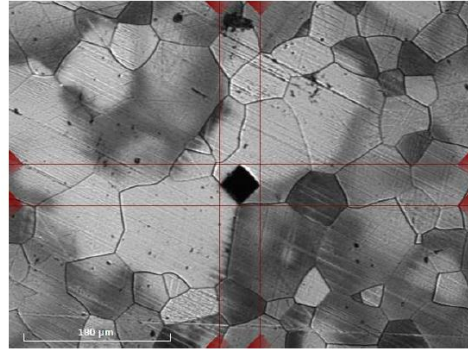
ID 8 (1/1)
Hardness 199.23 HV0.5
d1 0.0662 mm
d2 0.0702 mm
position x: 61.05 mm
y: 51.28 mm
Conversions
Time 10:36:39



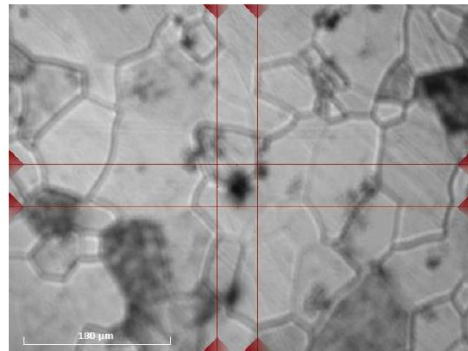
ID 9 (1/1)
Hardness 253.42 HV0.5
d1 0.0605 mm
d2 0.0605 mm
position x: 66.05 mm
y: 51.28 mm
Conversions
Time 10:36:53



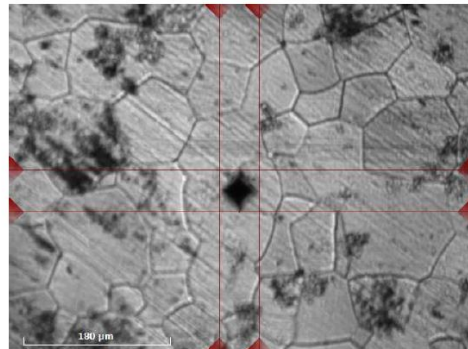
ID 10 (1/1)
Hardness 369.18 HV0.5
d1 0.0499 mm
d2 0.0503 mm
position x: 71.05 mm
y: 51.28 mm
Conversions
Time 10:30:12



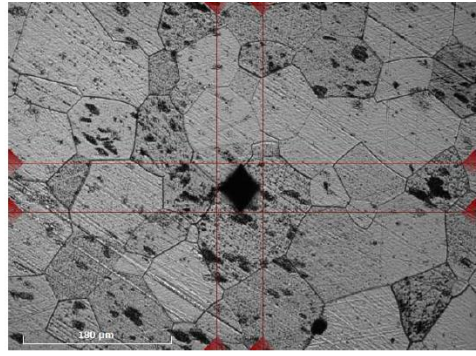
ID 11 (1/1)
Hardness 359.56 HV0.5
d1 0.0495 mm
d2 0.0521 mm
position x: 51.05 mm
y: 47.28 mm
Conversions
Time 10:30:57



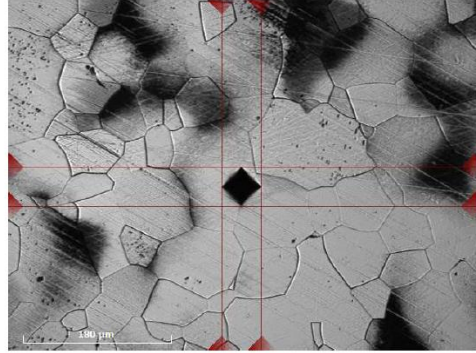
ID 12 (1/1)
Hardness 372.22 HV0.5
d1 0.0486 mm
d2 0.0512 mm
position x: 56.05 mm
y: 47.28 mm
Conversions
Time 10:31:39



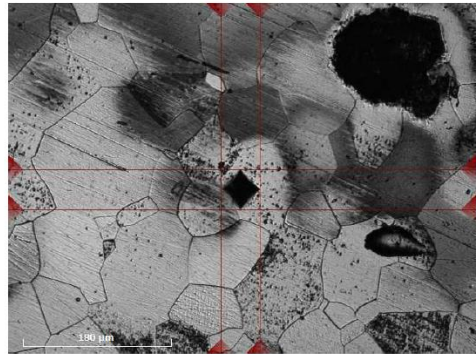
ID 13 (1/1)
Hardness 283.55 HV0.5
d1 0.0552 mm
d2 0.0592 mm
position x: 61.05 mm
y: 47.28 mm
Conversions
Time 10:32:22



ID 14 (1/1)
Hardness 407.81 HV0.5
d1 0.0481 mm
d2 0.0472 mm
position x: 66.05 mm
y: 47.28 mm
Conversions
Time 10:33:04



ID 15 (1/1)
Hardness 404.02 HV0.5
d1 0.0472 mm
d2 0.0486 mm
position x: 71.05 mm
y: 47.28 mm
Conversions
Time 10:33:46



APPENDIX AB



Figure B1: Raw titanium (Sponge)